AD-777 186

A STUDY OF ELECTRONICS RADIATION HARDNESS ASSURANCE TECHNIQUES. VOLUME II, PART 2, ELECTRICAL SCREENING FOR IONIZING RADIATION RATE AND TOTAL DOSE EFFECTS

I. Arimura, et al

Boeing Company

Prepared for:

Air Force Weapons Laboratory

January 1974

DISTRIBUTED BY:

NTIS

National Technical Information Service
U. S. DEPARTMENT OF COMMERCE
5285 Port Royal Road, Springfield Va. 22151

AIR FORCE WEAPONS LABORATORY
Air Force Systems Command
Kirtland Air Force Base
New Mexico 87117

UNCLASSIFIED
Security Classification

AD-777186

DOCUMENT CONTROL DATA - R & D

(Security classification of title, body of abstract and indexing annotation must be entered when the overall report is classified)

1. ORIGINATING ACTIVITY (Corporate author)
The Boeing Company
Seattle, Washington 98124

2a. REPORT SECURITY CLASSIFICATION
UNCLASSIFIED

2b. GROUP

3. REPORT TITLE
A STUDY OF ELECTRONICS RADIATION HARDNESS ASSURANCE TECHNIQUES
Volume II, Electrical Screening for Ionizing Radiation Rate and Total Dose Effects, Part 2

4. DESCRIPTIVE NOTES (Type of report and inclusive dates)
31 July 1970 through 16 July 1973

5. AUTHOR(S) (First name, middle initial, last name)
I. Arimura, et al.

6. REPORT DATE
January 1974

7a. TOTAL NO. OF PAGES
149

7b. NO. OF REFS
44

8a. CONTRACT OR GRANT NO.
F29601-71-C-0001

b. PROJECT NO.
8809, 133B, WDNE

c. Task
11, DE, 01

d.

9a. ORIGINATOR'S REPORT NUMBER(S)
AFWL-TR-73-134, Vol. II, Pt 2

9b. OTHER REPORT NO(S) (Any other numbers that may be assigned this report)

10. DISTRIBUTION STATEMENT
Approved for public release; distribution unlimited.

11. SUPPLEMENTARY NOTES

12. SPONSORING MILITARY ACTIVITY
Air Force Weapons Laboratory (ELP)
Kirtland Air Force Base, NM 87117

13. ABSTRACT
(Distribution Limitation Statement A)

This program determined physical failure modes of a range of discrete and integrated semiconductor devices exposed to ionizing rate, neutron, and total dose environments. From physical reasoning possible electrical parameter measurements were determined which had some probability of correlating with the radiation sensitivity and failure thresholds. It was determined that base transit time normalization for neutron degradation was generally effective for low-power transistors, but ineffective for power devices. Other AC and a few DC measurements also were found to be effective potential screens for neutron degradation. No particular advantage was noted for using electrical storage time constants compared to electrical storage time for screening primary photocurrents of low-power discrete devices. In some cases, the integrated circuits were obtained with nonstandard metallization, "special lead," topologies to enable electrical measurements to be made at internal circuit nodes. In this Volume (Volume II), the utility of these measurements as correlation parameters was compared to that obtained from measurements made using unmodified circuits. Excellent correlation was obtained between the neutron degradation of the logic circuits and the emitter-base turn-on voltage obtained from the measurements made using special leads. Electrical screens for total dose hardness assurance were found to be relatively ineffective even with parameter correlation factors of 0.7 to 0.8. Similar results were obtained from an evaluation of the low dose screening concept since relative device sensitivity varied with absorbed dose. A mathematical expression was developed for the neutron induced reduction of the energy required for second

DD FORM 1 NOV 65 1473

UNCLASSIFIED
Security Classification

UNCLASSIFIED

Security Classification

14 KEY WORDS	LINK A		LINK B		LINK C	
	ROLE	WT	ROLE	WT	ROLE	WT
Hardness Assurance Transient Radiation Effects Integrated Circuits Radiation Quality Assurance Irradiate-Anneal						

ABSTRACT (Cont'd)

breakdown in the investigated power transistor. Second breakdown of dielectrically isolated integrated circuit (logic) transistors was investigated and determined not to be a problem in neutron or ionizing rate environments. Mean time between failure was not significantly affected (1) by any of the annealing schedules, or (2) by a nondestructive second breakdown test used in the program, or (3) by exposure to an ionizing rate environment of 10^9 to 10^{10} rad (Si)/s. Additional Volumes (Volumes I and III) contain a description of the program, summary and conclusions, and homogeneity and irradiate-anneal studies.

UNCLASSIFIED

Security Classification

AFWL-TR-73-134, Vol. II, Pt 2

A STUDY OF ELECTRONICS RADIATION HARNESSS ASSURANCE TECHNIQUES

Volume II, Part 2
Electrical Screening for Ionizing Radiation Rate and Total Dose Effects

I. Arimura, et al.

The Boeing Company
Seattle, Washington 98124

Final Report for Period 31 July 1970 through 16 July 1973

This work was sponsored in part by the Defense Nuclear Agency under Nuclear Weapons Effects Research Subtask TD-072, Work Unit No. 1, Electrical Parameter Statistical Correlation to Radiation Effects.

1 N

FOREWORD

This report was prepared by The Boeing Company, Seattle, Washington, under Contract F29601-71-C-0001. The research was performed under Program Elements 62601F, 11213F, and 62707H; Projects 8809, 133B, and WDNE; Tasks DE, 11, and 01.

Inclusive dates of research were 31 July 1970 through 16 July 1973. The report was submitted 29 October 1973 by the Air Force Weapons Laboratory Project Officer, Mr. John L. Mullis (ELP).

Principal authors and contributors were Mr. Allan H. Johnston, Dr. L. L. Sivo, and Mr. D. W. Egelkrout. Technical direction and coordination of the program were performed by Dr. R. S. Caldwell and Mr. C. Rosenberg.

Capt J. L. Guidry, Capt G. B. Crocker and Capt P. J. Vail at the Air Force Weapons Laboratory also made significant contributions to the overall planning and execution of the program.

Mr. L. D. Milliman, Mr. K. D. Friddell, Mr. J. Thomas, and Dr. R. C. Kennedy assisted with the large tasks of Data Storage, Retrieval, and Analysis while Messrs. E. T. Ball, E. A. Gallaway, J. F. Foster, D. L. Cushing, S. D. Brooks, and S. Cady performed the Experimental Measurements. Documentation was very ably handled by Mrs. E. L. Taylor, Mr. C. R. Brittain, and Mr. R. Kent. Mr. D. K. Myers at Fairchild Semiconductor assisted with the low power device selection and Mr. K. Martin at Texas Instruments and Mr. R. Jarl at RCA provided timely support of the Irradiate-and-Anneal Program. Mr. J. Snyder and his staff at Sandia Laboratories were very helpful in providing the necessary reactor tests.

This technical report has been reviewed and is approved.

John L. Mullis

JOHN L. MULLIS
Project Officer

Gordon G. Wepfer

GORDON G. WEPFER
Lt Colonel, USAF
Chief, Phenomenology and Technology Branch

John P. Portasik

JOHN P. PORTASIK
Colonel, USAF
Chief, Electronics Division

PREFACE

This report describes the results of a comprehensive study which was designed to determine improved techniques for providing radiation hardness assurance on modern electronic systems. The two basic goals considered were (1) to determine from physical reasoning and large scale testing the effectiveness of established electrical screening parameters and the existence of additional ones which might be correlated with radiation responses and (2) to establish a statistical comparison between the various hardness assurance techniques including electrical screening, lot sampling and irradiate-and-anneal. For reasons of physical convenience, the report is divided into three volumes:

Volume I - Background, Approach, and Summary of Results
Volume II - Electrical Screening, parts 1, 2, and 3
Volume III - Lot Sampling and Irradiate-and-Anneal

This Volume (Volume II) contains a detailed description of the results obtained from the electrical screening portion of the program. The electrical screening approach examined correlations between certain initial electrical parameters and the radiation sensitivities of the devices. The correlation parameters were selected on the basis of physical reasoning and the radiation sensitivies were defined differently for the various radiation environments. Neutron hardness assurance is treated first and the various classes of devices such as low-power transistors, high-power transistors, JFETs and ICs are discussed separately. Ionizing radiation rate hardness assurance is treated second with subdivision determined again by the various classes of devices. MTBF results are also discussed for parts subjected to ionizing rate tests. Total dose hardness assurance is discussed third for the low-power transistors and for the op amp separately. Low dose screening is included in this section although it differs slightly from the "normal" techniques of electrical screening. Finally, second breakdown hardness assurance is discussed in its entirety.

CONTENTS

ILLUSTRATIONS

ILLUSTRATIONS (Cont'd)

ILLUSTRATIONS (Cont'd)

ILLUSTRATIONS (Cont'd)

TABLES

TABLE (Cont'd)

TABLES (Cont'd)

ABBREVIATIONS AND SYMBOLS

A	Ampere, area, surface area of second breakdown region
A_B	Base area
A_E	Emitter area
A_{EFF}	Effective emitter area
A_{OL}	Open-loop gain
A_{SB}	Cross Sectional area of a second breakdown site
AC	Alternating current
AH1	Effective emitter area determined from gain-bandwidth product, emitter base capacitance and current gain
AH3	Effective emitter area determined from gain-bandwidth product, current gain, and base doping concentration
AH4	Effective emitter area determined from gain-bandwidth product, breakdown voltage, and current gain
A-0-I	And-or-invert
BOT	Breakout transistor
BV	Breakdown voltage
BV_{CBO}	Breakdown voltage of collector-base junction with emitter open
BV_{EBO}	The emitter-base breakdown voltage of a transistor with the collector open
BV_{GSS}	Breakdown voltage of gate-channel in JFET. Source and drain shorted
BVCBO	Base to collector breakdown voltage, emitter open
BVCEO	Open base collector to emitter breakdown voltage, measured at a collector current of 10 milliamperes
BVEBO	Open collector, emitter to base breakdown voltage, measured at a base current of 10 milliamperes
C	Damage factor, average specific heat, capacitor

ABBREVIATIONS AND SYMBOLS (Continued)

C_{CB}	Collector-base junction capacitance
C_{GSS}	Gate-channel junction capacitance of JFET
C_{IB}	Emitter-base junction capacitance
C_{OB}	Collector-base junction capacitance
C_P	Damage factor of wafer transistors
C_{SBL}	Linear second breakdown neutron degradation constant
C_β	Neutron damage factor
C-B	Collector to base
CB - X, Y	Neutron damage factor for current gain measured at a collector current of X amperes and collector to emitter voltage of Y volts
C-E	Collector to emitter
CH	Channel
CMRR	Common-mode rejection ratio
COV	Coefficient of variation
COVAR	Covariance = $\frac{\text{standard deviation}}{\text{mean}}$
CRO	Cathode ray oscilloscope
CSBLXYZ	Linear second breakdown neutron degradation constant determined from neutron levels ϕ_x, ϕ_y, and ϕ_z
CSBXYZ	C_{SB} determined from neutron levels ϕ_x, ϕ_y, and ϕ_z
D	Diffusion constant
D_B	Diffusion constant for minority carriers in base region
D_E	Diffusion constant for minority carriers in emitter region
DC	Direct current
D.I.	Dielectric isolation

DUT	Device under test
E	Energy or electric field strength, second breakdown energy measured at $I_E = 5A$
E-5MSIA	Second breakdown energy for a 5 millisecond wide, 1 ampere pulse of emitter current
E-5MSIBO	Second breakdown energy for a 5 millisecond wide voltage pulse equal to the collector-emitter breakdown voltage, base open
E_{SB}	Energy required to produce second breakdown: measured at device terminals
E'_{SB}	Energy required to produce second breakdown: delivered to a localized site of second breakdown
F	F value
FSC	Fairchild Semiconductor Corporation
FM1	Transistor figure of merit determined from gain bandwidth product and base doping concentration
FM3	Transistor figure of merit determined from gain bandwidth product and collector to base breakdown voltage, emitter open
FM4	Transistor figure of merit determined from gain bandwidth product and collector to base breakdown voltage, emitter open
FT	A constant proportional to the gain-bandwidth product measured at an emitter current of 1 ampere
HA	Hardness assurance
HFE - X, Y	Common emitter DC current gain measured at a collector current of X amperes and a collector to emitter voltage of Y volts
I	Current
I_B	Base current (bipolar transistors) or input bias current (op amps, sense amps)
I_B^o	Initial (pre-radiation) base current or bias current
I_B^s	The surface component of the base current

ABBREVIATIONS AND SYMBOLS (Continued)

I_{B1}	The forward current into the base of a saturated transistor
I_{B2}	The current flowing out of the base of a saturated transistor when it is switched out of saturation
I_{BIAS}	Input bias current
I_{BS}	Base current of saturated transistor
I_C	Collector current
I_{CBO}	Collector-base junction leakage current
I_{CC}	Power supply current in positive supply lead
$I_{CC(0)}$	Power supply current of a digital circuit in a 0-state
I_{CO}	Pre-exponential saturation current
I_{CS}	Collector current of saturated transistor
I_{DS}	Drain current in JFET
I_{DSS}	Source to drain saturation current at zero gate bias
I_E	Emitter current
I_{EBO}	Emitter-base junction leakage current, collector open
I^o_{EBO}	Initial (pre-radiation) emitter-base junction leakage current, collector open
I^s_{EBO}	The surface component of the leakage current across the reverse biased emitter-base junction
I_{EE}	Power supply current in negative supply lead
I_F	Forward current of gate-channel diode in JFET
$I_{IN(R)}$	Reverse input current measurement for TTL circuits
$I_{IN(0)}$	Current out of TTL input with input voltage low
$I_{IN(1)}$	Current into TTL input with input voltage high
I_{OS}	Input offset current
I_{pp}	Primary photocurrent

ABBREVIATIONS AND SYMBOLS (Continued

I_{OL}	Output leakage current of an integrated circuit
I_R	Reverse current of gate-channel diode in JFET
I_{SK}	The output sink current of a TTL device with lower than normal supply voltage
I_{sp}	Secondary photocurrent
IC	Integrated Circuit
ICBO	Open emitter, collector to base leakage current measured at 50 volts
ICEO	Open base, collector to emitter leakage current measured at 30 volts
IEBO	Open collector, emitter to base leakage current at 5 volts
I'V'	Portion of second breakdown power not directly dissipated in a second breakdown site
J_E	Emitter current density
J.I.	Junction isolation
k	Damage constant, an abbreviation for Kilo-ohm used in circuit schematics
K_a	Thermal conductivity at second breakdown site averaged over temperature
K_F	Carrier removal damage factor
K_N	Total delay time normalized damage constant
K_R	Damage constant due to lifetime degradation in emitter-base depletion region
L	Diffusion length, length of JFET channel in direction paralleled to current flow
L_C	Diffusion length of minority carriers in collector region
L_E	Diffusion length of minority carriers in emitter region

LINAC	Linear accelerator
LSI	Large scale integration
M	Mass of material at a localized second breakdown site
M_{β}	Temperature sensitivity of the common emitter DC current gain
MB -3.0	Temperature sensitivity of the common emitter current gain measured at a collector current of 3 amperes and a collector to emitter voltage of 3 volts
MeV	Mega electron volts
MLR	Multiple linear regression
MLRP	Multiple linear regression prediction
MLR-R	Coefficient of multiple linear correlation
MLR-$\hat{r}$	Multiple linear regression partial correlation coefficient
MLR-r	Multiple linear regression coefficient
MOT	Motorola
MSI	Medium scale integration
MTBF	Mean time between failure
N	Value of exponent in the equation relating second breakdown energy and neutron fluence. N is determined from, carrier concentration 4 fluence levels
N_B	Base doping concentration
N_{BO}	Base doping concentration adjacent to emitter region
N_E	Minority carrier density in the emitter region
N_o	Channel doping concentration for JFET in cm^{-3}
NXYZ	Value of exponent in equation relating second breakdown energy and neutron fluence. NXYZ is determined from fluence levels of ϕ_x, ϕ_y and ϕ_z
N(CH)	Channel doping as calculated from BV_{GSS} measurements

ABBREVIATIONS AND SYMBOLS (Continued)

Noise $(1/f)_s$	Surface component of the 1/f noise
P	Power
P_{SB}	Power of a square pulse required to produce second breakdown
Q	A symbol for transistors used in schematic diagrams
R	Resistance
R_B	External resistance from the base of a transistor in an electrical circuit
R_D	Maximum percentage range in the data
R_E	Radius of emitter region
R_L	Load resistor
R_P	Maximum percentage range in the prediction
RBC	The reciprocal of base impurity concentration
RBV	A constant inversely proportional to the 2.8 power of the open collector-emitter, to base breakdown voltage measured at a base current of 10 milliamperes
RCA	Radio Corporation of America
RCC	The reciprocal of the collector impurity concentration
RCV	A constant inversely proportional to the 2.8 power of the open emitter, collector to base breakdown voltage measured at a base current of 10 milliamperes
RMS	Root mean square
S	Switch
Sat.	Saturation
SB	Second breakdown
SCR	Silicon controlled rectifier
SLR	Single linear regression
SSI	Small-scale integration

T	Absolute temperature (°K), Temperature
T_a	Ambient temperature
T_{off}	The turn-off time of an integrated circuit
t_{SB}	The temperature at a site of second breakdown at the onset of second breakdown
TI	Texas Instruments
TTL	Transistor-transistor logic
TUT	Transistor under test
V	Volt
V_{BE}	Base to emitter voltage
V_{BEON}	Emitter to base forward voltage
V_C	Collector voltage
V_{CB}	Collector to base voltage
V_{CC}	The positive supply voltage of an integrated circuit
V_{CE}	Collector to emitter voltage
$V_{CE(SAT)}$	Collector to emitter voltage for saturated transistor
V_{DS}	Drain voltage
V_{EB}	The voltage from the emitter to base of a transistor
V_{EE}	The negative supply voltage of an integrated circuit
V_{GS}	Gate to source voltage
V_{in}	Input voltage
$V_{IN(R)}$	The reverse input voltage of a TTL circuit
V_{OH}	The 1-state output voltage of a digital circuit
V_{OL}	The 0-state output voltage of a digital circuit

ABBREVIATIONS AND SYMBOLS (Continued)

V_{OS}	The offset voltage of an integrated circuit
V_P	Pinch off voltage for JFET
V_{SB}	Voltage across a device prior to second breakdown
V-I	Voltage-current
VBEON-X	Emitter to base forward voltage for an emitter current of X amperes
VCES-X	Collector to emitter saturation voltage at a collector current of X amperes
VSB-5A	Voltage across a device prior to second breakdown at an emitter current of 5 amperes
VSB-5MSIBO	Voltage across a device prior to second breakdown at a delay time of 5 milliseconds and with zero base current
W_B	Base width
W_C	Collector depletion width of a transistor
W_D	Depletion region width of emitter-base junction
$W_{1(2,3,4)}$	Wafer number 1 (2,3,4)
WB	The inverse square root of the common emitter gain-bandwidth product
Z	Channel width in direction perpendicular to thickness and length in JFET
a	Channel thickness in JFET
c	Capacitance
cm	Centimeter
f_T	Common-emitter gain-bandwidth product
F_α	Common base cutoff frequency
g_m	Post-irradiation transconductance
g_{mo}	Pre-irradiation transconductance

ABBREVIATIONS AND SYMBOLS (Continued)

h_{FE}	Common-emitter DC gain
h_{FE}', h_{FEI}	Common-emitter DC current gain for inverted transistor
h_{FEO}	Pre-irradiation gain
$h_{FE\phi}$	Gain after neutron irradiation
i_n	Equivalent input noise current
k	Boltzmann constant
keV	10^3 electron-volts
mA	10^{-3} amperes
mV	10^{-3} volts
mW	10^{-3} watts
n	Value of exponent in equation relating second breakdown energy and neutron fluence
n_I	Exponent of voltage dependence of emitter-base junction capacitance
n_i	Electron concentration in intrinsic silicon
n_p	Minority carrier density in a p-type semiconductor
ns	10^{-9} seconds
P_o	Equilibrium hole concentration
pF	10^{-12} farads
q	Electron charge
r	rads
rank-r	Rank correlation coefficient
r_B	Transverse base resistance
r_{BI}	Transverse base resistance for inverted transistor
r_c	Collector body resistance

r_{cs}	Resistance of collector region of saturated transistor
$r_{d(on)o}$	Pre-irradiation value of $r_{d(on)}$
$r_{d(on)}$	The on resistance of a JFET
rad(Si)	A deposited dose of 100 ergs per gram of silicon
s	Second
t	Time
t_B	Base transit time
t_d	Total delay time
t_{PD}	Propagation delay time of a logic circuit
t_{OFF}	Turn-Off time of the word switch
t_{PLH2}	The delay time of an integrated circuit when the output goes from low to high, measured at 50% of the equilibrium value
t_{rrGS}	Reverse recovery time of gate-channel diode in JFET
t_{SE}	Electrical storage time
t_{SAT}	Saturation time of the word switch
t-statistic	Measure of significance for multiple linear regression analyses
w_E	Width of emitter stripe
x_m	Modulation length
ΔI_B^s(burn-in)	The change in I_B^s during burn-in
$\Delta I_B^s(T)$	The change in I_B^s when measured at different temperatures
ΔI_{EBO}^s(burn-in)	The change in I_{EBO}^s during burn-in
ΔI_{EBO}^s	The change in I_{EBO}^s when measured at different temperatures
Δn	Excess electron concentration
ϕ_{BE}	Base-emitter junction contact potential

ABBREVIATIONS AND SYMBOLS (Continued)

Ω	Ohm
β	Grounded emitter DC current gain (i.e. h_{FE})
β_F	Forced beta of saturated transistor ($\equiv I_{CS}/I_{BS}$)
β_o	Initial (pre-radiation) grounded emitter DC current gain
$\dot{\gamma}$	Ionizing dose rate
ε	Permittivity of dielectric
ε_o	Permittivity of vacuum
θ	The electronic charge divided by the product of Boltzmann's constant and the absolute temperature
θ_{HS}	Hot spot thermal resistance
κ	Dielectric constant
μ	Mobility
μ_B	Carrier mobility in base region
μ_c	Carrier mobility in collector region
μ_n	Electron mobility
μ_p	Hole mobility
μA	Micro amperes
μF	10^{-6} farad
μs	10^{-6} second
ρ_B	Resistivity of base region
ρ_C	Resistivity of collector region
ρ_{SE}	Emitter sheet resistivity
σ	Electrical conductivity or standard deviation
τ	Excess minority carrier lifetime
τ_B	Minority carrier lifetime in base region

ABBREVIATIONS AND SYMBOLS (Continued)

τ_C	Minority carrier lifetime in collector region
τ_{no}	Minority carrier lifetime in highly p-type
τ_{po}	Minority carrier lifetime in highly n-type
τ_s	Electrical storage time constant
τ_s	Storage time constant for gate-channel diode in JFET
τ_{SB}	Second breakdown delay time
τ_{SBO}	Delay time to second breakdown measured in previous tests
τ	Hot spot thermal time constant
ϕ	Neutron Fluence
ϕ_C	Critical dose or threshold dose for failure
ϕ_1	First neutron fluence
ϕ_2	Second neutron fluence
ϕ_3	Third neutron fluence
ϕ_4	Fourth neutron fluence
ω_T	The gain-bandwidth product of a transistor $(f_T) \times 2\pi$
0-state	The low output voltage state of a digital circuit
1-state	The high output voltage state of a digital circuit
1N1	First neutron irradiation
2N1	Second neutron irradiation
3N1	Third neutron irradiation
4N1	Fourth neutron irradiation

SECTION III

IONIZING RADIATION RATE EFFECTS HARDNESS ASSURANCE

1. INTRODUCTION

This section discusses hardness assurance techniques for ionizing rate effects in discrete transistors, junction field-effect transistors (JFET), and integrated circuits. For discrete transistors, hardness assurance techniques were investigated for both primary and secondary photocurrent. The transistor types studied include high- and low-power transistors with a wide range of device geometries and electrical properties. The radiation rate depencence of primary photocurrent was also considered. For the JFET, gate primary photocurrent is the fundamental radiation parameter used in the correlation and hardness assurance studies. The integrated circuits included in this study are all dielectrically-isolated, radiation-hardened devices, and include both digital and linear circuit types. The circuit output response to ionizing radiation was used as the parameter of interest for hardness assurance and correlation studies. For the digital circuits, the radiation level was varied to find the particular radiation threshold level at which a given output response occurred.

A detailed description of the various device types and the schematic diagrams for the integrated circuits are contained in Paragraphs 2-a and 2-b, Section IV, Volume 1. A description of the radiation test conditions and techniques is included in Paragraph 4-c, Section IV, Volume 1.

2. LOW POWER TRANSISTORS

a. Primary Photocurrent

Steady-state primary photocurrents were measured for five types of low-power transistors and two types of IC breakout transistors using the Boeing Radiation Effects Laboratory 10-MeV Electron Linear Accelerator as an ionization source. Experimental details of the measurements were described previously in Paragraph 4-b, Section IV, Volume 1. Table 51 is a summary of the parts tested for primary and secondary photocurrents. The electrical screening parameters for primary photocurrents were investigated only for the first seven part types shown in Table 51.

The primary photocurrent, I_{pp}, measured for five types of low-power transistors are summarized in the sample histograms shown on Figures 49 through 53. The mean, standard deviation, maximum, minimum and range of photocurrents are summarized in Table 52. The range of responses for these part types (given by the maximum I_{pp} divided by minimum I_{pp}) varied from ~1.8 to ~3.5 (excluding one 2N3960 which exhibited a breakdown or anomalous I_{pp} a factor of 10 greater than the other devices of that type). However, the data at the very high rates are of questionabe accuracy, particularly for the rates in the high 10^{10} rad(Si)/s range. Accurate dosimetry was difficult at these rates since the electron beam spot was quite small and the position of the beam varied from shot-to-shot.

I_{pp}, based on the simple theory given in Paragraph 3-a, Section V, Volume 1 for collector-base primary photocurrent, is expected to vary linearly with ionizing radiation rate. The rate dependence of I_{pp} is an important quantity to establish since extrapolation of data to other rates is generally required for analyses of system performance. The rate dependence of I_{pp} was established for four of the part types by measuring I_{pp} at two rates. Table 52 includes a summary of linearity of the rate dependence of I_{pp}; the ratio of the photocurrent per unit rate at the higher and lower rates indicates the rate dependence is nearly linear for two of the part types with the 2N3960 and 2N2905A of questionable linearity. The linear dependence of I_{pp} with rate is shown in Figures 54 and 55 where the mean value of I_{pp} is plotted against dose rate for four of the part types. The bars associated with each data point are plus and minus one standard deviation for the distribution of photocurrents for the ~150 devices of each type.

The only well-known electrical technique for screening transistors against excessive photocurrents is the method of measuring electrical storage time, t_{SE}, as developed by Carr (Ref. 17). The technique was originally developed to evaluate different device types and works fairly well for this purpose when restricted (1) to silicon planar diffused and mesa npn transistors with power ratings less than 800 mW, (2) to dose rates between 10^6 and 10^8 rad(Si)/s, and (3) to transistors with electrical storage times between 10^{-8} and 10^{-5} seconds. Although t_{SE} can be used

acceptably when comparing different types of devices, it has not been demonstrated to be useful as a screening parameter for devices of a given type.

However, as discussed in the theory of primary photocurrents (Paragraph 3-b, Section V, Volume 1), the main contribution to I_{pp} originates almost entirely in the collector regions for non-Au-doped planar epitaxial devices. For these cases, the collector lifetime, τ_C, and diffusion length are the major parameters controlling I_{pp}. The electrical screening and correlation parameter then is the electrical storage time constant, τ_S, rather than t_{SE} since,

$$\tau_S \cong 1/2\ \tau_C$$

where τ_S is obtained from

$$t_{SE} = \tau_S \ln \frac{I_{B1} + I_{B2}}{I_{CS}/h_{FE} + I_{B2}} \qquad (12)$$

The results of the correlations between I_{pp} and t_{SE} and τ_S are shown in Table 53. Electrical storage time constant, τ_S, appears to offer practically no improvement as a screening parameter over electrical storage time, t_{SE}. This is partly the result of the poor quality of the "fit" of the data to Equation (12) which produced "noisy" values of τ_S and thus poor rank correlations.

These results are further verified by examining the scatter diagrams (shown in Figures 56 and 57) of I_{pp} versus t_{SE} and τ_S for one example in Table 53. It can be seen that, while a trend is obvious, these plots are truly scattered and neither of the parameters are particularly useful as a screen for I_{pp}.

The efficacy of other screens for I_{pp} were investigated. According to the theory presented in Paragraph 3-b, Section V, Volume 1, collector-base junction capacitance, C_{OB}, and possibly base transit time, t_B, should be the next best correlation parameters after τ_S. Neither of these parameters were particularly successful as I_{pp} screens. The largest

correlation coefficient for C_{OB} was +0.538 for the 2N2905 which is opposite in sign to that anticipated. At least t_B, however poorly, correlated with the I_{pp} in the proper direction.

Tables 54 and 55 briefly summarize the order of efficacy of potential screening parameters for the various device types. In general, t_{SE} or τ_S are the best screening parameter for primary photocurrent. C_{IB} as a potential screening parameter was unexpected since it was assumed that the junction areas were nearly constant for a given device type. However, C_{IB} is dependent upon the base doping concentration near the e-b junction and, thus could reflect a large gradient in base impurity doping concentration. The electric field produced by this gradient would enhance the carrier flow to the c-b junction and the subsequent photocurrent. The correlation with t_B is reduced by the presence of an internal electric field.

Since no single screening parameter appeared to be successful as a primary photocurrent screen, multiple linear regression (MLR) analyses were performed using the parameters predicted to be effective from theoretical reasons as well as those the data indicated were correlated to I_{pp}. These results (summarized in Table 56) were, in general, disappointing and while effective in reducing the prediction errors, were not sufficiently effective to implement as a screening technique.

b. Secondary Photocurrents

Secondary photocurrents, I_{sp}, were measured in a grounded base configuration. The main "turn-on" mechanism for this case is the transverse voltage generated by the IR drop of the primary photocurrent and transverse base resistance. This model (presented in Paragraph 3-b, Section V, Volume 1) predicts that the following parameters are important for screening I_{sp}:

1. I_{pp} (and parameters for which I_{pp} is dependent),
2. r_B, transverse base resistance,
3. h_{FE}, common-emitter DC current gain,
4. N_{BO}, base region impurity doping concentration, and
5. t_B, base transit time.

In general, the correlations for I_{sp} were much better than for I_{pp}. A summary of the correlation coefficient for potential I_{sp} screening parameters are shown in Table 57.

3. POWER TRANSISTORS

a. Primary Photocurrent

Primary photocurrents for power devices, though considerably larger as a result of larger device geometries, do not differ in principle from those of low-power devices. However, power devices do exhibit greater tendencies for secondary effects such as the onset of "anomalous" photocurrents due to transverse effects enhanced by their larger photocurrents and geometries.

An inspection of a histogram of I_{pp} for the RCA TA8007 in Figure 58 shows seven devices which exhibited these anomalous I_{pp}s even at rates as low as 3.0×10^7 rad(Si)/s. Two are shown on the histogram and the other five had such large I_{pp}s that they are shown as outside the range of the histogram. These devices all had low values of base doping concentration N_{BO}. The mean values of the doping level for all devices was $\sim 5.6 \times 10^{16}$ cm^{-3}, while the devices which exhibited anomalous turn-on all had values $\sim 2 \times 10^{16}$ cm^{-3}. This result is apparent in scatter diagrams of I_{pp} versus N_{BO} and r_B (Figures 59 and 60).

b. Secondary Photocurrent, I_{sp}, and Turn-on Threshold

The radiation rate threshold for I_{sp} "turn-on" varied nearly a factor of 25 for the TA8007 and nearly a factor of 4 for the BR200A. These ranges can be seen in the histograms shown on Figures 61 and 62. Based on a simple analytical description for I_{sp}, the key parameters for screening I_{sp} are: (1) h_{FE}, (2) r_B, and (3) I_{pp}.

The scatter diagrams in Figures 63 through 66 show the strong correlation between turn-on threshold and both h_{FE} and r_B. Thus, where transient photocurrents constitute the major failure threat, screens on high h_{FE} and r_B values would significantly truncate those failures which occur at the lower rates.

4. DUAL JUNCTION FIELD EFFECT TRANSISTOR

Primary photocurrent was measured at three dose rates for the dual JFET. The experimental arrangement was similar to that used for the bipolar transistors with the collector-base junction being replaced by the channel-gate junction. Source and drain were shorted together in this measurement and 30V was applied across the gate-channel junction.

Figure 67 shows the response (I_{pp}) as a function of dose rate, $\dot{\gamma}$, for the sample. In this plot the "A" and "B" halves are both shown.

We can see that the primary photocurrent is super-linear over the range of $\dot{\gamma}$ which was used. Therefore, photocurrent is following a relationship

$$I_{pp} = A\dot{\gamma}^{n} \tag{13}$$

where $n > 1$. For the mean of our sample n was found to be ~1.2.

This super-linearity is expected due to two-dimensional mechanisms and the fact that the reverse bias was relatively near the breakdown voltage of the gate-channel junction (BV_{GSS}).

a. Correlation Parameters

Parameters which are expected to correlate with I_{pp} are: the reverse recovery time of the gate-channel diode, t_{rrGS}, the storage time constant, τ_S, defined as

$$t_{rrGS} = \tau_S \ln \left(1 + \frac{I_F}{I_R}\right) \tag{14}$$

and the width of the depletion region which is inversely proportional to the depletion capacitance. It was expected that the lifetime measurements would correlate positively with I_{pp} and that the capacitance would correlate negatively with I_{pp}.

Table 58 shows a summary of rank correlation coefficients for the various parameters of interest. The parts have been divided into two groups labeled α and β; group α contains serial numbers 1-35, and

group β contains serial numbers 36-60. The reason for this grouping is that the two groups seem to come from different wafers or diffusions. Histograms of many of the electrical parameters appear as bimodal distributions with the groups appearing as two separate distributions. Hence, when a rank correlation is performed between two parameters which are each bimodally distributted, the correlation may be artifically high because of the separation of the two groups. This is shown by Figure 68 which shows a scatter diagram C_{GSS} (1V) versus I_{pp} [$\dot{\gamma} = 1.2 \times 10^8$ rad(Si)/s]. One can see from this plot and Table 58 that the rank correlation of the total (0.738) is high and that the correlation with capacitance within each group is significantly lower.

It is apparent from Table 58 that the best correlations were obtained with the parameters which are a function of lifetime. The storage time constant, τ_S, in general correlates as well or better than the reverse recovery time, and it appears that this parameter is the most likely candidate for a screening parameter for primary photocurrent. Note that there is a marked difference in the correlations between I_{pp} and τ_S observed in the two subgroups. The α subgroup data correlates much better than the β subgroup. This is, perhaps, more apparent in Figure 69 which shows a scatter diagram of the "A" chips.

b. Multiple Linear Regression Analyses

Multiple linear regression techniques were used to predict primary photocurrent using the correlation parameters discussed in the preceding section. Since the JFETs were apparently grouped into two subgroups, which implied that the parts came from either two wafers or diffusions, this allowed a measure of the predictive ability of the regression coefficients of the MLR parameters. For this to be the case, the independent variables used in the regression must be variables which physically describe the dependent variable. Were this not the case, the MLR coefficients would fit the data for which the coefficients were generated, but would not accurately fit another set of parts with slightly different physical properties.

MLR's were therefore run using t_{rrGS}, τ_S and C_{GSS} and functions of these parameters. Table 59 summarizes the results of these analyses. We can see from this table that MLR techniques do not work well for the prediction of the response of devices with electrical parameters much different than those of the devices from which the MLR coefficients were generated unless the independent variables are theoretically plausible. The first two sets of MLR's shown used independent variables related to I_{pp} but with a meaningless functional relationship. Hence, the prediction errors are large. The third run, however, used τ_S and $1/C_{GSS}$ which are expected to be related to I_{pp} and, as expected, the regression works well. As Figure 69 showed in the previous material (Paragraph 4-b) the groups (α and β) show quite different degrees of correlation with τ_S. The addition of the capacitance term, however, allowed a much better estimate of I_{pp} than obtained with τ_S alone.

c. Conclusion

As would be expected lifetime measurements give the best correlation and prediction for I_{pp} in the dual JFET. Therefore, an MLR technique or an electrical screen using t_{rrGS} or several values of t_{rrGS} to give a fitted value of τ_S should provide the best HA screen for devices of this type.

5. INTEGRATED CIRCUITS

The transient ionization response of the integrated circuits was measured with direct exposure to 10 MeV electrons from a linear accelerator. The pulse width used was sufficiently wide to assure time equilibrium, and pulse widths ranged from approximately 100 ns for the TTL devices to 3 μs for the op amp. The decision to use a wide radiation pulse was reached because of the difficulty of measuring the response of fast circuits to narrow pulses and because of the more universal applicability of hardness assurance data obtained with wide radiation pulses, i.e., if the circuit is hard to a pulse width sufficient for time equilibrium, it is generally hard for any pulse width. Extreme care was taken to assure repeatability in the transient ionization measurements. Threshold response data was in general repeatable to better than ±5% relative

accuracy. Because this type of experimentation forces continual adjustments of the radiation intensity, it is very time consuming, and to minimize the expenditure of effort data was not taken for all sections of multiple devices. Additional general information on the experimental procedures is given in Paragraph 4-c, Section IV, Volume 1.

a. TTL Circuits

(1) Failure Criteria

The TTL circuits were loaded with a resistor-diode network that simulated maximum fanout for both logic states. The loading conditions for the 1-state are particularly important when measuring the ionization response because this causes the pull-up transistor to be in the active region which minimizes the output transient. In general, the failure criterion used for either logic state for these circuits was a 100 mV transient voltage shift at the output terminal, i.e., the failure criterion was equivalent to a 100 mV reduction in the allowable noise margin. This seems low, but it is the typical fraction of the normal 400 mV noise margin which is relinquished by the system designers for transient radiation. Most of the available noise margin is usually required for normal electrical design purposes. Since these circuits fail in either state because of secondary photocurrent in internal transistors, the radiation response is strongly nonlinear with dose rate, and moderate differences in response criteria will cause only slight differences in the radiation level for transient failure. One practical difficulty which arose during the 1-state tests was the stability of the power supply voltage. The 10 μf capacitor placed close to the device to bypass the power supply leads still allowed V_{CC} to change by as much as several hundred millivolts. This in turn affected the 1-state output voltage. To solve this problem, it was necessary to place a large (4000 μf) capacitor a few feet away from the experiment, out of the radiation beam. This held the supply voltage to within 20 mV during the transient pulse.

The transient voltage shift was used as a failure criterion instead of the absolute DC output voltage because: (1) it was experimentally more convenient to measure a consistent pulse amplitude, (2) failure mechanisms involving secondary photocurrent are likely to be more

consistent from unit to unit, and (3) circuits which have DC logic levels close to the worst-case values for these parameters will fail with transient output voltages of a few hundred millivolts.

(2) Failure Mechanisms

The expected failure mechanism for the 1-state response of the TTL devices is turn-on of the output transistor. Obvious correlation parameters for secondary photocurrent are the h_{FE} and r_B of the output transistor and the value of the external base resistance. Storage time, capacitance and stored charge were expected to correlate with primary photocurrent.

The expected failure mechanism for the 0-state is turn-on of the pull-up transistor. One obvious correlation parameter is the value of the external base resistance. For all of the TI circuits except the inverter, this resistor was significantly lower than for the corresponding circuits made by Motorola (1KΩ versus 4KΩ for the standard gate). Because the secondary photocurrent of the pull-up transistor may cause transient increase in the $V_{CE(SAT)}$ of the output transistor, the dynamic resistance of the circuit in the 0-state is also important.

(3) Radiation Data

Transient radiation data for the five TTL device types were taken for approximately 140 units of each type. The sample histogram of the data in Figure 70 shows the transient threshold data for the TI inverter (1-state). The data for all of the device types is summarized in Table 60, which lists the mean, standard deviation, ratio of maximum to minimum value, and worst or most radiation sensitive value. This is simply a tabular presentation of the radiation data which allows the reader to make a comparison of the data for different device types and different test conditions. Since the data for the TI buffer has a maximum to minimum ratio of only 2, one can anticipate more difficulty in obtaining high rank correlation coefficients for this device.

The limited spread in the radiation data for most of these devices was a major limitation in investigating the effectiveness of various electrical parameters in screening the radiation response distributions. The parts had already been through a stringent selection procedure

because of the electrical specifications and processing controls which were included in the parts specifications. This is probably the reason that the AC and switching measurements were relatively ineffective. Any device with extreme AC parameters had already been eliminated. Another aspect is that the basic resolution and accuracy of these AC measurements are significantly lower than those of the DC parameters and hence, these measurements would be expected to be less effective in correlations with tightly grouped radiation data. An alternative approach would have been to deliberately allow some fraction of the devices in the test population to be out of tolerance. This would have broadened the range of the electrical parameters, and made it easier to assess correlation effectiveness. However, this approach would also raise a question about the applicability to practical groups of devices which do undergo a stringent initial electrical screen.

In the following material, it is apparent that the results are best for devices which have a wide spread in radiation parameters. The relative accuracy of the radiation dosimetry and the electrical measurements are less important for devices with wide spreads in radiation behavior. In most applications, a range of 3 to 4 in the spread of radiation behavior would be acceptable, and there would be no need to apply techniques to further truncate the distribution. The main goal of hardness assurance is to eliminate devices from one end of the distribution, and it is difficult to accomplish this goal if the sample of parts used do not have sufficient variability.

(4) TI Inverter

Some interesting results were obtained for the TI inverter 1-state response. High rank correlations were obtained for h_{FE}, as shown in Table 61. However, when h_{FE} was applied as a screening parameter, eliminating devices with highest h_{FE} values, two devices stubbornly persisted in the lower, more radiation sensitive, side of the histogram, and it was apparent that, in spite of the high correlation coefficient, h_{FE} was not working well as a single correlation parameter. The electrical parameters of the two devices were examined in more detail, and it was found that both devices had abnormal values of V_{OH}, one being very high,

the other very low - in fact, the low device was just beneath the 2.4V specification limit. The reason for the high V_{OH} reading was an open internal resistor. This same problem occurred for one of the Motorola circuits, and is further discussed in Paragraph 5-b of this Section. When V_{OH} was included as a screening parameter, the results shown in Figure 71 were obtained. These results suggest that abnormal device behavior, in spite of electrical test limits, can still affect radiation behavior, and support the concept of monitoring a wide number of device parameters to achieve hardness assurance. The significance of V_{OH} as a parameter for electrical evaluation of TTL circuits is discussed in detail in Paragraph 5-b of this Section. These results show that radiation hardness can be improved by monitoring appropriate data, adding additional tests, and imposing tighter limits for some parameters. The existing limits in the Honeywell specification were not sufficient for this purpose.

A further interesting result was obtained for the TI inverter. Returning to Figure 71, one device is conspicuously located on the leading edge of the histogram even after the h_{FE} and V_{OH} screens were applied. This device had the highest value of propagation delay time, and this value was significantly greater than that of any of the other devices. This is one of the few examples of successful application of switching parameters for the TTL ICs. Conversations with Honeywell at the beginning of this program yielded the information that both manufacturers were having difficulty meeting the switching time specifications for these parts, and this had a major effect on device yields. Certainly, as discussed in Paragraph 3-b, Section IV, Volume 1, storage time is an expected correlation parameter for primary photocurrent, and the fact that measurements affected by storage time were of limited success in this program is probably due to the stringent selection imposed by the vendors in meeting the Honeywell specifications. For more loosely processed parts, theory and the results for the TI inverter support the inclusion of switching times in any hardness assurance program.

(5) TI Buffer

The TI buffer was the only digital circuit which used primary photocurrent compensation. The LINAC test results revealed that this compensation was not completely effective. For a 100 mV transient output response, the uncompensated Motorola buffer was actually harder. However, for higher transient voltage shifts, the compensation worked reasonably well; the dependence of output voltage on dose rate was much less sharp for the TI buffer than for any of the other TTL circuits. For this reason, the responses at a fixed rate could be used to compare different units of this circuit.

The range of responses for the TI buffer was only a factor of 2, and because of the limited range and the compensation, it was difficult to find good correlation parameters for this circuit. Nevertheless, for higher output responses, a single correlation parameter, V_{CS}, was found which was reasonably successful. Figure 72 shows a histogram of the output responses, with the high and low offset voltage units eliminated from the distribution. This parameter, which is expected to correlate with lifetime, was successful in eliminating the worst units from the already narrow histogram. Considering the fact that this is a compensated circuit, the results are quite promising. The rank correlation factors of several parameters of interest are summarized in Table 62.

(6) TI A-O-I Gate

The TI A-O-I gate was selected because it contains two phase splitter transistors which are connected in parallel. The increased photocurrent in the common collector resistor of the phase splitter transistors makes these circuits more sensitive to ionizing radiation than the simple gates, which have only a single phase splitter transistor. No abnormal V_{OH} values were observed for any of the A-O-I gates.

Rank correlation coefficients for these devices are summarized in Table 63. There were no parameters with high rank correlation coefficients for this device type. However, the results of an MLR run, shown in Table 64, show a relatively low rms error of 16%, and a maximum error of only 45% when 5 parameters are used to obtain MLR coefficients.

As with all the MLR runs for the ICs, the first half of the devices were used to obtain the MLR coefficients and the radiation response of its entire population was predicted using these coefficients. The rms and maximum errors apply to the prediction of all units.

(7) Motorola Inverter

The Motorola inverter population also had two devices with abnormal V_{OH} behavior, and the radiation thresholds of these units were also abnormally low. One of these devices had extremely high leakage current, and although it passed the vendor's electrical tests, would not have passed an additional 100% test by the user because the I_{OL} measurement was "out of spec". However, even though the other device met all specifications, curve tracer tests revealed that the cause of the high V_{OH} value for this unit was that R_3, the resistor from the base of the output transistor, was open! This greatly increased the sensitivity of the device to transient radiation. A more detailed discussion of the cause and significance of abnormal V_{OH} values, along with suggestions for eliminating this problem with additional electrical tests, is included in Paragraph 5-b of this Section.

Rank correlation coefficients between several electrical parameters of the Motorola inverter and the ionization threshold are listed in Table 65. Once the two abnormal devices were identified, the range of the ionization response data was reduced an order of magnitude. The results of two MLR computer runs are shown in Table 66. The first run includes all devices; the second run was generated with the two abnormal devices removed. The first MLR run had an rms error in excess of 100%, and the maximum error is even higher. However, when the two devices were removed, large reductions in the rms and maximum errors were obtained. This example illustrates the significant effect of a small number of abnormal devices or bad data points on the results of an MLR calculation. High quality data must be used in order to obtain reasonable results with multiple linear regression.

(8) Motorola Buffer

Results for the Motorola buffer were better for the 0-state than the 1-state. Unfortunately, the 1-state is the more sensitive of the two states. Rank correlation coefficients of various electrical parameters vs. ionization response are shown in Table 67. However, an examination of the 1-state data, presented in Figure 73, shows that the data is already well truncated on the lower, more radiation sensitive side. Except for one device, the minimum values are only a factor of 2 below the mean value of the distribution. With this type of histogram, low rank correlations are expected because of the large peak on the low side. Slight errors or "noise" in either the radiation or electrical data will cause large rank differences in such a skewed distribution. When this is considered, the results for the Motorola buffer are not unreasonable. Regression techniques were also applied for the Motorola buffer, and these results are presented in Table 68. Again, the 0-state results are better than the results for the 1-state, but the wider range of the 1-state data at the high end would be expected to affect the MLR results for this case.

b. The Effect of Resistor Reliability on Radiation Response

(1) Open Resistor Problem

One extremely soft device was found in each group of inverters from the two manufacturers. The only significant difference in the electrical behavior of these two devices was a slightly higher value of V_{OH}. Additional measurements, which were made on these devices with a curve tracer, proved conclusively that the high V_{OH} readings were caused by an open R_3 resistor from the base of the output transistor to ground (see Figure 74). This also explains the extreme sensitivity of these particular devices to ionizing radiation.

After identifying this problem, it is disquieting to realize that these parts still meet all electrical specifications, in spite of the open resistor. Similar devices could easily be installed in "radiation-hard" systems, and would lower the transient failure level of such systems by more than one order of magnitude. In the following section, we will

discuss the means of detecting this problem and implementing tighter electrical specifications to screen this fault at the vendor or at an incoming inspection level.

(2) Method of Detecting Open Base-Emitter Resistors

The V_{OH} readings for the two faulty devices were approximately 300 mV higher than the average value of 2.7V which occurs when $V_{CC} = 4.5V$ and $V_{IN} = 0.8V$ for the inverters. There are several factors which can cause V_{OH} to be high, but the distribution of V_{OH} readings for normal devices is tightly grouped around 2.7V with a total spread of less than 100 mV. High V_{OH} readings can be caused by the following conditions: (1) high leakage in the output transistor, (2) an open R_4, (3) an open R_3, or (4) a short between base and emitter of Q_3 or Q_4 (see Figure 74 for a circuit schematic). Condition (3), R_3 open, can be verifield by examining the V-I characteristics of the 1-state output as the input voltage is changed from 0.4 to 1.2 volts. In normal devices, the output voltage will change approximately 300 mV as the input voltage is changed from 0.4 to 0.8V. This is caused by the phase splitter transistor turning on, because of the inverted saturation of Q_1. In order for the phase splitter to turn on with 0.8V applied to the input, R_3 must be present. If R_3 is open, the phase splitter and the output transistor will turn on simultaneously at input voltages above 1V but there will be no change in 1-state output voltage until the input level exceeds 1V. The output V-I characteristics of a normal device and a device with R_3 open are shown in Figure 74.

Another resistor which could be open, and still allow the circuit to pass electrical specifications is R_4. This would greatly increase the sensitivity of the circuit in the 0-state, because Q_4 effectively has an open base if R_4 is open. This particular problem was not observed on any of the devices in this program, but is nevertheless an important consideration given the incidence of open R_3 resistors encountered in these devices. The other resistors (R_1, R_2 and R_5) are all necessary for proper circuit operation, and the circuit would not pass electrical or functional tests unless these resistors are connected properly within the circuit.

(3) Electrical Screening Methods

One screening method for the presence of R_3 is simply to put a maximum as well as a minimum value on V_{OH}. The maximum value could be assigned as 2.85V with V_{CC} = 4.5V and V_{IN} = 0.8V, which would eliminate this particular problem for devices with the pull-down resistor connected to ground. The limit would have to be adjusted upwards for devices which use a pull-down resistor across the base-emitter junction of Q_4, which is typical of all the TI devices except the inverter. For circuits with different resistor values, such as the buffers, slightly different values of V_{OH} may be required.

For complex MSI circuits, it may be impossible to verify proper resistor connections for points buried within the circuit from measurements with the external leads. There are two approaches to this problem. One is to improve resistor reliability so that resistor contact failures will have a very low probability of occurring. Based on our results, the present technology has not solved this problem. An alternative approach is to measure critical internal V_{OH} values with extra pads during the wafer probing, or the resistor could be measured directly. This approach assumes that the resistor reliability problem is not affected by the die bond, packaging and burn-in. This is probably a poor assumption, because of the high temperatures which occur during the die bonding and electrical stress caused by burn-in procedures.

(4) Conclusions and Recommendations

We have discovered circuits with open internal resistors which are much more sensitive to ionizing radiation than normal circuits. Users of hardened circuits should be aware that this problem does not occur with sufficient regularity to be discovered with the typical sample testing that is done to evaluate hardened parts, but does occur often enough to seriously effect system hardness. Techniques for screening such devices with tighter V_{OH} measurement limits have been suggested, and it is recommended that these methods be applied to eliminate these bad devices. Additional effort should also be made to solve the problem at the manufacturing level.

c. Other Integrated Circuits

This section presents the ionization results of the TI word switch, Motorola sense amplifier and Fairchild μA744 operational amplifier. The ionization test results are summarized in Table 69, which shows the mean value and range of the ionization response data for each of these devices.

(1) TI Word Switch

The primary photocurrent and the radiation threshold for a secondary photocurrent of 200 mA were used as radiation response criteria for the word switch. The ionization response data were very tightly grouped, with a ratio of maximum to minimum value of about 1.5 for both the I_{pp}s and the response thresholds. Considering the estimated relative inaccuracy of the dosimetry, which could be as high as 5%, correlation factors would be expected to be somewhat worse for the word switch than for devices with higher spreads in radiation data. A table of rank correlation coefficients for I_{pp} and the I_{sp} threshold is shown in Table 70.

Although the distributions of I_{pp} and I_{sp} were narrow, the increased flexibility of measurements with the word switch resulted in good screening parameters for I_{sp}. Figure 75 shows a histogram of the initial data, and also shows the improvement after using h_{FE} and the external base-emitter resistance value as screening parameters. Storage time also worked as a screening parameter for this circuit. Since the initial histogram was already very tight, with a steep lower side, it is encouraging that the application of these relatively simple parameters (see Paragraph 3-b, Section V, Volume 1 for a theoretical discussion) further narrows the distribution.

A multiple linear regression run was also made to see how well the word switch turn-on threshold could be predicted. The results, shown in Table 71, have an rms prediction error of 3.9% with a maximum prediction error of 11.5%. These were the best MLR results obtained for any of the integrated circuits, and the success of the results for the word switch is probably due to the increased flexibility of measurements which are possible when the output transistor is accessible.

(2) Motorola Sense Amplifier

Radiation testing of the Motorola sense amplifier was complicated by the wide variations in offset voltage between units, which was further aggravated by the fact that the offset voltage specification was relaxed in order to obtain the devices on a reasonable schedule. The first stage of a plated-wire sense amp always operates in a linear, non-saturating mode, and the offset voltage problem was resolved by operating the devices at a fixed output voltage of 1.5 volts. This is the center of the operating characteristics of the typical logic gate which would be driven by the sense amp. The radiation failure criterion was that a 3 mV differential input signal from the pulse generator would no longer drive the output beyond the TTL noise margin limits of 0.4 or 2.4 volts during the radiation pulse. The 1.5 volt operating level was achieved by using an operational amplifier to provide the necessary input biasing voltage. The op amp was located in the data room in order to eliminate its radiation response, and a large frequency compensation capacitor was used to prevent the op amp from responding to the radiation transient. A diagram of this experimental arrangement is shown in Figure 76.

The sense amplifier is a complex circuit, and based on the range of offset voltages encountered for the 4-input channels, the internal transistors were not as well matched as the transistors in modern junction-isolated circuits. The internal mismatches in V_{BE} are important in establishing bias currents in the various stages, and the mismatches in V_{BE} make it unlikely that external measurements will correlate with transient radiation behavior. The types of measurements which can be made are also severely restricted by the limited number of pins and fixed resistor values. An examination of the LINAC data showed that, although there was often a correlation between the data for different channels on the same device, there were also cases where large differences occurred between the channels on the same device. Rank correlations of several electrical parameters with the ionization response of the sense amplifiers are shown in Table 72. All of these correlation coefficients are very low, and are an indication of the difficulty of establishing good correlation parameters for this device. The MLR approach was also unsuccessful, as can be seen from the results listed in Table 73.

(3) Fairchild Operational Amplifier - μA744

As mentioned previously in (Paragraph 2-b, Section IV, Volume 1), the Fairchild μA744 is a radiation hardened, dielectrically isolated operational amplifier which is not gold doped. Therefore, this device exhibits long radiation storage time once saturation occurs, and also is more sensitive to ionizing radiation than some of the newer hardened op amps which are gold doped. Three different ionization response measurements were made on this circuit, (1) the output voltage response at 4.3×10^6 rad(Si)/s, (2) the radiation level required to just saturate the circuit, and (3) the radiation recovery (storage) time at 9×10^8 rad(Si)/s. For these tests, the circuit was connected as an inverting voltage amplifier with a gain of 10. Power supply voltages were ±12 volts.

The rank correlations of several electrical parameters with the radiation responses are summarized in Table 74. As expected, the electrical saturation recovery time was one of the best correlation parameters (see Paragraph 3-b, Section V, Volume 1). However, because of the complex behavior of this device, no single parameter worked very well in screening the more sensitive devices. For the high transient response at the edge of this saturation threshold, the electrical saturation recovery was a good correlation parameter. A multiple linear regression run was made to compare this approach with the single parameter approach. These results are listed in Table 75, and are not particularly good. The five units with the highest low-level response were not screened by either the single parameter screen or the MLR approach.

These results indicate that complex linear circuits will be difficult to handle when measurements are restricted to those possible with external leads. It would be interesting to examine the feasibility of breakout transistor measurements as screening parameters for the ionization response of linear circuits. This would certainly increase the flexibility of measurements, although both pnp and npn transistor types would have to be made available.

d. Summary and Conclusions

The most significant result of the ionization response study on ICs was the discovery that open internal resistors occurred for devices from two manufacturers, which increased the radiation sensitivity of these devices by approximately one order of magnitude. Electrical screening procedures were developed which will screen such devices with tighter limits on one electrical parameter for TTL small scale integrated (SSI) circuits.

The normal ionizing rate response data of most of the devices were tightly grouped. Because of this narrow range of data, the uncertainty in dosimetry and the small errors in electrical measurements tended to obscure fundamental correlations. The electrical measurement problem was further complicated by the fact that the ICs were procured to a rigid set of specifications which screened out devices with extreme electrical behavior and narrowed the distribution of electrical parameters. This magnified the effect of the errors and resolution limits in the electrical measurements.

In spite of the narrow distributions, correlation and screening parameters were found which further truncated the already narrow distribution. In general, the results were best for circuits which allowed a reasonable inference of internal transistor parameters from external measurements. For very complex circuits, with limited access to internal transistor parameters, such as the sense amp and op amp, results were considerably worse.

6. MTBF RESULTS FOR PARTS SUBJECTED TO IONIZING RATE TESTS

Although the general applicability of a gamma-rate screen was not a part of this program, it was felt that MTBF testing of parts subjected to high dose rate environments would yield results of immediate applicability to some military systems. To this end a group of inverters and buffers were submitted to life testing after exposure to the ionizing rate tests. Neither catastrophic nor drift failures were observed in the exposed group of 49 inverters although the control group (99 parts) showed three failures, 2 catastrophic and 1 drift. For the buffers, 2 drift and 1 catastrophic failure were observed out of the exposed group of

48, although the control group of 94 parts showed no failures of either kind. Converting the catastrophic failure numbers to failure rates at a 60% confidence level results in Table 76.

2N696 151 0.0 F40 25C 7-28-72 BRL-109 07 MAY 73

NO.	PER CENT	TEST IPP	5.30 E8
0	0.0	4.26E-02	.
0	0.0	4.49E-02	.
0	0.0	4.72E-02	.
0	0.0	4.96E-02	.
0	0.0	5.19E-02	.
0	0.0	5.42E-02	.
0	0.0	[illegible]	.
0	0.0	5.89E-02	.
0	0.0	6.12E-02	.
1	0.6	6.35E-02	.090
4	2.5	6.58E-02	.039041065115
1	0.6	6.82E-02	.088
9	5.7	7.05E-02	.080033050054057063081104140
5	3.2	7.29E-02	.032040079082113
8	5.1	7.52E-02	.056060094099101103111124
8	5.1	7.75E-02	.044045055061062086151157
18	11.4	7.99E-02	.014025029042047049058059069076098105107108116120122129
14	8.9	8.22E-02	.006012034037-48071073074084093106138148152
14	8.9	8.45E-02	.024035046053067072091092095100114118119123
11	7.0	8.68E-02	.027031051064075078080083089102133
15	9.5	8.92E-02	.033043070097112121126130131132141143146154156
6	3.8	9.15E-02	.007019052096109153
12	7.6	9.38E-02	.008017013028036060077110117135147149
6	3.8	9.62E-02	.083087137139144158
7	4.4	9.85E-02	.006009013026128135145
1	0.6	1.01E-01	.086
8	5.1	1.03E-01	.020023125127134142150155
3	1.9	1.05E-01	.604015022
1	0.6	1.08E-01	.016
1	0.6	1.10E-01	.021
0	0.0	1.12E-01	.
1	0.6	1.15E-01	.000
1	0.6	1.17E-01	.011
1	0.6	1.19E-01	.010
0	0.0	1.22E-01	.
0	0.0	1.24E-01	.
0	0.0	1.26E-01	.
0	0.0	1.29E-01	.
0	0.0	1.31E-01	.

MEDIAN	MEAN	STD. DEV.	COVAR.(%)
8.430E-02	8.068E-02	1.084E-02	12.59

156 0 5 10 15 20 25 30

Figure 49. Histogram of Primary Photocurrents at 5.3 x 10^8 rad(Si)/s for 2N696

2N2222	151	0.0	F40 25C 7-21-72 BRL-108 07 MAY 73
NO.	PER CENT	TEST IPP	1.35E10 MEDIAN 2.270E-01 MEAN 2.201E-01 STD. DEV. 3.494E-02 COVAR.(%) 15.88
0	0.0	8.75E-02	.
0	0.0	9.45E-02	.
0	0.0	1.01E-01	.
0	0.0	1.08E-01	.
0	0.0	1.15E-01	.
0	0.0	1.22E-01	.
0	0.0	1.29E-01	.
0	0.0	1.35E-01	.
4	2.5	1.43E-01	.008009010026
4	2.5	1.50E-01	.005071094132
2	1.3	1.57E-01	.017091
3	1.9	1.64E-01	.036043112
2	1.3	1.71E-01	.024147
8	5.1	1.78E-01	.003015082087069073149150
8	5.1	1.85E-01	.014020035045054055064099
7	4.5	1.92E-01	.007012016021038046070
7	4.5	1.99E-01	.006022028044047075130
11	7.0	2.06E-01	.018023025031040053061065101123157
9	5.7	2.13E-01	.004019029030034059074079143
7	4.5	2.20E-01	.027033050056072103120
10	6.4	2.27E-01	.039052062067068077087089115144
13	8.3	2.34E-01	.049051057066084092100104105111119136159
3	5.1	2.41E-01	.011048050093114125131155
13	6.3	2.48E-01	.063076078083085090097098102108116134148
9	5.7	2.65E-01	.095106109118124127141142153
14	8.9	2.62E-01	.058068096107110126128129133137138145146152
9	5.7	2.69E-01	.086113117135139140151154156
0	0.0	2.76E-01	.
0	0.0	2.83E-01	.
1	0.6	2.90E-01	.158
0	0.0	2.97E-01	.
0	0.0	3.04E-01	.
0	0.0	3.11E-01	.
0	0.0	3.18E-01	.
0	0.0	3.25E-01	.
0	0.0	3.32E-01	.
0	0.0	3.39E-01	.
0	0.0	3.48E-01	.
0	0.0	3.53E-01	.
149			0 5 10 15 20 25 30

Figure 50. Histogram of Primary Photocurrents at 1.35 x 10^{10} rad(Si)/s for 2N2222

```
2N2905            151 0.0       F40 25C        7-30-72    BRL-110                                         07 MAY 73
NO.        PER         TEST                                             MEDIAN       MEAN         STD. DEV.          COVAR.(%)
           CENT        IPP         6.00 E9                              9.250E-02    9.023E-02    1.658E-02          18.38

 0         0.0         2.37E-02    .
 0         0.0         2.74E-02    .
 0         0.0         3.11E-02    .
 0         0.0         3.47E-02    .
 0         0.0         3.84E-02    .
 0         0.0         4.21E-02    .
 0         0.0         4.58E-02    .
 0         0.0         4.95E-02    .
 0         0.0         5.32E-02    .
 0         0.0         5.69E-02    .
 6         3.8         6.06E-02    .107111113114115133
 4         2.5         6.43E-02    .117123140142
 6         3.3         6.80E-02    .108110119125129134
15         9.4         7.17E-02    .095116126127128130136139141144146149151153157
13         8.1         7.54E-02    .016033037084087132137145150152154155159
 5         3.1         7.91E-02    .069109112124131
10         6.3         8.28E-02    .029032057080066091104118148156
 7         4.4         8.85E-02    .005008088093098143158
12         7.5         9.02E-02    .007012011014046054064068085089094106
15         9.4         9.39E-02    .010027038056058069086088092096097100120138
11         6.9         9.76E-02    .004017024025031032035044063103105
14         8.8         1.01E-01    .006019023034040045046052059062099101102135
10         6.3         1.05E-01    .016018050061070071075078080090
 8         5.0         1.09E-01    .005020021047049051072078
 3         1.9         1.12E-01    .022026074
 2         1.3         1.16E-01    .023077
 5         3.1         1.20E-01    .011036043055147
 2         1.3         1.24E-01    .067079
 1         0.6         1.27E-01    .065
 1         0.6         1.31E-01    .058
 1         0.6         1.35E-01    .000
 0         0.0         1.38E-01    .
 0         0.0         1.42E-01    .
 0         0.0         1.46E-01    .
 0         0.0         1.49E-01    .
 0         0.0         1.53E-01    .
 0         0.0         1.57E-01    .
 0         0.0         1.61E-01    .
 0         0.0         1.64E-01    .
------------------------------------------------------------------------------------------------------------------------
151                                0         5         10        15        20        25        30
```

Figure 51. Histogram of Primary Photocurrents at 6.0 x 10^9 rad(Si)/s for 2N2905A

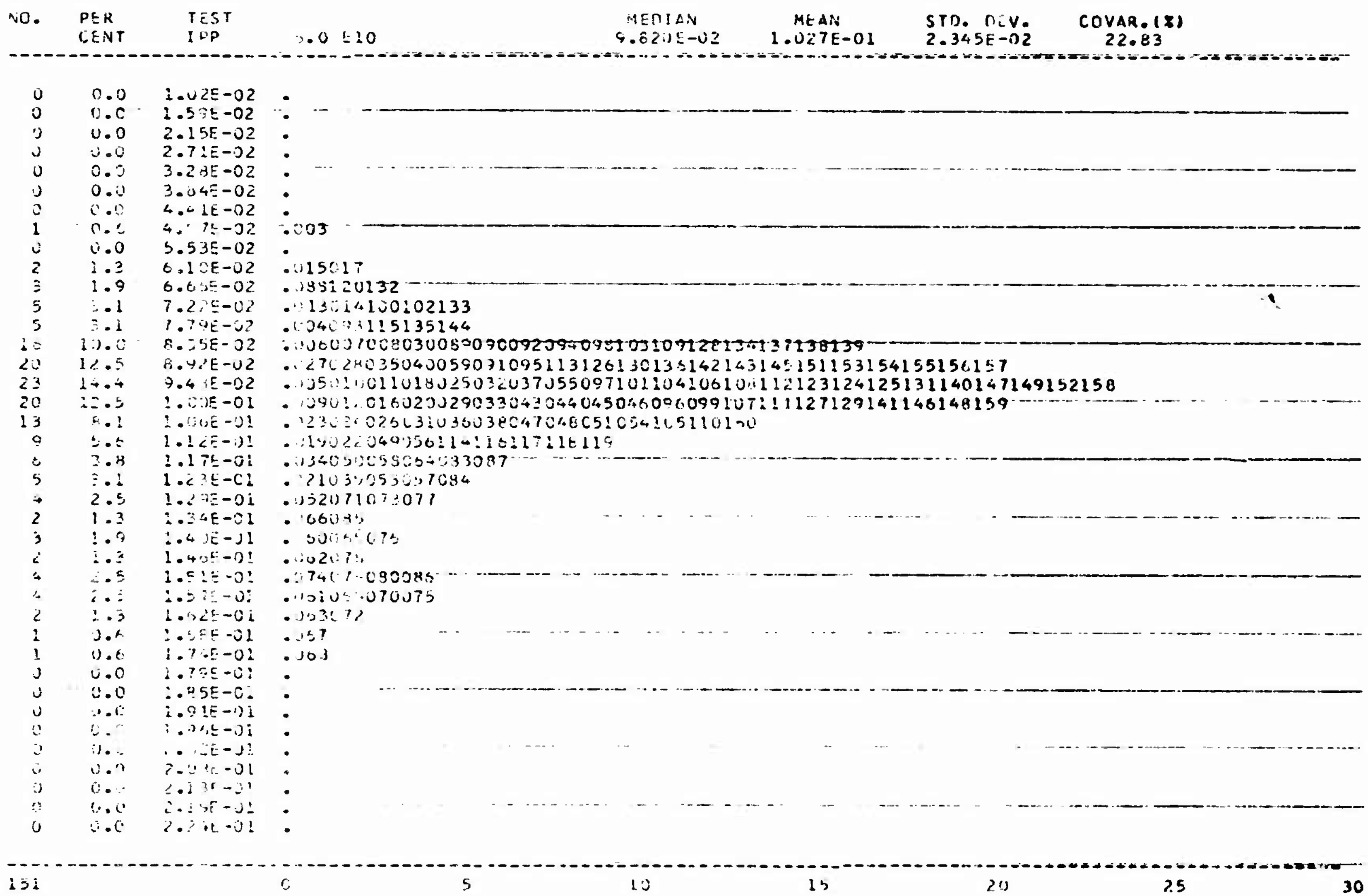

Figure 52. Histogram of Primary Photocurrents at 6.0 x 10^{10} rad(Si)/s for 2N3960

Figure 53. Histogram of Primary Photocurrents at 8.0 x 10^{10} rad(Si)/s for 2N709

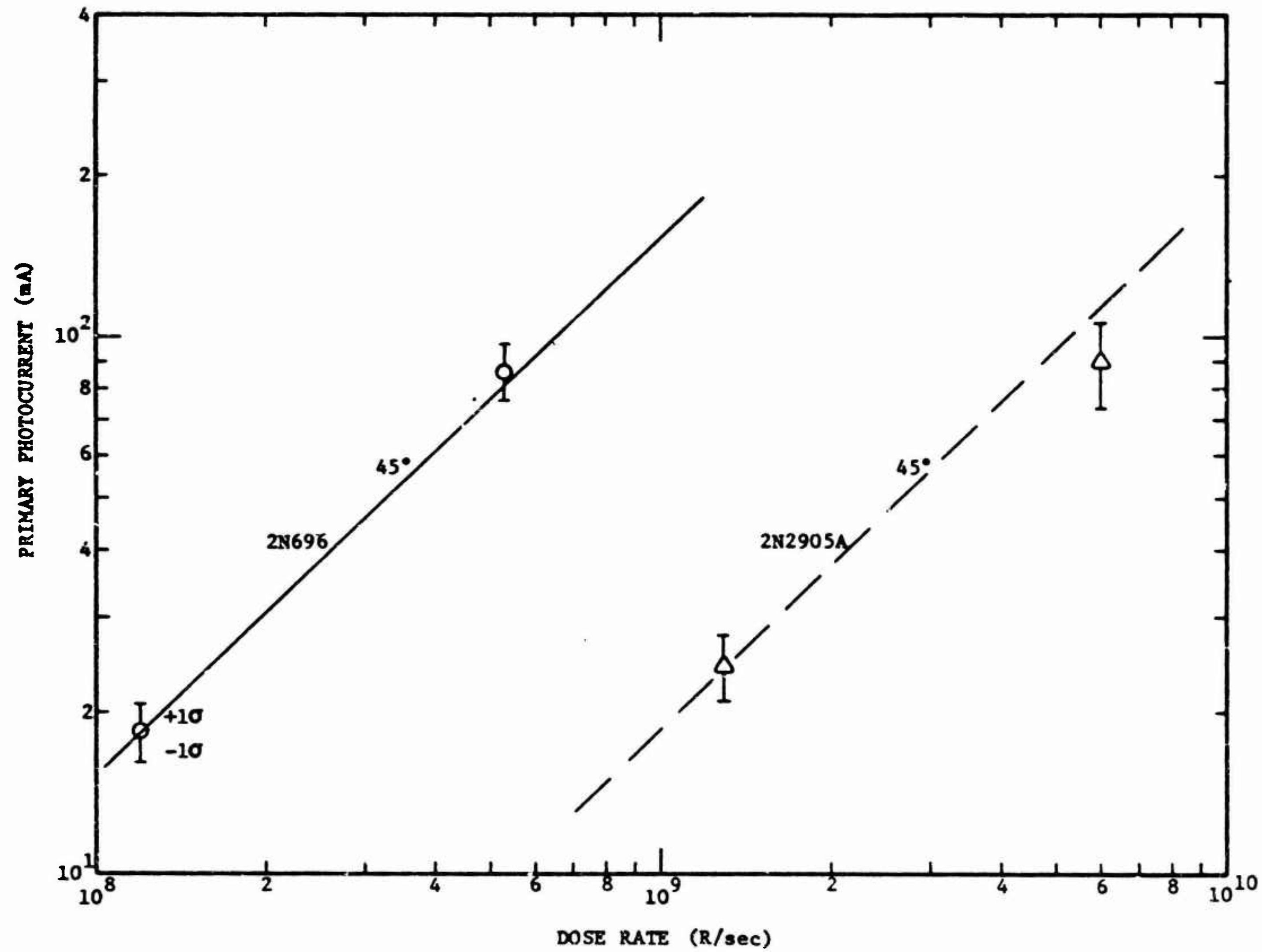

Figure 54. Dose Rate Dependence of Mean Primary Photocurrent for 2N696 and 2N2905A

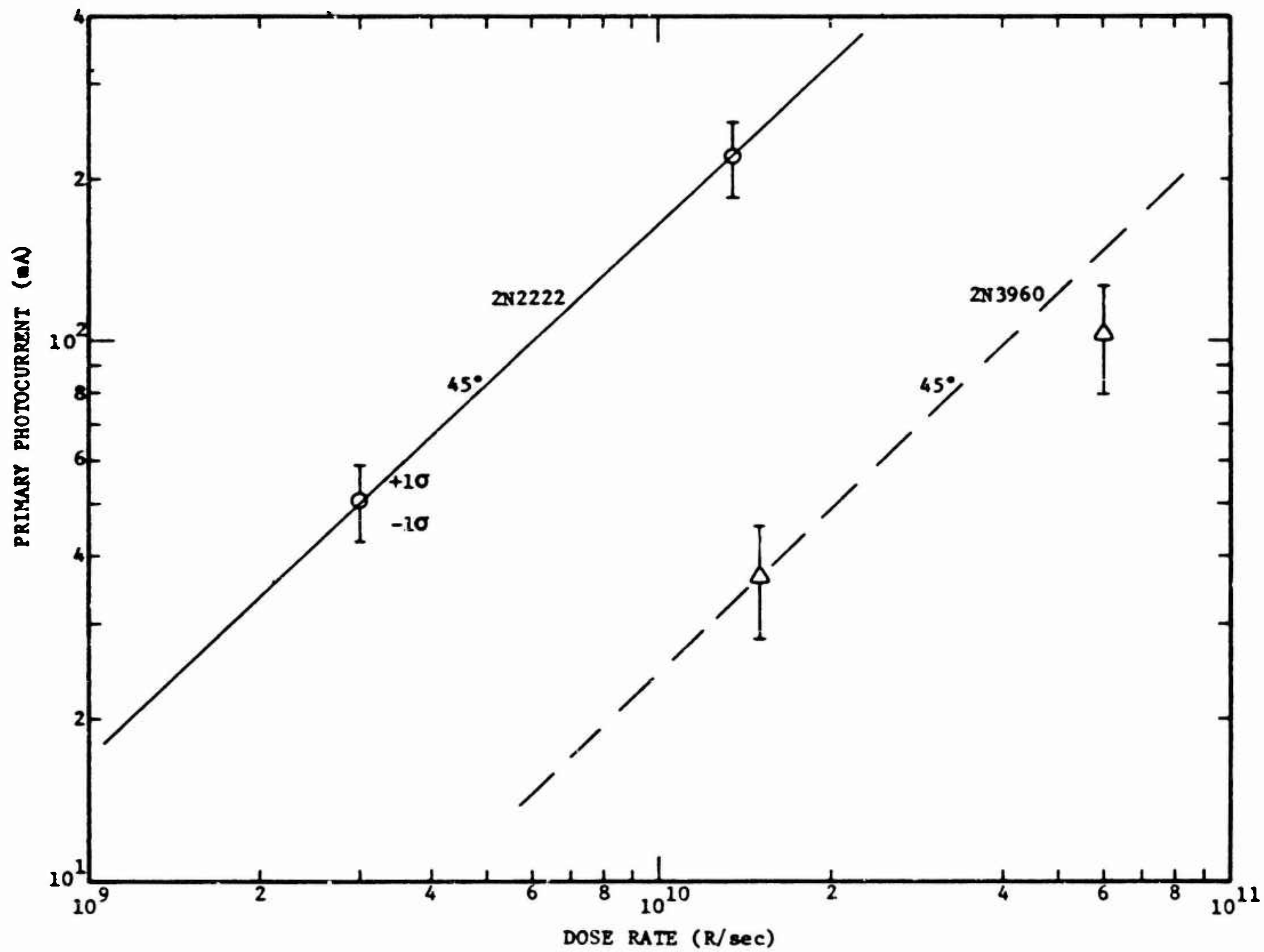

Figure 55. Dose Rate Dependence of Mean Primary Photocurrent for 2N2222 and 2N3960

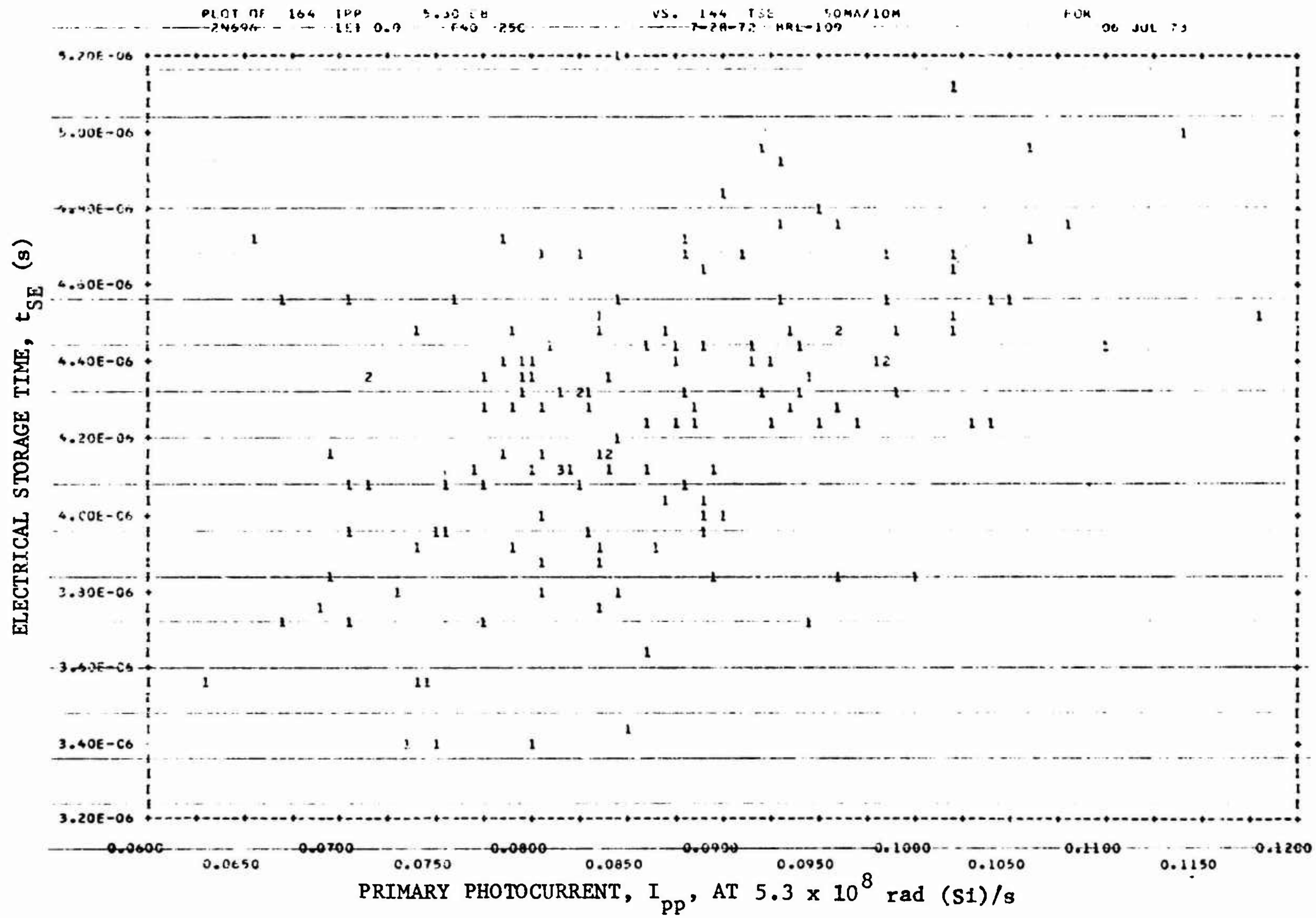

Figure 56. Scatter Diagram of I_{pp} [5.3×10^8 rad(Si)/s] versus t_{SE} (50 mA/10mA) for 2N696

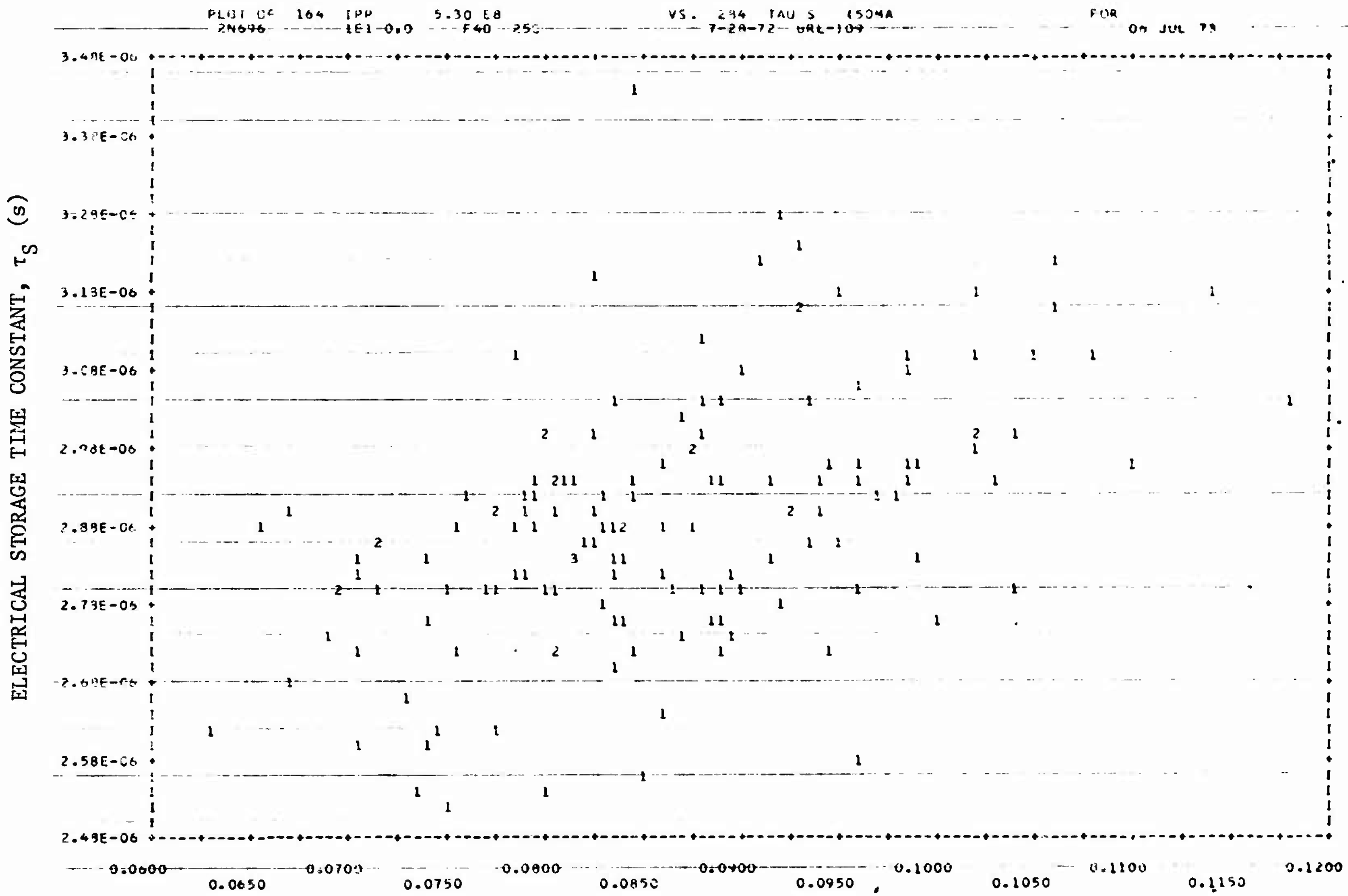

PRIMARY PHOTOCURRENT, I_{pp} (A), at 5.3×10^8 rad(Si)/s

Figure 57. Scatter Diagram of I_{pp} [5.3×10^8 rad(Si)/s] versus τ_S for 2N696

```
RCA 7A        1F1 0.0 F50/F40   29C       F500/F40C0  3-20/4-11-72   DPCC02                          06 JUL 73
--------------------------------------------------------------------------------------------------------------
NO.    PER      TEST                                      MEDIAN         MEAN        STD. DEV.     COVAR.(4)
       CENT     IPP       3.0 E7                          8.450E-02      8.499E-02   1.463E-02      17.21
--------------------------------------------------------------------------------------------------------------

  0     0.0   -2.79E-02  .
  0     0.0   -1.98E-02  .
  0     0.0   -1.17E-02  .
  0     0.0   -3.60E-03  .
  0     0.0    4.52E-03  .
  0     0.0    1.26E-02  .
  0     0.0    2.08E-02  .
  0     0.0    2.89E-02  .
  0     0.0    3.70E-02  .
  0     0.0    4.51E-02  .
  0     0.0    5.32E-02  .
  0     0.0    6.13E-02  .
 15    10.0    6.94E-02  .006009013015021033034037057067071082085093098
 45    30.0    7.76E-02  .007008012014017018019020022026028029044053055056058063065068070075079084088089091092097100
 40    26.7    8.57E-02  .010011016025027030032036041042043047048050051052054061062064066072073074076087089095099103
 28    18.7    9.38E-02  .023024031035038040045046049059069075080081083086109123124127130133134135136139144145
  0     0.0    1.02E-01  .
  4     2.7    1.10E-01  .108110111112
  1     0.7    1.18E-01  .106
  0     0.0    1.26E-01  .
  0     0.0    1.34E-01  .
  0     0.0    1.42E-01  .
  0     0.0    1.51E-01  .
  0     0.0    1.59E-01  .
  0     0.0    1.67E-01  .
  1     0.7    1.75E-01  .039
  1     0.7    1.83E-01  .094
  0     0.0    1.91E-01  .
  0     0.0    1.99E-01  .
  0     0.0    2.07E-01  .
  0     0.0    2.16E-01  .
  0     0.0    2.24E-01  .
  0     0.0    2.32E-01  .
  0     0.0    2.40E-01  .
  0     0.0    2.48E-01  .
  0     0.0    2.56E-01  .
  0     0.0    2.64E-01  .
  0     0.0    2.72E-01  .
  0     0.0    2.80E-01  .

--------------------------------------------------------------------------------------------------------------
135                       0          5          10          15          20          25          30

THE FOLLOWING DEVICE(S) ARE OUTSIDE THE RANGE OF THE HISTOGRAM

00010001  1.000E 30   00010002  1.000E 30   00010003  1.000E 30   00010004  1.000E 30   00010005  1.000E 30
00000060  1.220E 00   00000077  8.900E-01   00000096  1.570E 00   00000101  1.520E 00   00000105  3.260E-01
00010146  1.000E 30   00010147  1.000E 30   00010148  1.000E 30   00010149  1.000E 30   00010150  1.000E 30
```

Figure 58. Histogram of I_{PP} at 3.C x 10^7 rad(Si)/s for TA8007 Showing Devices with "Anomalous" Photocurrents

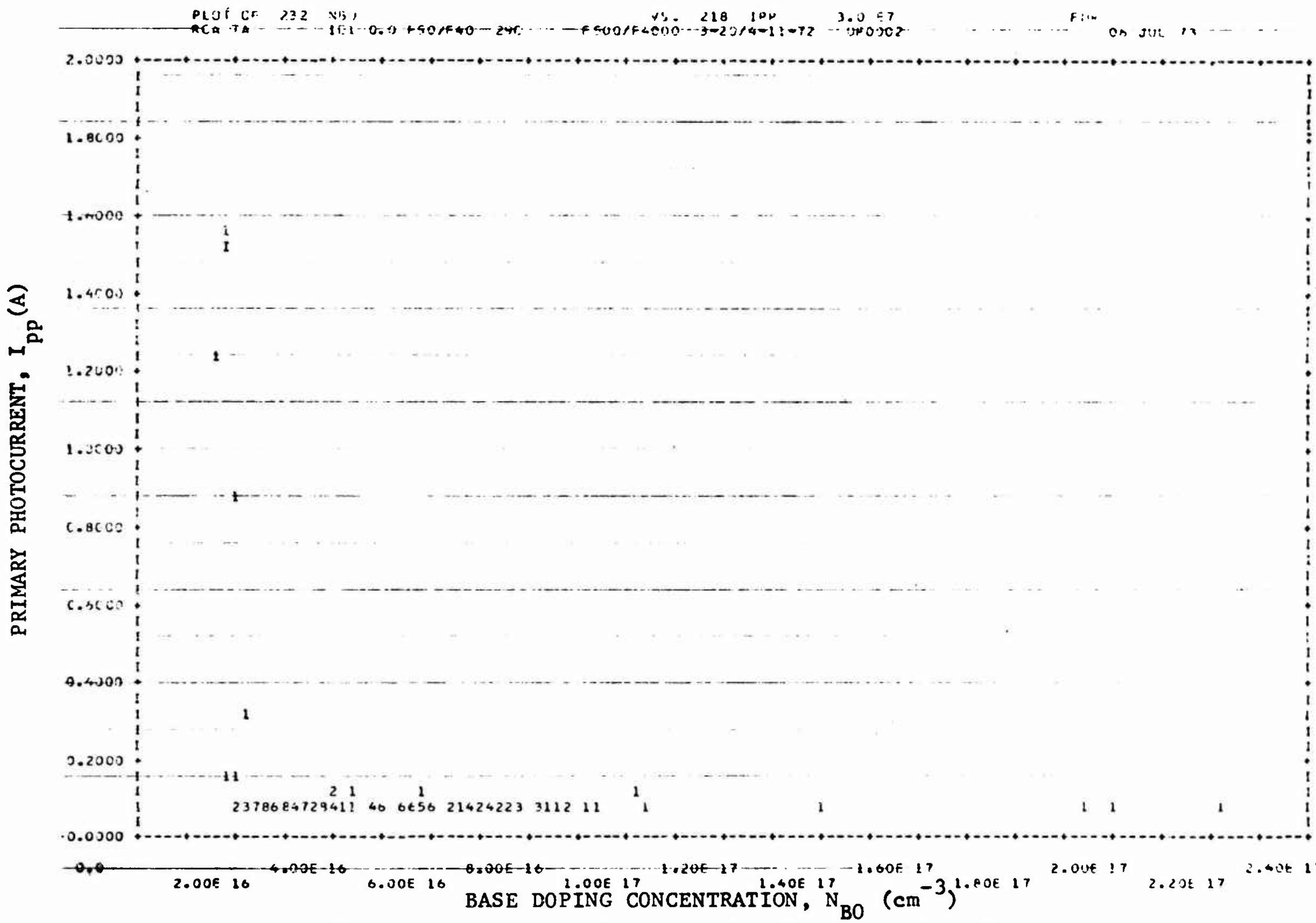

Figure 59. Scatter Diagram of Base Doping Concentration, N_{BO}, versus Primary Photocurrent, I_{pp}, at 3.0×10^7 Rad(Si)/s for TA8007

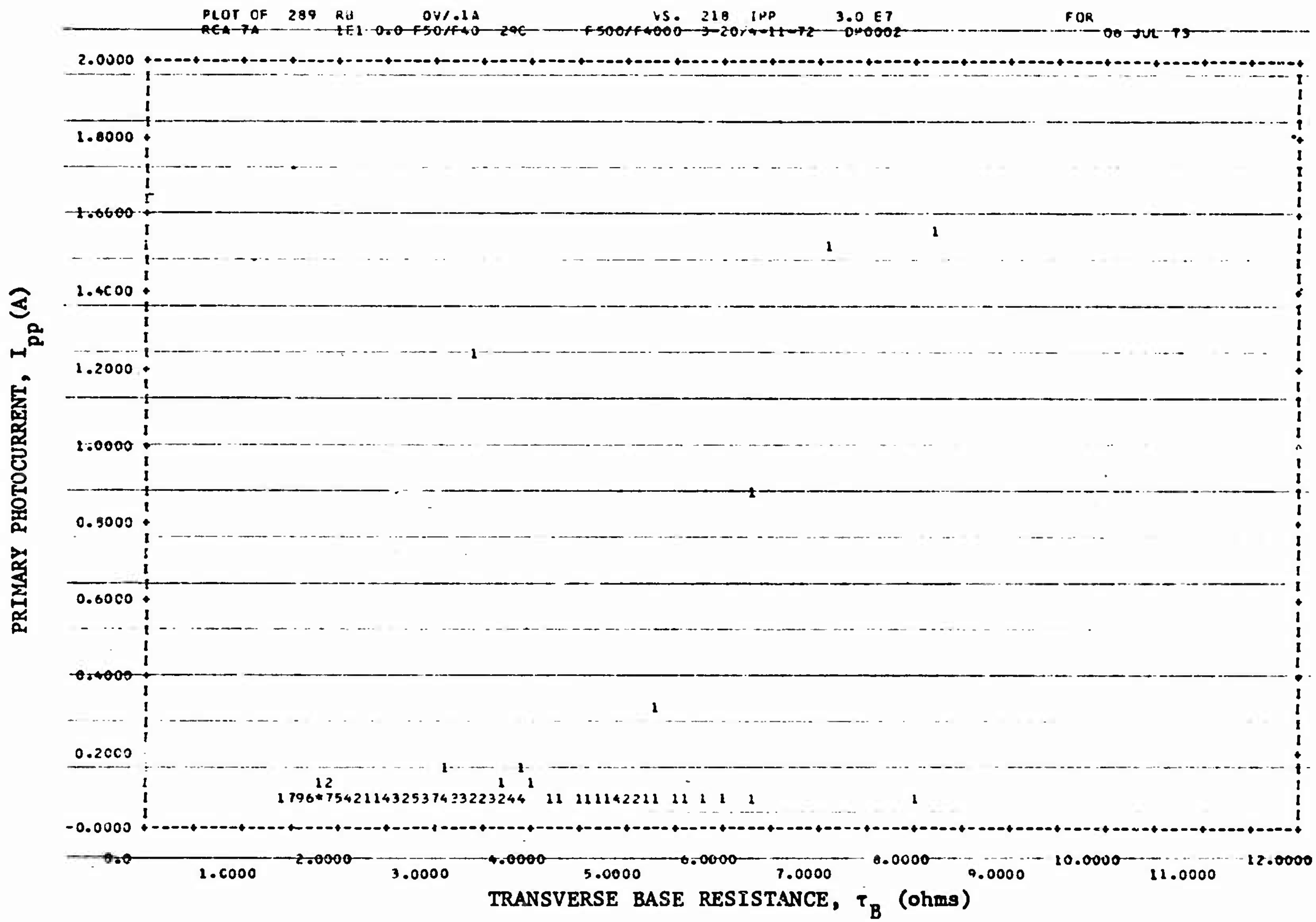

Figure 60. Scatter Diagram of r_B versus I_{pp} at 3.0×10^7 rad(Si)/s for TA8007

NO.	PER CENT	TEST THI	ISP=2A
0	0.0	-1.21E 08	.
0	0.0	-1.10E 08	.
0	0.0	-9.77E 07	.
0	0.0	-8.59E 07	.
0	0.0	-7.40E 07	.
0	0.0	-6.22E 07	.
0	0.0	-5.03E 07	.
0	0.0	-3.84E 07	.
0	0.0	-2.66E 07	.
0	0.0	-1.47E 07	.
0	0.0	-2.83E 06	.
2	1.3	9.01E 06	.076101
14	9.3	2.08E 07	.016039054059060072073077081083094095105127
23	15.3	3.27E 07	.009013020024030031035040043044045046051055069074076080099100110111112
19	12.7	4.45E 07	.009011049062070075097118119123124130134125136139141144145
10	6.7	5.65E 07	.007019028050088090109131138143
11	7.3	6.83E 07	.023029041078082086103106126137140
3	2.0	8.02E 07	.064102142
3	2.0	9.20E 07	.022047048
12	8.0	1.04E 08	.010037052061066089092115115120122132
12	8.0	1.16E 08	.012014015036038053079054087091104109
6	4.0	1.28E 08	.027034063114117128
6	4.0	1.39E 08	.025033042067098121
7	4.7	1.51E 08	.063071085107116125133
2	1.3	1.63E 08	.065035
5	3.3	1.75E 08	.026032056058129
0	0.0	1.87E 08	.
2	1.3	1.99E 08	.013017
1	0.7	2.11E 08	.021
1	0.7	2.23E 08	.057
1	0.7	2.34E 08	.006
0	0.0	2.46E 08	.
0	0.0	2.58E 08	.
0	0.0	2.70E 08	.
0	0.0	2.82E 08	.
0	0.0	2.94E 08	.
0	0.0	3.06E 08	.
0	0.0	3.17E 08	.
0	0.0	3.29E 08	.
140			

MEDIAN	MEAN	STD. DEV.	COVAR.(%)
6.820E 07	8.135E 07	5.226E 07	64.24

0 5 10 15 20 25 30

Figure 61. Histogram of Threshold Rate for Turn-On (I_{sp} = 2A) for RCA TA8007 in Shorted-base Configuration

NO.	PER CENT	TEST THI	ISP=1A
0	0.0	-2.13E 07	.
0	0.0	-1.70E 07	.
0	0.0	-1.27E 07	.
0	0.0	-8.37E 06	.
0	0.0	-4.05E 06	.
0	0.0	2.77E 05	.
0	0.0	4.60E 06	.
0	0.0	8.92E 06	.
0	0.0	1.32E 07	.
0	0.0	1.76E 07	.
0	0.0	2.19E 07	.
5	3.3	2.62E 07	.009011014016036
9	6.0	3.05E 07	.006008010012013015049058088
21	14.0	3.48E 07	.018022024026028033034038039040042044048050053056070075081090091
12	8.0	3.92E 07	.019021023025029041043047059060062079
3	2.0	4.35E 07	.035076083
2	1.3	4.78E 07	.064099
2	1.3	5.22E 07	.077113
8	5.3	5.65E 07	.057072089094098101107110
11	7.3	6.08E 07	.007055067087095118122124130131135
10	6.7	6.51E 07	.045063068069074097114117127132
9	6.0	6.94E 07	.017020052080093112115120129
16	10.7	7.38E 07	.046054071084085086102103106108116125135138139142
9	6.0	7.81E 07	.032037092092123126128133145
9	6.0	8.24E 07	.051065096100109121134137144
8	5.3	8.67E 07	.027033065073104105111119
3	2.0	9.11E 07	.061140143
2	1.3	9.54E 07	.031141
0	0.0	9.97E 07	.
0	0.0	1.04E 08	.
0	0.0	1.08E 08	.
0	0.0	1.13E 08	.
0	0.0	1.17E 08	.
0	0.0	1.21E 08	.
0	0.0	1.26E 08	.
0	0.0	1.30E 08	.
0	0.0	1.34E 08	.
0	0.0	1.39E 08	.
0	0.0	1.43E 08	.
139			0 5 10 15 20 25 30

MEDIAN	MEAN	STD. DEV.	COVAR.(%)
6.470E 07	5.827E 07	2.019E 07	34.64

Figure 62. Histogram of Threshold Rate for Turn-on (I_{sp} = 1A) for Solitron BR200A in Shorted-base Configuration

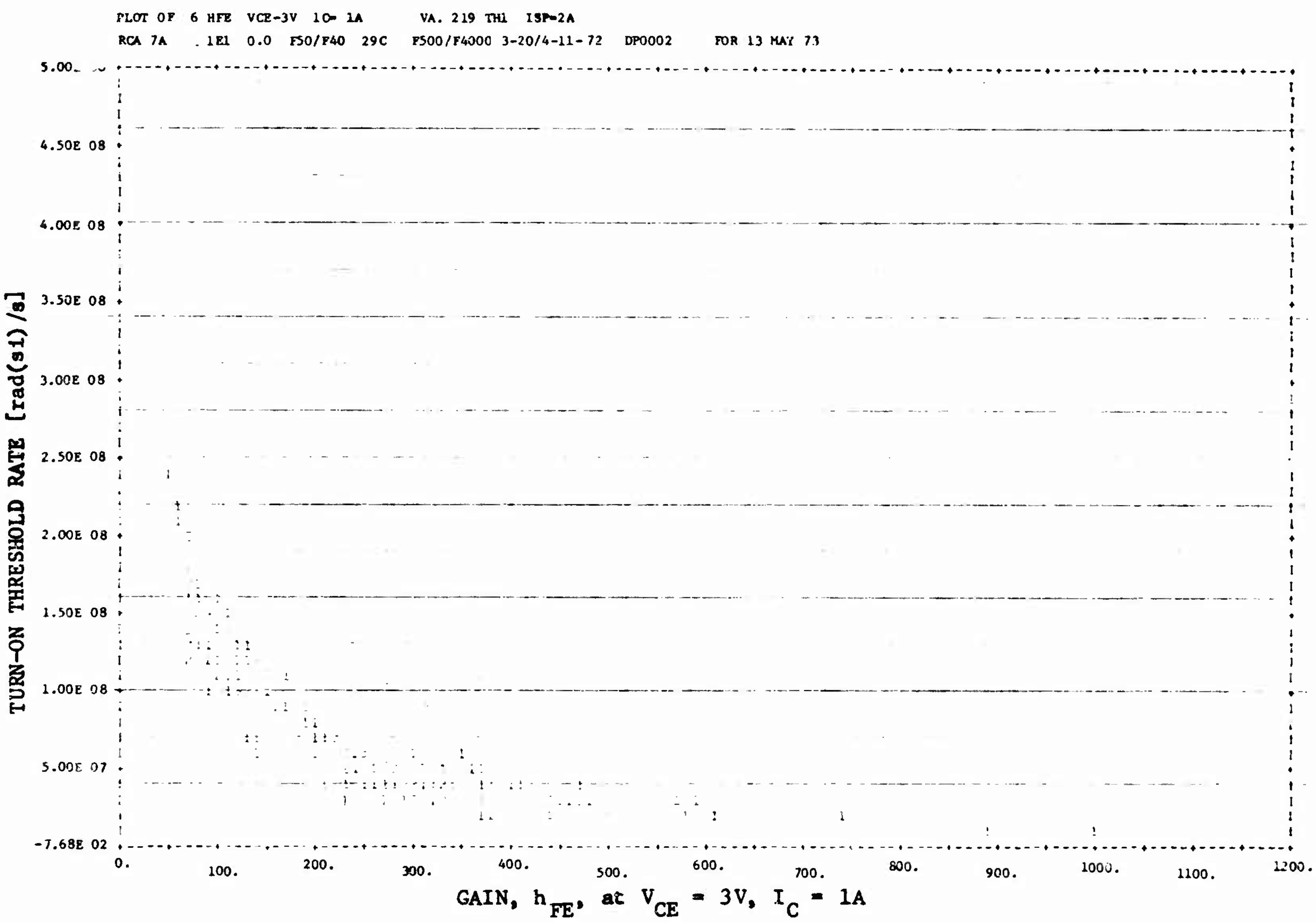

Figure 63. Scatter Diagram of h_{FE} (3V/1A) versus Trun-On Threshold Rate for RCA TA8007

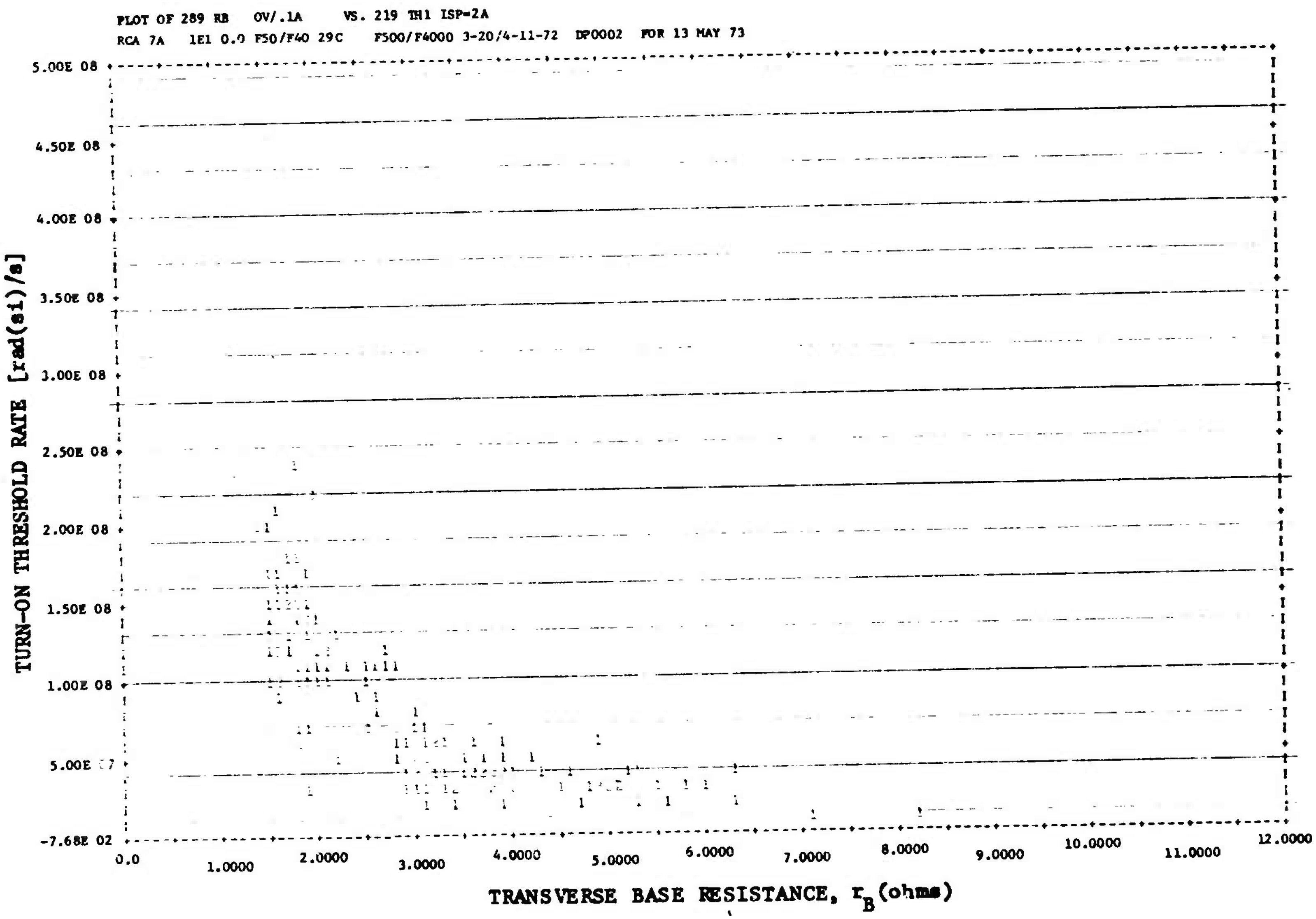

Figure 64. Scatter Diagram of r_B versus Turn-On Threshold Rate for RCA TA8007

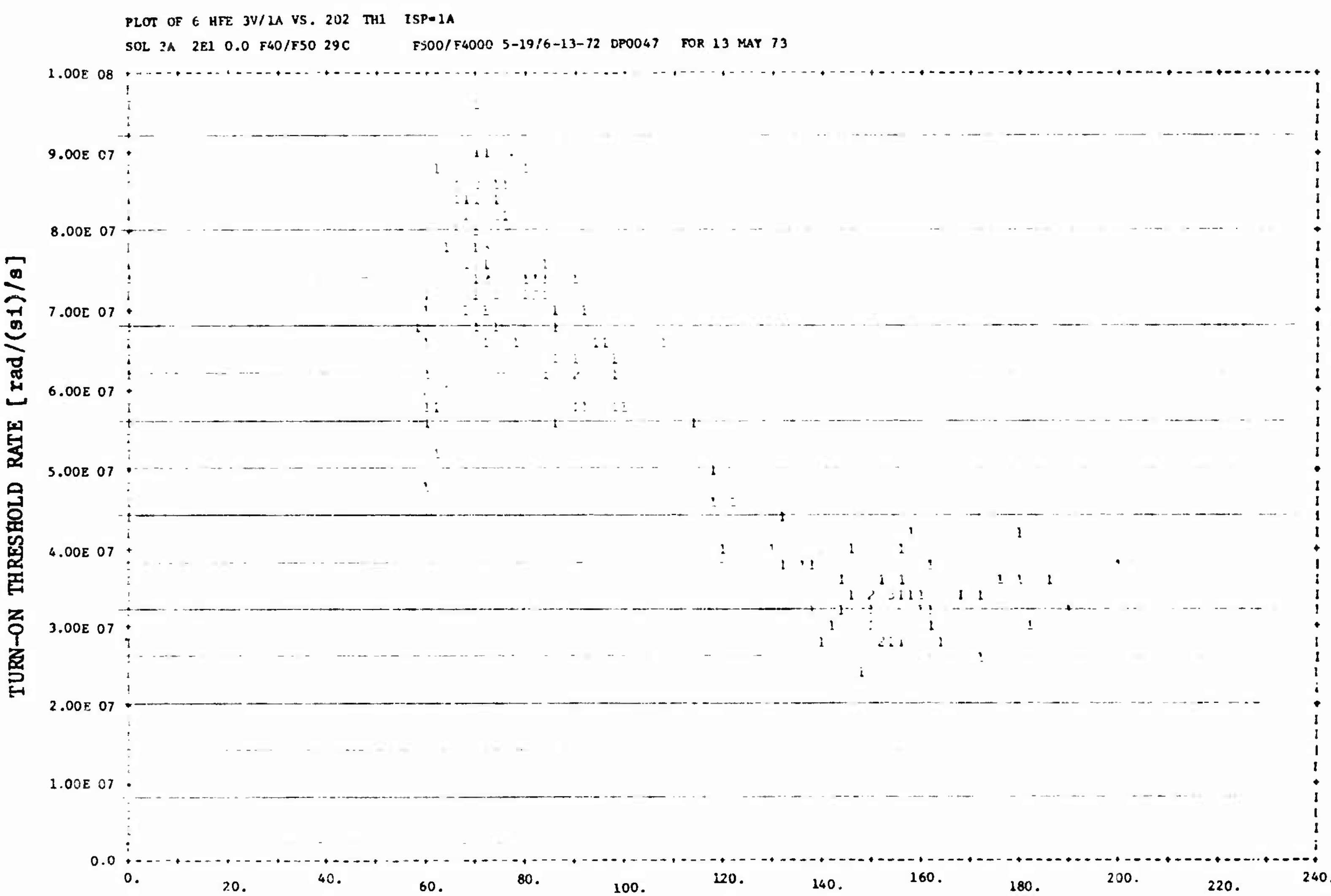

Figure 65. Scatter Diagram of h_{FE} (3V/1A) versus Turn-On Threshold Rate for Solitron BR200A

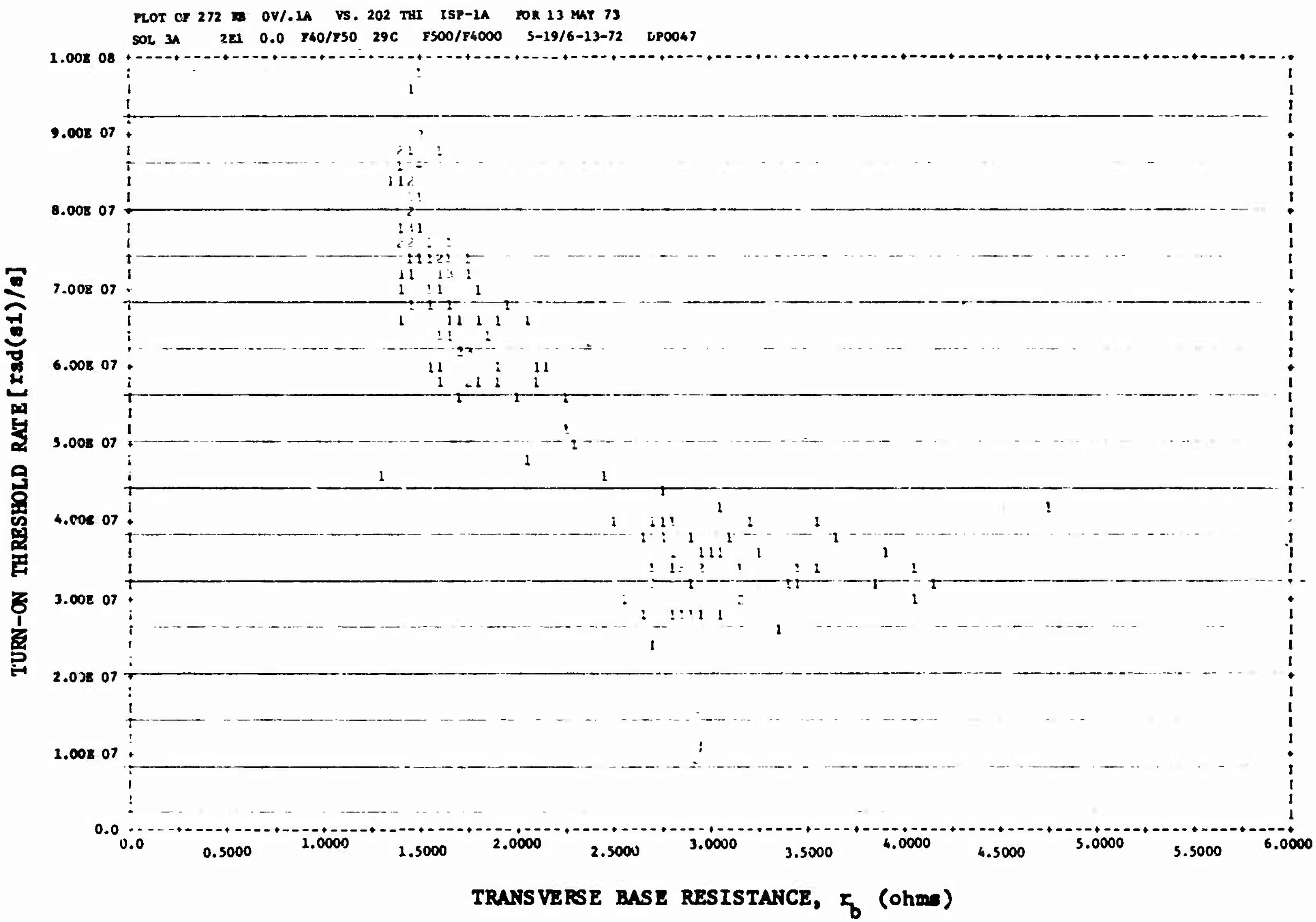

Figure 66. Scatter Diagram of r_B versus Turn-On Threshold Rate for Solitron BR200A

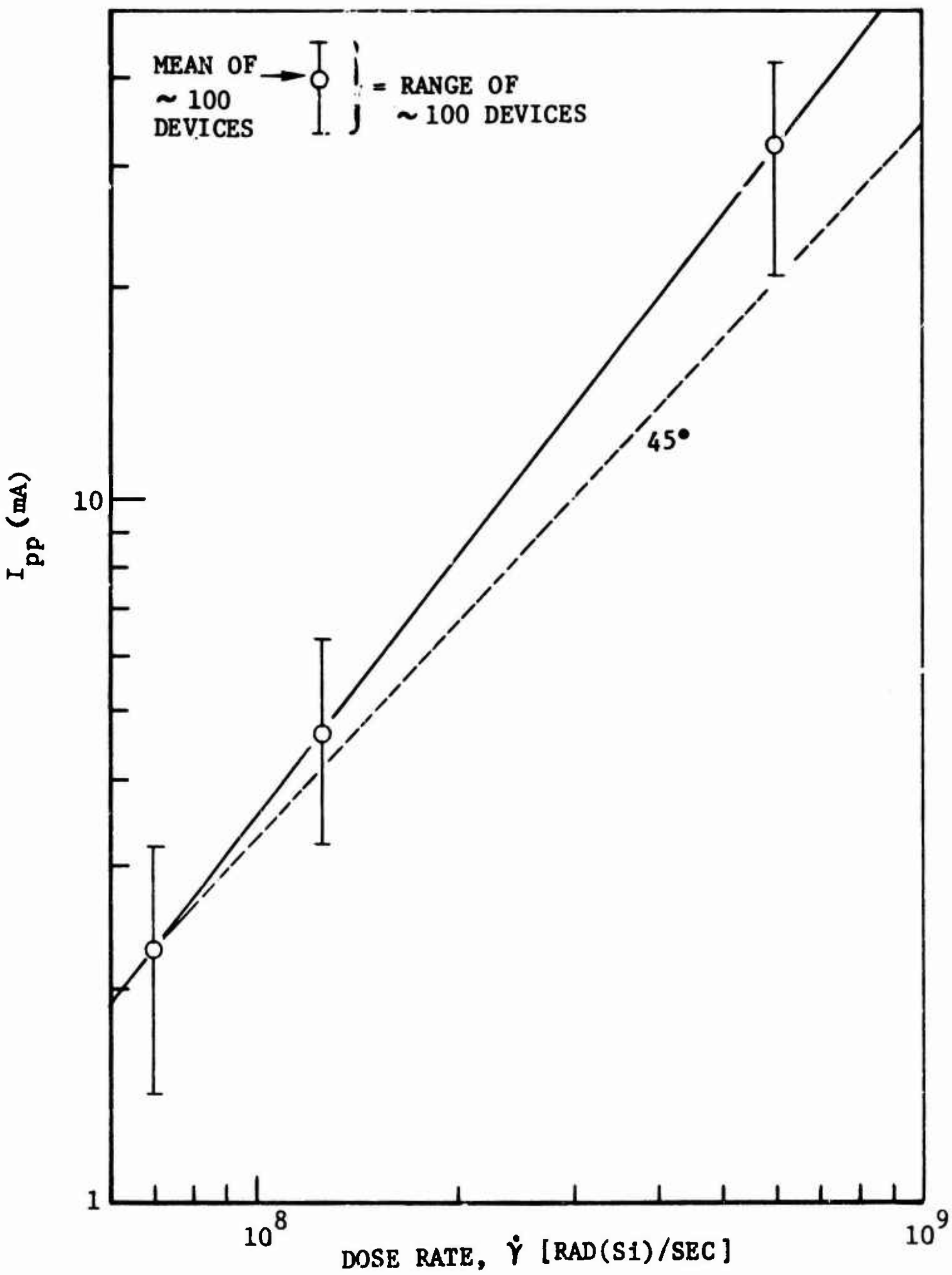

Figure 67. Superlinearity of Primary Photocurrent, I_{pp} as a Function of Dose Rate for the Dual JFET

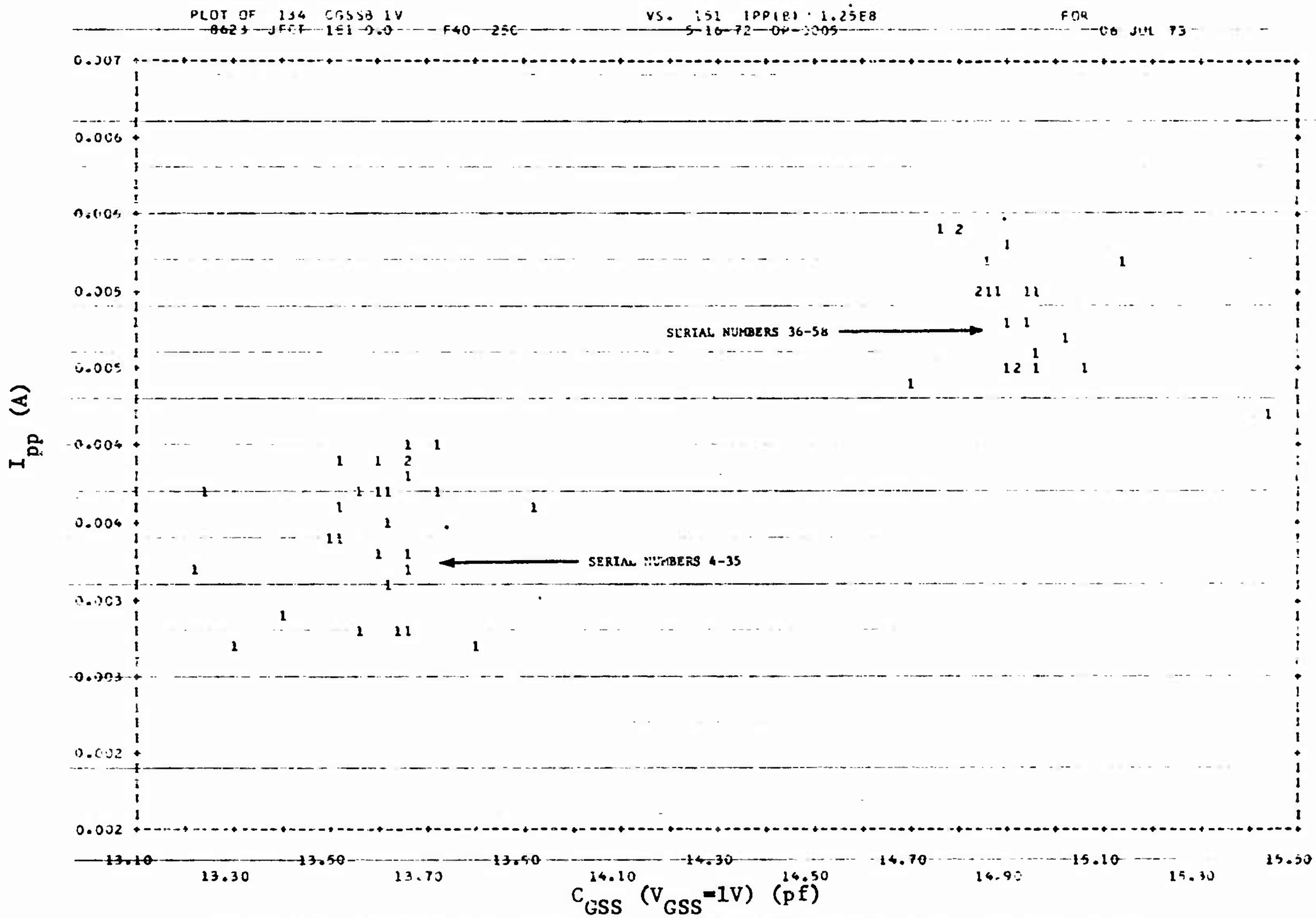

Figure 68. Correlation Between C_{GSS} (V = 1V) and I_{pp} for the Dual JFET

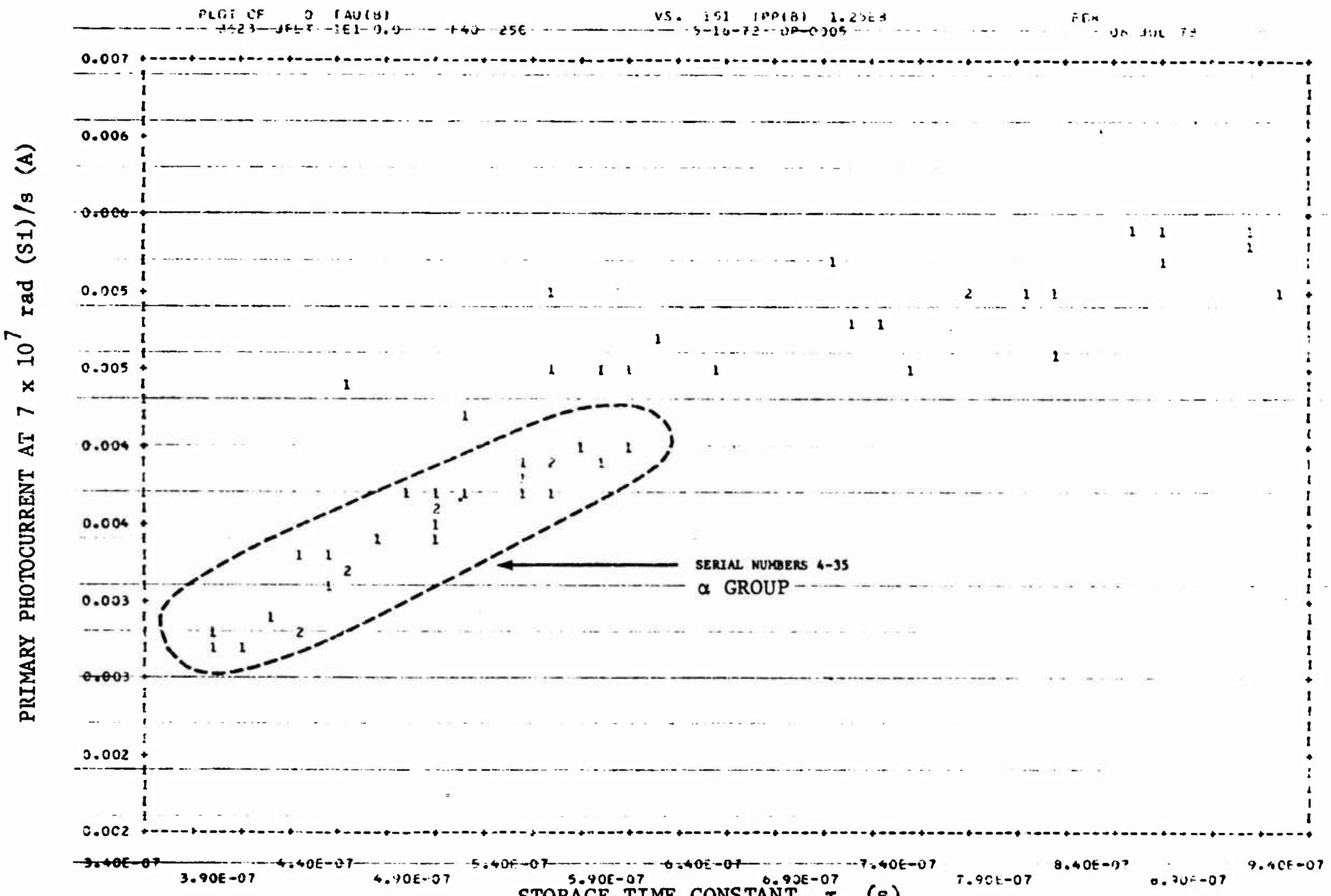

Figure 69. Correlation Between τ_S and I_{pp} for the Dual JFET

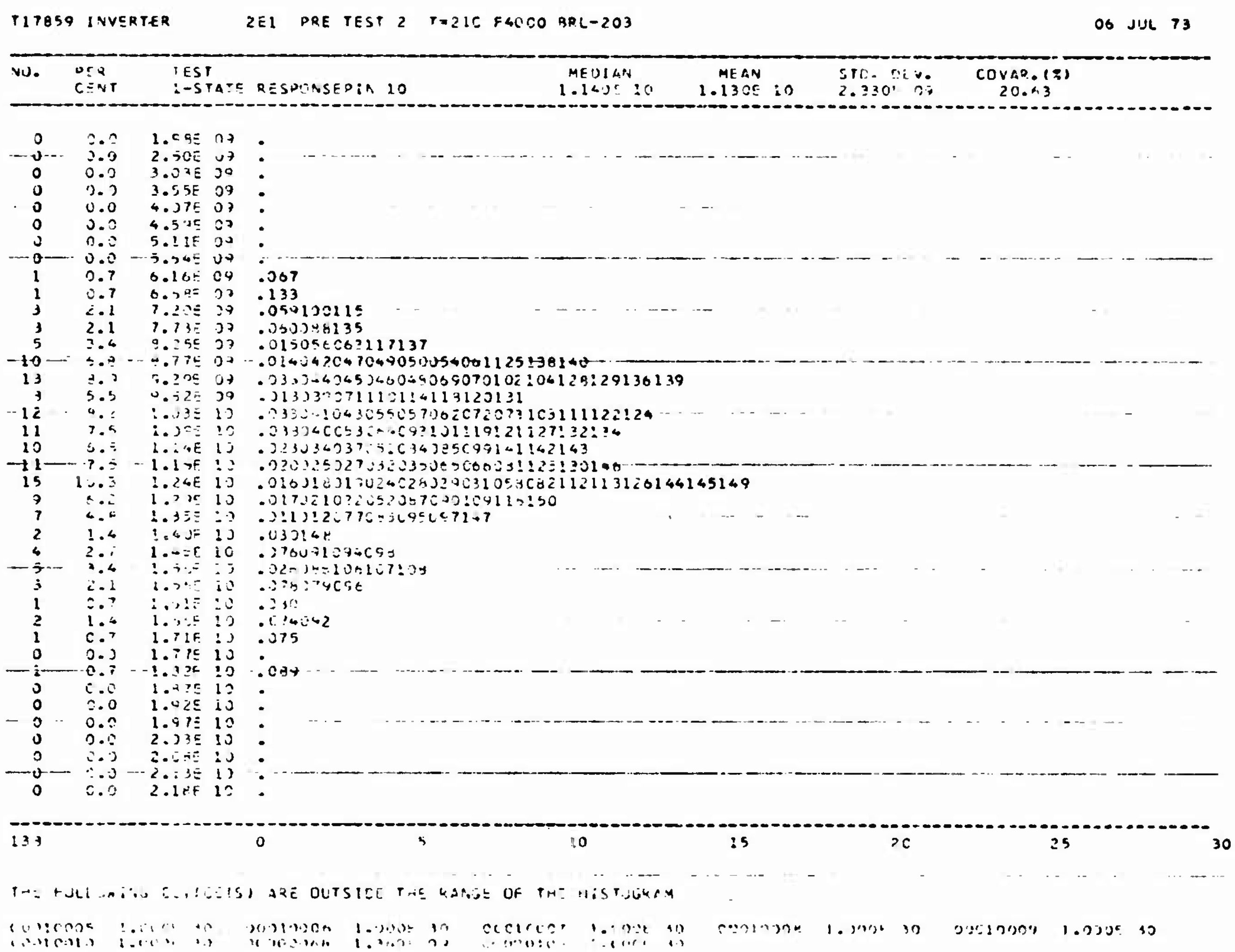

Figure 70. A Sample Histogram of the Radiation Response Threshold Data (TI Inverter 1-State Response)

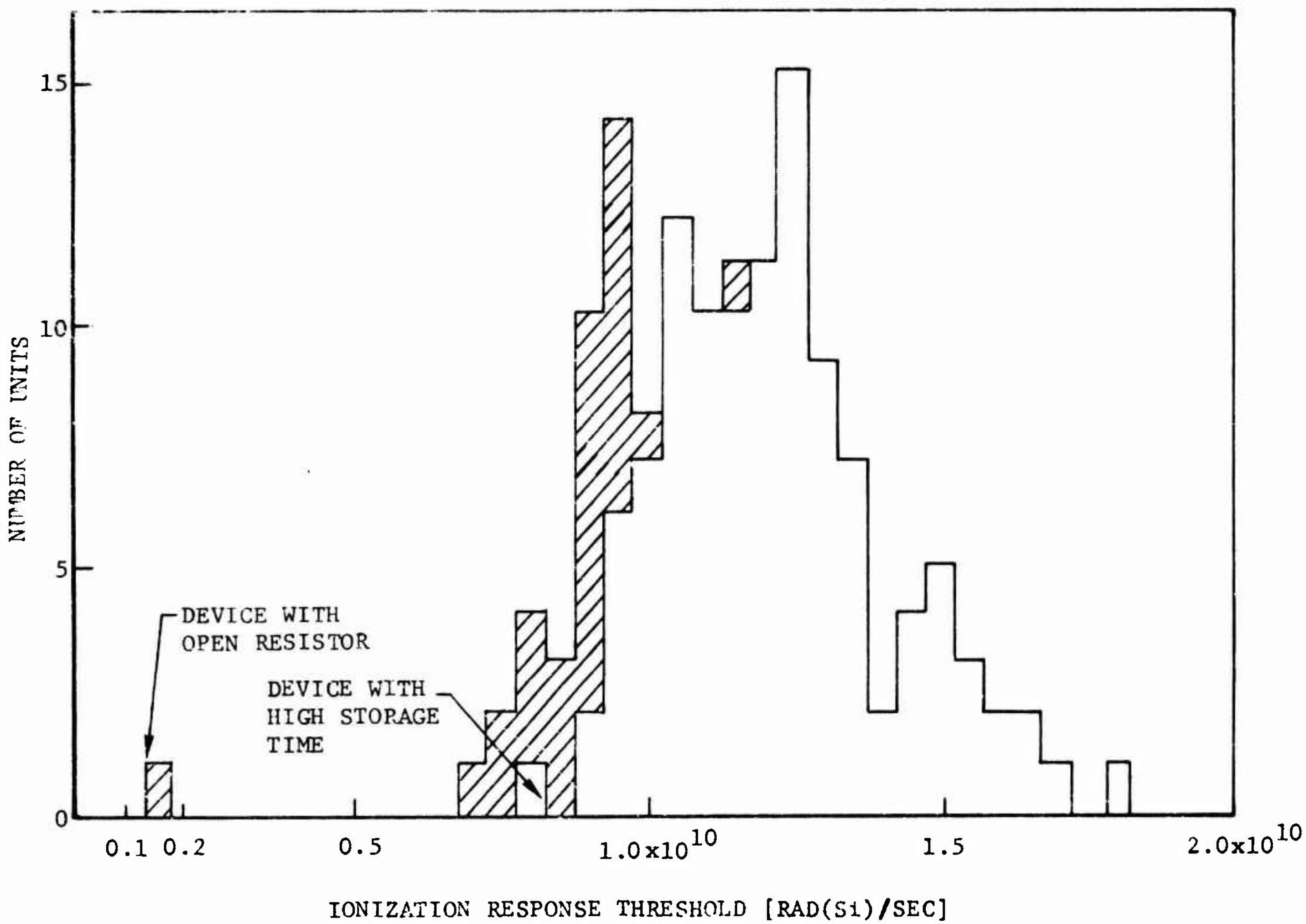

Figure 71. Histogram of TI Inverter 1-State Response Thresholds Showing Truncation With Electrical Storage Time

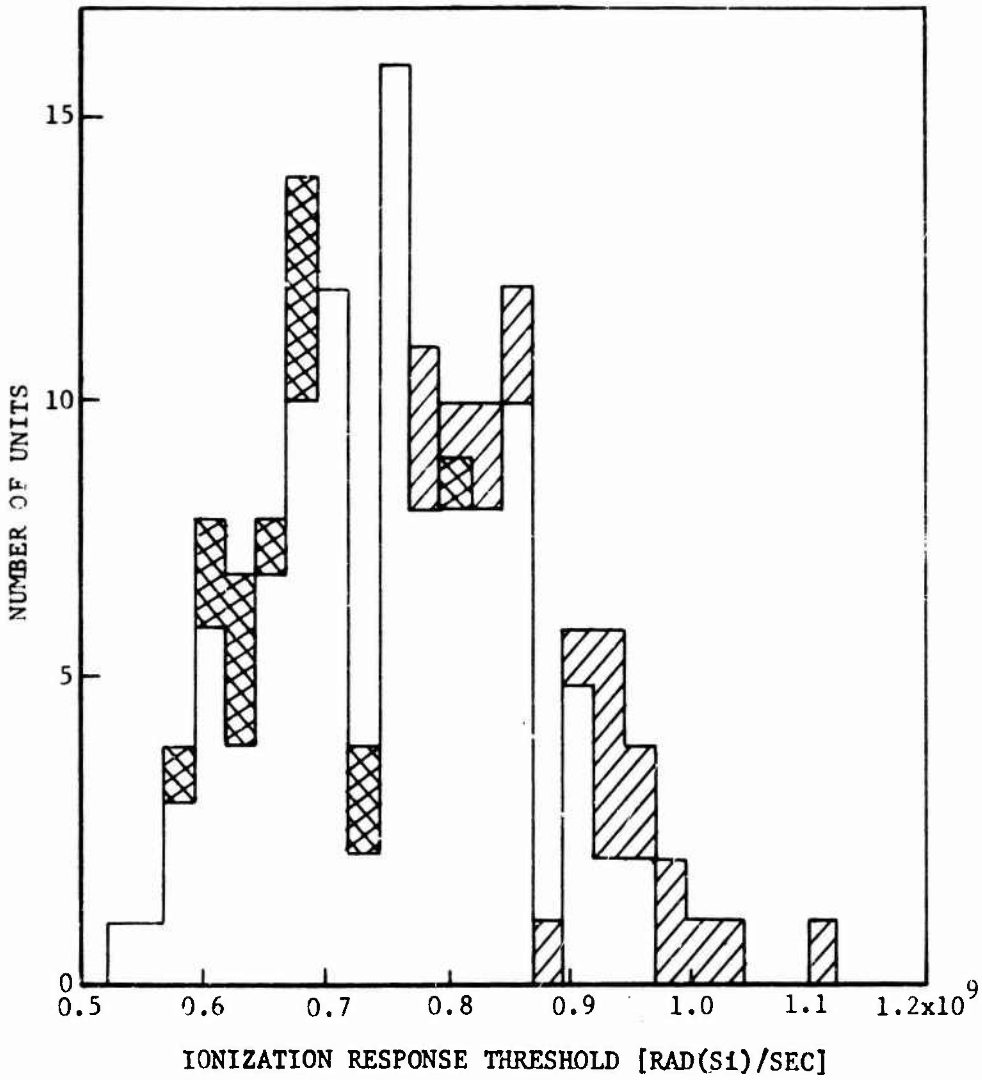

Figure 72. Truncation of TI Buffer Radiation Responses with Offset Voltage

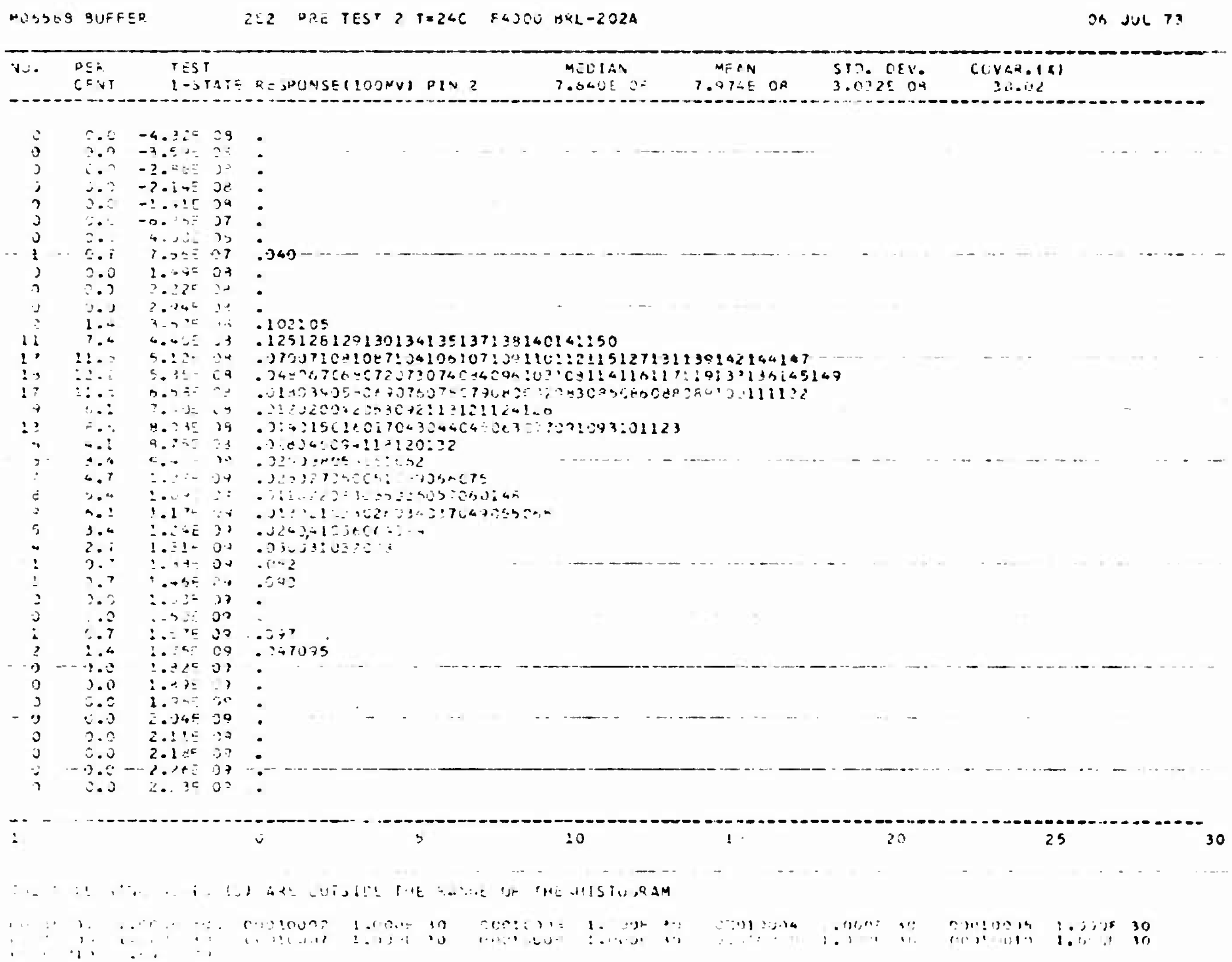

Figure 73. Histogram of Radiation Response Threshold Data (Motorola Buffer 1-State Response)

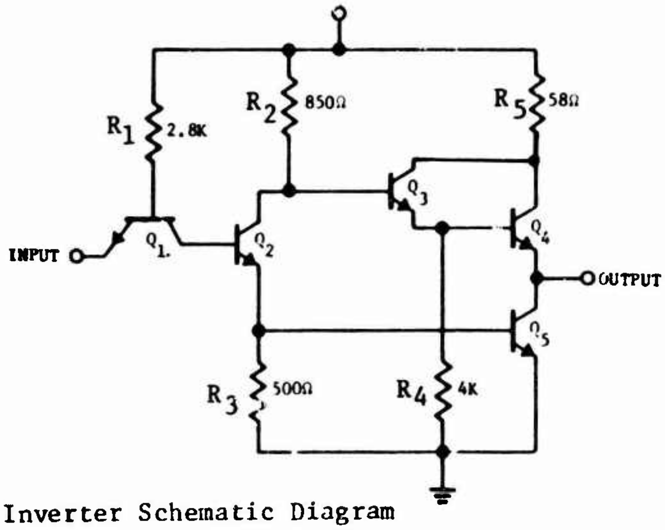

a) Inverter Schematic Diagram

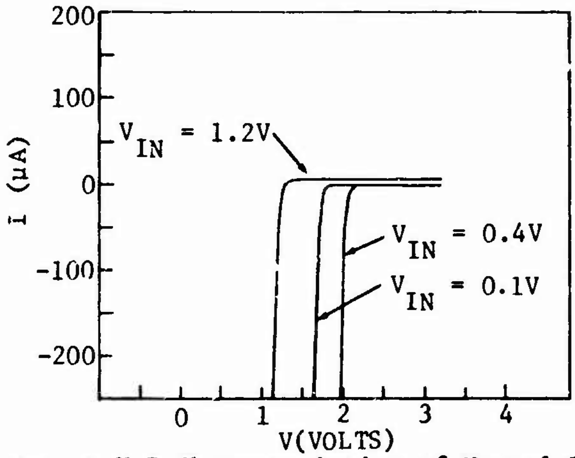

b) Output V-I Characteristics of Normal Device

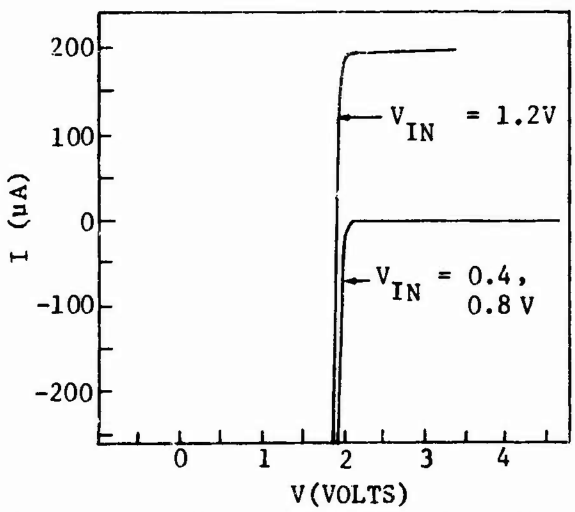

c) Output V-I Characteristics of Device with Open R_3

Figure 74. Method Used to Detect Open Internal Resistors in the Inverter Circuits

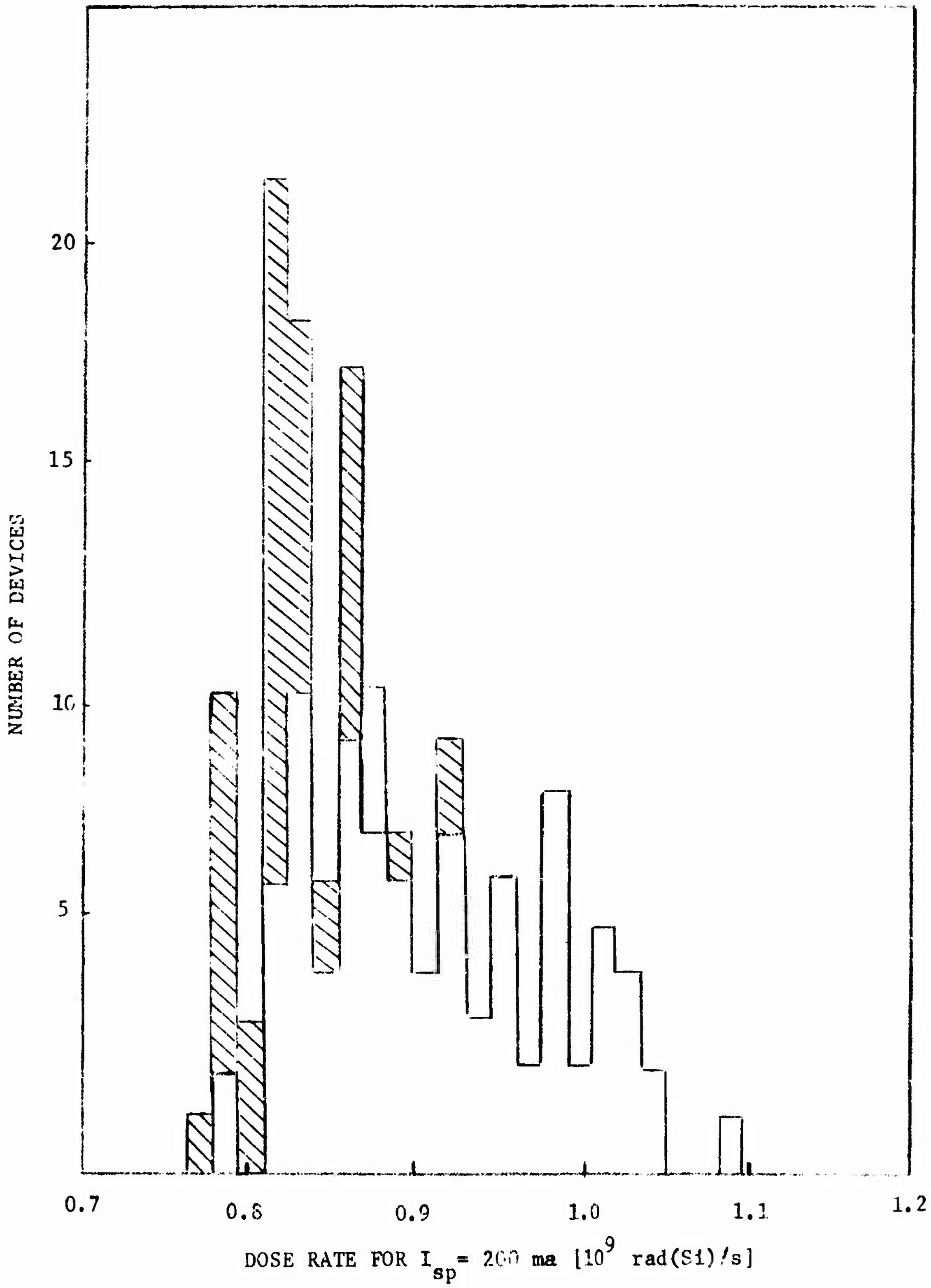

Figure 75. Truncation of the Word Switch Secondary Photocurrent Thresholds with h_{FE} and r_B

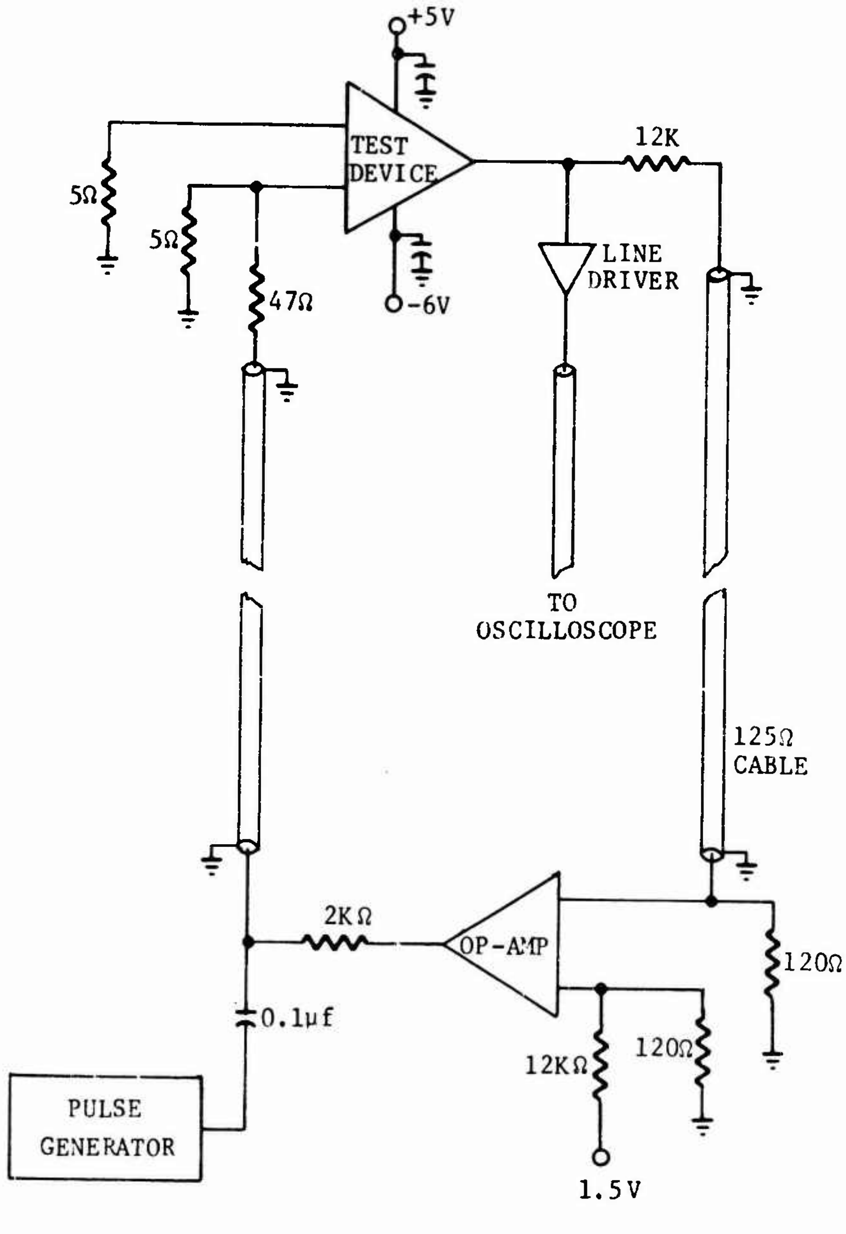

Figure 76. Experimental Method Used in LINAC Tests of the Motorola Sense Amplifier

Table 51
Summary of Low Power Transistors Tested
for Transient Ionization Effects

Mfr.	Device Type	Construction[a]	Gold-Doped	Base Area (cm^2)	Approx. No. Parts Tested
FSC	2N696	NPN PE	No	3.43×10^{-3}	150
FSC	2N2222	NPN PE	No	8.47×10^{-4}	150
FSC	2N2905A	PNP	No	9.35×10^{-4}	150
FSC	2N709	NPN PE	Yes	3.65×10^{-5}	417
FSC	2N3960	NPN PE	No	3.65×10^{-5}	150
MOT	MT7111 Hex Inv. BOT	NPN PE IC Breakout (DI)	Yes	4.6×10^{-5}	30
MOT	MT7113 Buffer BOT	NPN PE IC Breakout (DI)	Yes	3.03×10^{-4}	30
TI	TI7111 Hex Inv BOT	NPN PE 3 IC Breakouts (DI)	Yes	---	87
TI	TI7113 Buffer BOT	NPN PE 3 IC Breakouts (DI)	Yes	---	87

(a) PE = Planar Epitaxial
(b) DI = Dielectric Isolation

Table 52

Summary of Photocurrent Data for Low-Power Transistors

Device Type	Response Mechanism	Exposure Rate [rad(Si/s]	Photocurrent				
			Mean (mA)	Standard Dev. (mA)	Range (mA)	Max/Min	Normalized mA/[rad(Si)/s]
2N696	I_{pp}	1.2×10^{8}	18.4	2.3	24.9 - 13.6	1.83	1.47×10^{-7}
	I_{pp}	5.3×10^{8}	86.1	10.8	119 - 63.5	1.88	1.62×10^{-7}
	I_{sp}	5.3×10^{8}	531	67.6	722 - 403	1.79	
2N2222	I_{pp}	3.0×10^{9}	50.7	8.2	65.3 - 29.4	2.22	1.69×10^{-8}
	I_{pp}	1.4×10^{10}	220	34.9	290 - 143	2.02	1.63×10^{-8}
	I_{sp}	1.4×10^{10}	668	201	1.08 - 369	2.93	
2N2905A	I_{pp}	1.3×10^{9}	24.4	3.4	31.7 - 15.4	2.06	1.88×10^{-8}
	I_{pp}	6.0×10^{9}	90.2	16.6	135 - 60.6	2.22	1.50×10^{-8}
	I_{sp}	6.0×10^{9}	226	88.5	383 - 40.5	9.46	
2N709	I_{pp}	8.0×10^{10}	50.8	7.5	80.9 - 31.9	2.53	6.35×10^{-10}
	I_{sp}	8.0×10^{10}	92.5	66.7	271 - 36.7	7.40	---
2N3960	I_{pp}	1.5×10^{10}	36.7	8.6	320* - 15.6	20.5*	2.44×10^{-9}
	I_{pp}	6.0×10^{10}	102.7	23.5	174 - 49.7	3.5	1.71×10^{-9}
	I_{sp}	6.0×10^{10}	209.2	63.4	386 - 65.4	5.90	---
BOT (MOT Hex Inv)	I_{pp}	7.3×10^{10}	26.6	2.4	32.5 - 23.2	1.40	3.65×10^{-10}
	I_{sp}	7.3×10^{10}	167.7	39.1	269 - 108	2.49	---
BOT (MOT Buffer)	I_{pp}	1.3×10^{10}	13.9	2.0	19.4 - 10.6	1.83	1.07×10^{-9}
	I_{pp}	6.4×10^{10}	67.0	12.2	99.0 - 43.0	2.30	1.05×10^{-9}
	I_{sp}	6.4×10^{10}	493	114.5	708 - 203	3.49	---

*"Anomalous" I_{pp} due to secondary effects (such as transverse base resistance), decreased ~ X5 after repeated testing.

Table 53

Comparison of Electrical Storage Time and Storage Time Constant, as Screening Parameters for Primary Photocurrent

Device Type	Exposure Rate [rad(Si)/s]	Rank Correlation Coefficient of I_{pp} vs:				
		Electrical Storage Time, t_{SE}		Electrical Storage Time Constant, τ_S		
		I_{CS} = 10mA, I_B = 2mA	I_{CS} = 50mA, I_B = 10mA	I_{CS} = 5mA	I_{CS} = 10mA	I_{CS} = 50mA
2N696	1.2×10^{8}	.391	.331	.426	.464	.398
	5.3×10^{8}	.514	.463	.531	.529	.504
2N2222	3.0×10^{9}	.283	.264	.274	.278	.309
	1.4×10^{10}	.133	.123	.125	.130	.146
2N2905A	1.3×10^{9}	-.154	.607	.243	.471	.604
	6.0×10^{9}	-.050	.594	.289	.470	.586
2N3960	1.5×10^{10}	.566	.570	.559	.557	.482
	6.0×10^{10}	.595	.610	.534	.536	.358
		I_{CS} = 10mA, I_B = 4mA	I_{CS} = 20mA, I_B = 4mA	I_{CS} = 10mA		I_{CS} = 20mA
2N709	8×10^{10}	---	---	---		---
BOT (MOT Buffer)	1.3×10^{10}	.495	.377	.465		-.161
	6.4×10^{10}	.478	.537	.371		.425

Table 54

Summary of Rank Correlation Coefficients for Various Screening Parameters versus I_{pp} for Low-Power Transistors

Device Type	Dose Rate [rad(Si)/s]	Rank Correlation Coefficient of I_{pp} vs: C_{OB}	t_B	BV_{CBO}	h_{FEI}	r_{BI}	C_{IB}
2N696	1.25×10^8	.013	-.099	.426	.176	.105	-.282
	5.3×10^8	.079	-.123	.445	.248	.111	-.354
2N2222	3.0×10^9	-.334	.320	.317	-.066	.156	.413
	1.35×10^{10}	-.296	.184	.189	-.237	-.036	.501
2N2905A	1.3×10^9	.498	-.246	.249	.501	.182	.013
	6.0×10^9	.538	-.312	.168	.511	.317	-.082
2N3960	1.5×10^{10}	-.305	.566	.478	.000	-.585	.038
	6.0×10^{10}	-.232	.299	.354	-.152	-.370	.144
MT7113	1.3×10^{10}	.180	.133	.295	.096	-.100	.284
	6.4×10^{10}	.133	-.075	.214	.180	.168	.076

Table 55

Relative Efficacies of Various Screening Parameters for Primary Photocurrents

Rank	Device Type: 2N969	2N2222	2N2905A	2N709	2N3960	MT7111	MT7113
(1)	τ_S	C_{IB}	t_{SE}	C_{OB}	t_{SE}	C_{OB}	t_{SE}
(2)	t_{SE}	$V_{CE(SAT)}$	τ_S	BV_{CBO}	τ_S	C_{IB}	τ_S
(3)	BV_{CBO}	C_{OB}	$V_{CE(SAT)}$		r_{BI}	t_{SE}	BV_{CEO}
(4)	I_{EBO}		C_{OB}			h_{FEI}	h_{FE}
(5)	$V_{CE(SAT)}$		h_{FEI}				
(6)	C_{IB}						

Table 56
Summary of MLR Predictions of I_{pp} for 2N696, 2N2905A and 2N2222
Low-Power Transistors Using Total Sample

Device Type	Dose Rate [rad(Si)/s]	No. Screening Parameters	Prediction Errors (%)			
			Mean	RMS	Max	Min
2N696	1.25×10^{8}	3	1.2	11.5	33.3	-24.8
	5.3×10^{8}	3	1.1	10.6	28.3	-25.9
	1.25×10^{8}	12	1.2	10.4	36.8	-21.5
	5.3×10^{8}	12	0.7	9.0	31.7	-17.2
2N2905A	1.3×10^{9}	3	2.2	14.4	49.3	-34.1
	6×10^{9}	3	2.9	18.3	45.6	-30.6
	1.3×10^{9}	12	1.1	11.2	45.6	-19.8
	6×10^{9}	12	—	14.4	37.2	-28.7
2N2222	3×10^{9}	3	—	17.3	56.5	-26.8
	1.35×10^{10}	3	—	17.7	52.8	-22.2
	3×10^{9}	12	—	15.8	53.5	-22.8
	1.35×10^{10}	12	—	16.2	52.6	-23.6

Table 57

Summary of Rank Correlation Coefficients for I_{sp}

Device Type	Exposure Rate [rad(Si)/s]	Rank Correlation Coefficients of I_{sp} vs.								
		I_{Fp}	r_B	h_{FE}	N_{BO}	t_B	τ_S	t_{SE}	$V_{CE(SAT)}$	Other
2N2905 A	6.0×10^{9}	.744	.619	.860	-.473	-.744	.818	.845	.839	.865 (h_{FEI})
2N696	5.3×10^{8}	.858	.334	.426	-.368	-.232	.736	.722	.739	.421 (h_{FEI})
2N2222	1.35×10^{10}	.305	.765	.258	.053	.525	.782	.773	-.620	.649 (h_{FEI})
2N709	---	---	---	---	---	---	---	---	---	---
2N3960	6.0×10^{10}	.305	.388	.281	.195	.274	.288	.212	.246	.239 (h_{FEI})
MT 7111	---	---	---	---	---	---	---	---	---	---
MT 7113	6.4×10^{10}	.155	.101	.498	-.594	-.558	.425	.537	-.596	0.542 (h_{FEI})

Table 58

Summary of Rank Correlation Coefficients for Primary Photocurrent - Dual JFET

Electrical Parameter / Dose Rate [rad(SI)/s]	Chip[a]	Group[b]	t_{rrGS} I_F = 10mA I_R = 2mA	t_{rrGS} I_F = 10mA I_R = 5mA	t_S	C_{GSS} (V_{GSS}=1V)	C_{GSS} (V_{GSS}=20V)
7×10^7	A	α	.951	.951	.933	.262	.239
7×10^7	A	β	.735	.758	.724	-.479	-.470
7×10^7	A	TOT	.946	.944	.944	.732	.722
7×10^7	B	α	.921	.833	.936	.232	.484
7×10^7	B	β	.794	.795	.795	-.599	-.510
7×10^7	B	TOT	.910	.876	.931	.722	.766
1.2×10^8	A	α	.930	.940	.910	.265	.223
1.2×10^8	A	β	.790	.818	.768	-.495	-.471
1.2×10^8	A	TOT	.949	.951	.946	.719	.708
1.2×10^8	B	α	.913	.808	.949	.249	.441
1.2×10^8	B	β	.823	.828	.825	-.457	-.420
1.2×10^8	B	TOT	.918	.882	.943	.738	.769
6×10^8	A	α	.925	.931	.903	.278	.239
6×10^8	A	β	.785	.754	.781	-.534	-.577
6×10^8	A	TOT	.954	.950	.951	.721	.642
6×10^8	B	α	.862	.771	.859	.183	.352
6×10^8	B	β	.762	.769	.748	-.383	-.387
6×10^8	B	TOT	.905	.873	.928	.717	.750

(a) The dual JFET has two chips, A and B, in the package.
(b) Group α = serial numbers 1-35
Group β = serial numbers 36-60

Table 59

Summary of MLR for I_{pp} - Dual JFET

Dependent Variable	Chip	Dose Rate [rad(Si)/s]	No. of Independent Variables	Coef [a] of MLR	F	RMS Prediction Error (%)	Range of Data for 23 Predicted Devices (%)
I_{PP}	A	1.25×10^8	2 [b]	.856	27.4	26.2	29.3
I_{PP}	A	6×10^8	2 [b]	.841	23.0	30.8	22.7
I_{PP}	B	1.25×10^8	2 [b]	.817	20.0	40.8	23.7
I_{PP}	B	6×10^8	2 [b]	.794	16.3	17.7	25.1
I_{PP}	A	1.25×10^8	2 [c]	.856	27.5	26.6	29.3
I_{PP}	A	6×10^8	2 [c]	.824	20.1	31.4	22.7
I_{PP}	B	1.25×10^8	2 [c]	.811	19.2	45.0	23.7
I_{PP}	B	6×10^8	2 [c]	.800	16.8	15.1	25.1
I_{PP}	A	1.25×10^8	2 [d]	.915	64.0	9.68	29.3
I_{PP}	A	6×10^8	2 [d]	.891	48.3	10.4	22.7
I_{PP}	B	1.25×10^8	2 [d]	.953	123	13.0	23.7
I_{PP}	B	6×10^8	2 [d]	.876	41.2	13.1	25.1

(a) MLR coefficients were generated using 27 devices and the I_{pp} of the other 23 were predicted using these.

(b) Independent variables were τ_S, N (calculated from capacitance data).

(c) Independent variables were t_{rrGS} ($I_F = 5$ mA, $I_R = 10$ mA)

(d) Independent variables were τ_S, $I/C_{GSS}(20V)$.

Table 60

Summary of TTL Transient Ionization Data

Device	Data Description (a)	Mean Value	Worst Value	Standard Deviation	Ratio [Max/Min]
TI Inverter	1-State Threshold	1.13×10^{10}	5.7×10^{9}	2.3×10^{9}	3.2
	0-State Threshold (100 mV)	5.6×10^{9}	2.8×10^{9}	1.2×10^{9}	3.4
	0-State Threshold (200 mV)	9.2×10^{9}	4.0×10^{9}	2.9×10^{9}	4.7
TI Buffer	Modified Response - 1.2×10^{9}	0.20V	0.32V	0.019V	~2
	Modified Response - 3×10^{9}	0.77V	1.12V	0.11V	~2
	Unmodified Response - 3×10^{9}	0.34V	0.42V	0.038V	2.1
TI A-O-I Gate	300 mV Threshold	1.27×10^{9}	0.54×10^{9}	2.6×10^{9}	5
	600 mV Threshold	2.47×10^{9}	1.5×10^{9}	4.2×10^{8}	2.7
Motorola Inverter	1-State Threshold (Pin 6)	1.03×10^{10}	3.5×10^{9}	2.5×10^{9}	60
	0-State Threshold (Pin 8)	3.45×10^{9}	1.2×10^{9}	1.3×10^{9}	5.3
	0-State Threshold (Pin 6)	6.9×10^{9}	1.2×10^{9}	2.0×10^{9}	~9
Motorola Buffer	0-State Threshold	8.8×10^{9}	4.5×10^{9}	1.9×10^{9}	2.3
	1-State Threshold	7.9×10^{8}	8.7×10^{7}	3.0×10^{8}	~20

(a) "Modified" refers to the circuits which contain special leads.

Table 61

Some Rank Correlations for the $\dot{\gamma}$ Response of the TI Inverter

Initial Electrical Parameter	Correlation Factors for $\dot{\gamma}$ Response of Various Parameters	
	0-State (Output Low)	1-State (Output High)
V_{OH}	-0.616	-0.427
$I_{IN(1)}$	-0.715	-0.493
I_{SK}	-0.647	-0.520
V_{OS}	-0.679	0.738
Switching Time (Low to High)	-0.438	-0.746
Active Rise Time	-0.693	-0.630
ω_T	0.422	0.591
h_{FE}	-0.703	-0.721
Rise Time (Low to High)	-0.591	-0.771

Table 62

Some Rank Correlations for the $\dot{\gamma}$ Response of the TI Buffer

Initial Electrical Parameter	Correlation Factors for $\dot{\gamma}$ Response of Various Parameters	
	1-State Response at 3 x 10^9 rad(Si)/s (Side A)	1-State Response at 3 x 10^9 rad(Si)/s (Side B)
I_{SK}	0.436	0.462
I_{SINK}	0.709	0.521
V_{OS}	-0.705	-0.502
h_{FE}	0.510	0.405
Active Rise Time (Output voltage)	0.639	0.440
Switching Time (Low to High)	0.130	0.464
Switching Time (High to Low)	-0.414	-0.274
$I_{IN(1)}$	0.522	0.504
V_{BE}(Q5) [Note(a)]	0.550	----

(a)Special Lead Measurement

Table 63

Some Rank Correlations for the Ionization Response Threshold of the TI A-O-I Gate

Electrical Parameter	Rank Correlation with TI A-O-I Gate Ionization Response Threshold
I_{OS}	-.284
$I_{CC(0)}$	.273
V_{OS}	-.092
t_{PD}	-.323
Output Capacitance	-.289
Stored Charge	.170
h_{FE} (I_{SK})	.126
R_6 [(a)] Resistance	-.248

(a) R_6 is the emitter-to-base resistor of the output transistor.

Table 64

MLR Results for TI A-O-I Gate Transient Response Threshold

Parameters Used For Regression	Prediction Error[a] (%) RMS	Maximum
I_{CC} R_6[b] Resistance (Calculated) Propagation Delay Time I_{pp} Correlation Factor $1/I_{OS}$	16	45

(a)The first 70 units were used for regression coefficients which were then used to predict the values of all 140 units.

(b)R_6 is the emitter-to-base resistor of the output transistor.

Table 65

Some Rank Correlations for Ionizing Rate Response of the Motorola Inverter

Initial Electrical Parameter	Correlation Factors for $\dot{\gamma}$ Response of various parameters	
	0-State (Output Low)	1-State (Output High)
V_{OH}	-0.161	-0.342
$I_{IN(1)}$	0.042	-0.131
I_{SK}	0.049	-0.160
V_{OS}	0.133	0.121
Switching Time (Low to High)	0.084	-0.304
h_{FE}	0.083	0.218

Table 66

Effects of Electrical Screens on the Regression Results for the Motorola Inverter 1-State $\dot{\gamma}$ Threshold

Description	Parameters Used For Regression	F Value	Prediction Error[a] (%)	
			RMS	Maximum
MLR Based on Circuit Measurements (Devices #41 & #47 included)	h_{FE} V_{OH} R_4[c]	13.2	136	891
MLR Based on Circuit Measurements (Devices #41 & #47 excluded)[b]	h_{FE} V_{OH} R_4[c]	5.2	27	145

(a) The first 70 units were used to generate the regression coefficients. The 1-state $\dot{\gamma}$ threshold was then predicted for (a) the 2nd 70 units when Devices #41 and #47 were included and (b) all 138 units when the two devices were excluded.

(b) The two devices were excluded because of faulty pretest electrical characteristics:

(1) Device #47 had excessive output leakage current (112 μA at V_{OH} = 5.5V)

(2) Device #41 had an open base-emitter resistor (R_3)

(c) R_4 is the external base-emitter resistor on the pull-up transistor.

Table 67

Some Rank Correlations for the $\dot{\gamma}$ Threshold of the Motorola Buffer

Initial Electrical Parameter	Correlation Factor for $\dot{\gamma}$ Response of Various Parameters	
	0- State Response (Output Low)	1- State Response (Output High)
I_{SK}	-0.695	0.040
V_{OS}	0.217	0.234
V_{OH}	0.331	-0.173
h_{FE}	-0.708	-0.052
Switching Time (Low to High)	-0.532	0.131
Switching Time (High to Low)	0.178	-0.027
Stored Charge (Peak Current)	0.546	0.096
R_3 [a]	-0.267	-0.081
Depletion Width plus Diffusion Length	0.381	0.193

(a) R_3 is the emitter-to-base resistor on the output transistor

Table 68

Regression Results for the Motorola Buffer $\dot{\gamma}$ Threshold

Description	Parameters Used For Regression	F Value	Prediction Error[a] (%) RMS	Maximum
MLR Based on Circuit Measurements for 0-State Threshold	. h_{FE} . Stored Charge . Rise Time (low to high) . Switching time (Low to High) . R_3 (c)	27	15.7	36
MLR Based on Circuit Measurements for 1 state Threshold (Device #40 included)	. h_{FE} . V_{OL} . V_{OS} . Switching Time (High to Low) . Fall Time (High to Low) . R_4	2.1	99	964
MLR Based on Circuit Measurements for 1-State Threshold (Device #40 excluded) (b)	. h_{FE} . V_{OL} . V_{OS} . Switching Time (High to Low) . Fall Time (High to Low) . R_4(c)	2.1	56	163

(a) The first 70 units were used to generate the regression coefficients, and then predictions were made on all 140 units.

(b) Device #40 was excluded to observe the effect on the regression coefficients because the measured $\dot{\gamma}$ Threshold for Device #40 was a factor of four (4) lower than the other devices.

(c) R_3 and R_4 are the external base-emitter resistors for the output and pull-up transistors, respectively.

Table 69

Summary of Ionizing Rate Data (Non-TTL Integrated Circuits)

Device	Data Description	Mean	Worst Value	Standard Deviation	Max /Min
TI Word Switch	I_{pp} @ $3.5\times10^{8*}$	3.59 mA	4.1 mA	0.19 mA	1.33
	I_{pp} @ $3.3\times10^{9*}$	25.1 mA	30.4 mA	2.2 mA	1.5
	I_{sp} Threshold	$8.9\times10^{8*}$	$7.7\times10^{8*}$	$7.2\times10^{7*}$	1.4
Fairchild μA744 Op Amp	Response @ $4.3\times10^{6*}$	0.59V	1.1V	1.5V	9.5
	Sat. Threshold	$1.62\times10^{7*}$	7.0×10^{6}	$4.8\times10^{6*}$	8
	Sat. Time @ $9\times10^{8*}$	15.6 μs	41 μs	5.8 μs	45
MOT Sense Amp	Threshold	$2.26\times10^{8*}$	$2.7\times10^{7*}$	$7.9\times10^{7*}$	12
	CH 2 Threshold	$1.36\times10^{8*}$	$1.5\times10^{7*}$	$5.1\times10^{7*}$	18

* Dose rates in [rad(Si)/s]

Table 70

Some Rank Correlation Factors for the Ionization Response of the Word Switch

Electrical Parameter	Rank Correlation Coefficient	
	I_{pp} @ 3.3×10^9 rad(Si)/s	I_{sp} Threshold
Storage Time	.308	-.701
90 Ω Resistor[a]	-.166	-.725
h_{FE}	-.240	-.692
V_{BE}	-.167	-.496
Capacitance	-.251	.097
I_{pp} Correlation Factor	-.039	-.695
t_{OFF}	.499	.484

(a) Base-emitter resistor of the output transistor

Table 71

Multiple Linear Regression Results for the I_{sp} Threshold of the TI Word Switch

Parameter Used For Regression	Prediction Error[a] (%)		F Value
	RMS	Maximum	
Storage Time 90 Ω Resistor Value[b] h_{FE} Output Capacitance	3.91	11.5	71.1

(a) The first 70 units were used to generate the regression coefficients, and the coefficients were then used to predict all 140 units.

(b) Base-emitter resistor of the output transistor.

Table 72

Some Rank Correlation Coefficients for the Ionizing Rate Response of the Motorola Sense Amp

Initial Electrical Parameter	Rank Correlation Coefficient	
	Response Threshold Channel 1	Response Threshold Channel 2
Power Supply Current	.055	.127
V_{OL}	.057	.141
V_{OH}	.132	-.125
V_{OS}	-.141	-.177
I_{OS}	-.001	-.037
I_{BIAS}	-.080	.100
A_{OL}	.129	-.209
Recovery Time	-.053	-.087
Channel Select Time	-.108	-.238
Output Resistance	-.207	-.149

Table 73

An Example of MLR Predictions for the Ionizing Rate Response of the Motorola Sense Amp

Electrical Parameter	Prediction Error[(a)] (%)		F Value
	RMS	Maximum	
Power Supply Circuit Output Current (1V) V_{OH} V_{OS} A_{OL} Recovery Time	109	676	2.2

(a) First 70 units used to generate MLR coefficients. All 140 units used for prediction.

Table 74

Some Rank Correlation Coefficients for the Ionization Response of the μA744 Op Amp

Initial Electrical Parameter	Rank Correlation Coefficients for Transient Ionization Data	
	Response at 4.3×10^6 rad(Si)/s	Saturation Threshold
Saturation Recovery Time	.515	-.857
Slew Rate	.506	-.728
I_{CC}	.625	-.721
A_{OL}	.127	-.178
Input Capacitance	.205	-.502
I_{BIAS}	.255	-.533
I_{OS}	-.165	.292

Table 75

MLR Results for the Ionization Response of the μA744 Op Amp

Initial Electrical Parameters Used For Regression	RMS Prediction Error For Output Response At 4.3×10^6 rad(Si)/s	F Value For Regression	RMS Prediction Error For Saturation Threshold	F Value For Regression
Saturation Time Slew Rate Power Supply Current Input Capacitance Offset Current	107%	18.1	40%	23.6

Table 76

Failure Rates for Parts Subject to Ionizing Rate Tests

Device	Catastrophic Failure Rates (a) (Percent/1,000 hours at 60% Confidence)	
Type \ Group	Control	Stressed
Hex Inverter	1.1	.63
Dual Buffer	3.3	1.4

(a) Drift failures were not included in the failure rate calculations, (1) for the reasons stated in Paragraph 1d, Section V, Volume I and (2) because the particular circuits would still have functioned properly in normal practical applications.

SECTION IV

IONIZING RADIATION TOTAL DOSE HARDNESS ASSURANCE

1. INTRODUCTION

This section discusses the results of the work carried out on the total dose aspects of hardness assurance.

The primary objectives of the study were first, to identify certain surface related electrical parameters which could be used as precursors of radiation sensitivity and hence, which could enable one to predict the expected total dose damage. The second objective was to assess the feasibility of the low dose screening technique. Specifically, the objective was to test the assumption that the devices exhibiting the highest radiation sensitivities during a low dose exposure are the ones most likely to fail at higher doses.

Paragraphs 2 and 3 present the electrical and low dose screening results, respectively, for a group of low-power transistor. Similarly Paragraphs 4 and 5 perform the same functions for an operational amplifier.

2. ELECTRICAL SCREENING - LOW-POWER TRANSISTORS

a. Approach

The following material presents the results of the effort expended in evaluating electrical measurement techniques suitable for screening low-power transistors for total dose effects. The devices selected as vehicles for the study were: 2N709 (npn), 2N930 (npn) and 2N2905A (pnp).

The technical approach to the problem of evaluating electrical screening parameters was to determine the rank correlation coefficients between certain promising surface related, initial parameters and radiation sensitivity. The use of the rank correlation technique immediately implies that the scope of the program was primarily geared to the prediction of the relative radiation sensitivities between devices of different types and of a given type.

The rationale behind the selection of the correlation parameters for the bipolar transistors was discussed in Paragraph 4-a, Section V, Volume 1 and will not be repeated here. The summary of the results of the rank correlation calculations are shown in Table 77 in a sort of generalized form which gives an overview of the total dose task. (The specific list which would also indicate the exact bias conditions is prohibitively long.) As discussed in Paragraph 4, Section V, Volume 1 and as is evident in the tables, correlation was sought in the majority of cases between certain surface dependent initial parameters (or combinations of these) and the "radiation sensitivity" of the device. The radiation sensitivity was thought to be adequately represented by the absolute or relative radiation induced change in the base current. For increased measurement sensitivity the base current was measured at low injection levels (with both fixed V_{BE} and fixed I_E conditions) where the surface effects are dominant. Of course, there are other quantities of practical importance in Table 77, besides the radiation sensitivities, for which correlations with initial parameters were sought, e.g., the absolute and relative changes in gain.

Total dose effects are extremely variable both between device types and between devices of a given type. The three types of low-power transistors, 2N930, 2N709 and 2N2905A, had high, moderate and low radiation sensitivities, respectively. This is shown in Figure 77 where the mean value of the relative change in gain is plotted as a function of dose. (The lower end of the operating current range was used in these plots for increased sensitivity.) The histograms of Figures 78 through 89 illustrate the variability in radiation sensitivity of presumably identical devices. The radiation sensitivities are represented here by low injection ΔI_B, I_B/I_B^o, $\Delta(1/h_{FE})$ $(= \frac{\Delta I_B}{I_C})$, and h_{FE}/h_{FEO}. Tables 78 through 80 show the mean and the covariance of these quantities at various injection levels to give a better overall picture. (Note that the following bias conditions were applied during gamma exposures. 2N709: V_{CB} = +10V and I_E = 20 μA, 2N930: V_{CB} = +26V and I_E = 50 μA, 2N2905A: V_{CB} = -30V and I_E = 40 μA.)

b. Discussions and Conclusions

By scrutinizing the rank correlation tables the following conclusions can be drawn:

1. One of the promising initial parameters, the low frequency 1/f noise showed little correlation with radiation sensitivity. A possible explanation may be that the 1/f noise contains a current dependent term which prevents the determination of the density of the slow states in ungated devices. Hence, any ranking of the devices on the basis of noise will not necessarily mean a corresponding ranking in the density of the slow states. This latter quantity was the one with which correlation with radiation sensitivity was anticipated. Apparently, the current dependence of the 1/f noise obscured any significant correlation.
2. Surprisingly the radiation induced ΔI_B (low injection) did not always correlate well with ΔI_B (high injection) especially at the high end of the operating current range for the 2N709 and the 2N2905A. The correlation is quite good for 2N930. Consequently the practice of using ΔI_B (low injection) for predicting radiation sensitivity at high injection levels, just because ΔI_B (low injection) offers a great increase in measurement sensitivity, has to be treated with caution. The explanation of this effect is not clear at the present time.
3. No significant correlation was found between the radiation sensitivity and various initial parameters, e.g., burn-in changes, I_B, I_{EBO} (or BV_{EBO}) measured at various temperatures, etc. In fact, the correlation is practically nonexistent for the 2N930, slight for the 2N709, and moderate for the 2N2905A. Even the moderate values (≈0.7 - 0.8) of the rank correlation coefficients for the 2N2905A are far too low to expect any of the various initial parameters to be meaningful screening parameters.

The lack of a strong correlation discussed above is perhaps not too surprising. For example: it is well established that the magnitude of the surface components of the pre- and post-irradiation I_B is controlled by two primary factors, namely, by the amount of charge within the oxide and by the density of interface states in the mid gap region. Either of these factors can be dominant in certain cases. Also, it has been shown in the past that in certain oxides there was a correlation between the pre- and post-irradiation density of the interface states (Ref. 18). In such cases, one may expect a correlation between the initial I_B and the radiation induced change in I_B as long as the surface component is always dominated by the interface states; this could have been the case for the 2N2905A. It should be noted that the radiation induced excess base currents (good indicators of radiation sensitivity) tended to be higher in those 2N2905A devices which had higher base currents initially.

In constrast, the amount of radiation induced charge accumulation has not been found to correlate with the initial amount of oxide charge (or the initial interface state density). Hence, whenever the oxide charge dominates the surface component of either or both of the pre- and post-irradiation I_Bs, one does not expect to find any correlation between the initial I_B and the radiation induced changes in I_B. Such might have been the case for the 2N709 and even more so in the 2N930 since the rank correlation coefficients were very low.

4. The consistently high correlation between h_{FEO} and Δh_{FE} is not significant since contrary to expectations it does not guarantee high correlation between pre- and post-irradiation gains, h_{FEO} and h_{FE}, respectively.

The high rank correlation between h_{FEO} and Δh_{FE}, simply implies that devices with higher initial gain will suffer in general more gain loss. This is quite obvious e.g., whenever

the radiation induced base current increase, ΔI_B, is approximately the same for all devices of a given type. Although ΔI_B does vary among the devices (see histograms of ΔI_B in Figures 78, 82, 86) apparently the spread is not large enough to obscure the correlation between h_{FEO} and Δh_{FE}.

5. The utility of the high correlation between h_{FEO} and h_{FE} seems to be limited and the results should be viewed with caution. The correlation appears to offer a useful screening technique against h_{FE} failure [defined by $h_{FE} < (h_{FE})_{min}$] since the initial h_{FEO} distribution can be simply truncated. Figures 90 through 92 containing 2N2905A, 2N709and 2N930 data show the futility of this approach since all of the low gain devices do not fail first. (Incidentally, observe that that the h_{FEO} versus Δh_{FE} correlation is high in all cases; clearly a useless result especially for the 2N930 devices.)

It should be noted that the relatively high rank correlation values for the 2N2905A and in one case for the 2N709 are partially due to the fact that the gain degradations at the higher currents were relatively small. The rank correlation is expected to go down with higher relative gain loss. Furthermore, and this may be the root of the problem, since the degree of correlation between pre- and post-irradiation gain is very much oxide dependent, one cannot be sure ahead of time that a high h_{FEO} versus h_{FE} correlation will exist for any given untested device type. This can be checked out only by extensive experimental work which is just what we are trying to avoid by a simple electrical screen.

In other words, any given initial parameter which shows a good correlation with radiation sensitivity only in certain transistor types but not in others and whose behavior is not predictable, will have only limited significance, if any. Right now such seems to be the case with those initial parameters yielding reasonable good correlation in the 2N2905A but not in the 2N709 or the 2N930.

6. Higher gain devices tend to suffer more relative gain loss ($\Delta h_{FE}/h_{FE}$) in certain device types. The effect is clearly indicated for the 2N2905A, slightly indicated for the 2N709 and is completely absent for the 2N930. Again, the problem of complete inconsistency in behavior among the device types makes it impossible to generalize.

3. LOW-POWER TRANSISTORS - LOW DOSE SCREENING

The basic idea behind low dose screening is that devices which exhibit a relatively large radiation sensitivity during a low dose exposure are the ones which are most likely to fail after exposure to a larger dose. The approach to test this hypothesis was rather direct; comparisons were made of the tails of the histograms of radiation sensitivities at low and at high doses. The radiation sensitivities were defined in terms of I_B changes at both low and high injection levels. First, an arbitrary value of ΔI_B^* at high dose was selected and it was asserted that all devices with values of $\Delta I_B \geq \Delta I_B^*$ were to be rejected by the screen. The position of each ΔI_B of the devices in this group was then located on the low dose historgrams. Were they also located at the appropriate tail? In general they were <u>not</u> and hence, the reliability of low dose screening is very much in doubt. This conclusion was also supported by the rank correlation coefficients between the quantities ΔI_B (low dose) and ΔI_B (high dose). As shown in Table 81 the values of the correlation coefficients are much lower than might have been expected.

In the following material, the results and conclusions for each device type will be discussed separately.

a. 2N930

Histograms of ΔI_B @(3.0×10^5 rads) and ΔI_B @(1.0×10^5 rads) were compared at four test conditions. Devices in the part of the histogram with the largest ΔI_B @(3.0×10^5 rads) were generally scattered through a relatively large part of the histogram showing the ΔI_Bs at 1.0×10^5 rads (see Figure 93). These data are summarized in Table 82 where it is shown, specifically, that to eliminate the N devices having largest ΔI_B in the R rows of the 3.0×10^5 rads histogram would require

screening out M devices contained in the P rows of the 1.0×10^5 rads histogram. Both Table 82 and Figure 93 emphasize the fact that low dose screening does not seem to be a viable technique for our 2N930 transistors.

b. 2N2905A

The data for the 2N2905A can be treated in the same fashion as that for the preceding device type, 2N930.

To eliminate the N devices having largest ΔI_B in the R rows of the 5.6×10^6 rads histogram would require screening out M devices contained in the P rows of the 1.7×10^5 rads histogram (see Figure 94 and Table 83). On the basis of these data, the low dose screening does not seem to be a viable technique for our 2N2905A transistors.

c. 2N709

Histograms of ΔI_B (1.7×10^5 rads) were compared with histograms of ΔI_B (1.3×10^6 rads) at three bias conditions, I_E = 100 μA, 10 mA, and 3 μA. In the I_E = 100 μA and 10 mA data devices in the part of the 1.3×10^6 rads histogram with the largest ΔI_B were found in the higher tail of the lower dose (1.7×10^5 rads) histogram. The best predictability seems to occur for the 100 μA bias condition. The results at I_E = 3 μA showed significantly poorer predictability and were more like the data analyzed for the 2N930 and the 2N2905A. One apparent difference in the histograms of ΔI_B for the 2N709 is that the maximum values of ΔI_B were 1.5 to 4 times the mean, whereas for the 2N930 and 2N2905A device types the large values of ΔI_B were typically only 20% to 50% greater than the mean. In other words, the coefficient of variation for the 2N709 distribution was much larger for the 2N709 than for the other device types. Table 84 summarizes the capability to eliminate the N devices in the R rows of largest ΔI_B in the 1.3×10^6 rads histogram by screening out P rows containing M devices in the 1.7×10^5 rads histogram. Figure 95 shows an example of the procedure used in the analysis. As seen in this figure and in Table 84, the low dose screening does not seem to be a viable technique for our 2N709 transistors.

4. ELECTRICAL SCREENING - μA744 OPERATIONAL AMPLIFIER

The problems of predicting total dose damage for the μA744 operational amplifiers are in many ways similar to those encountered with the bipolar transistors. The most sensitive parameters of an op amp in a total dose environment are the input bias currents which are simply the base currents of the input transistors. It is important to note, however, that the radiation induced increase in I_B is somewhat reduced, one might say partially compensated, by the constant emitter current biasing circuit.

The rationale behind the selection of the primary correlation parameters, the bias currents, was discussed in Paragraph 4-b, Section V, Volume 1 in some detail and will not be repeated again. The radiation sensitivity is defined by the absolute or relative changes in the bias currents, similar to the procedure used for bipolar transistors.

The μA744 op amp exhibited a "medium" radiation sensitivity in I_B during total dose exposure. Although not very high it was by no means negligible! (It should be noted that the op amps were irradiated at bias voltages of +15V and -5V respectively in order to maximize the reverse biases across the junctions during exposure.) The initial base current, I_B^o distribution is illustrated in Figure 96, and the effects of the radiation are shown in the ΔI_B and the I_B histograms in Figures 97 and 98. The data emphasizes one very important message. The use of a failure level definition of $I_B \geq 750$ μA essentially a Honeywell specification will reject 6%, 17% and 21% of the op amps after doses of 2.7×10^5 rads, 1.3×10^6 rads and 5.6×10^6 rads, respectively.

Table 85 shows the rank correlation coefficients between the various initial parameters (noise and others related to I_B) and the radiation sensitivities of the op amps. As seen, there is a definite hint of correlation between the relative changes in the bias currents and the initial parameters. However, the values of the coefficients (≤ 0.5) are not high enough to have any statistical significance for screening purposes.

5. LOW DOSE SCREENING - μA744 OPERATIONAL AMPLIFIER

The approach to test the applicability to the μA744 of the basic premise of the low dose screening, "devices exhibiting high radiation sensitivity at low dose are the ones most likely to fail at high dose" was the same as presented for bipolar transistors. Namely, the tails of the histograms of the "radiation sensitivity" (measured by the change in the bias current, I_B) at low and high doses were compared to determine if the devices maintained their relative positions in the two histograms. As for the bipolars, the simple approach to low dose screening did not work. Too many devices would have had to be eliminated after the low dose test in order to make sure that those few exhibiting excessively high radiation sensitivity at the high doses were indeed removed. This conclusion is further supported by the following poor rank correlation value between low and high dose radiation sensitivities.

Low Dose Sensitivity	High Dose Sensitivity	Correlation Coefficient
$[I_B(2.7 \times 10^5 \text{ rads}) - I_B^o]$	$[I_B(5.6 \times 10^6 \text{ rads}) - I_B^o]$	0.629

After eliminating from consideration all devices with poor or suspect data we found that those devices in the 5 rows of the histogram corresponding to the largest values of ΔI_B at 5.6×10^6 rads were scattered almost randomly through 15 rows of the highest ΔI_Bs in the 2.7×10^5 rads histogram. Precisely, to screen out the N devices in the highest R rows of the 5.6×10^6 rads histogram requires elimination of the highest P rows containing M devices in the 2.7×10^5 rads histogram. The results are summarized in Table 86. Again, the conclusion is the same as for the bipolar transistors i.e., the low dose screening did not seem to be a viable technique for our μA744 op amps.

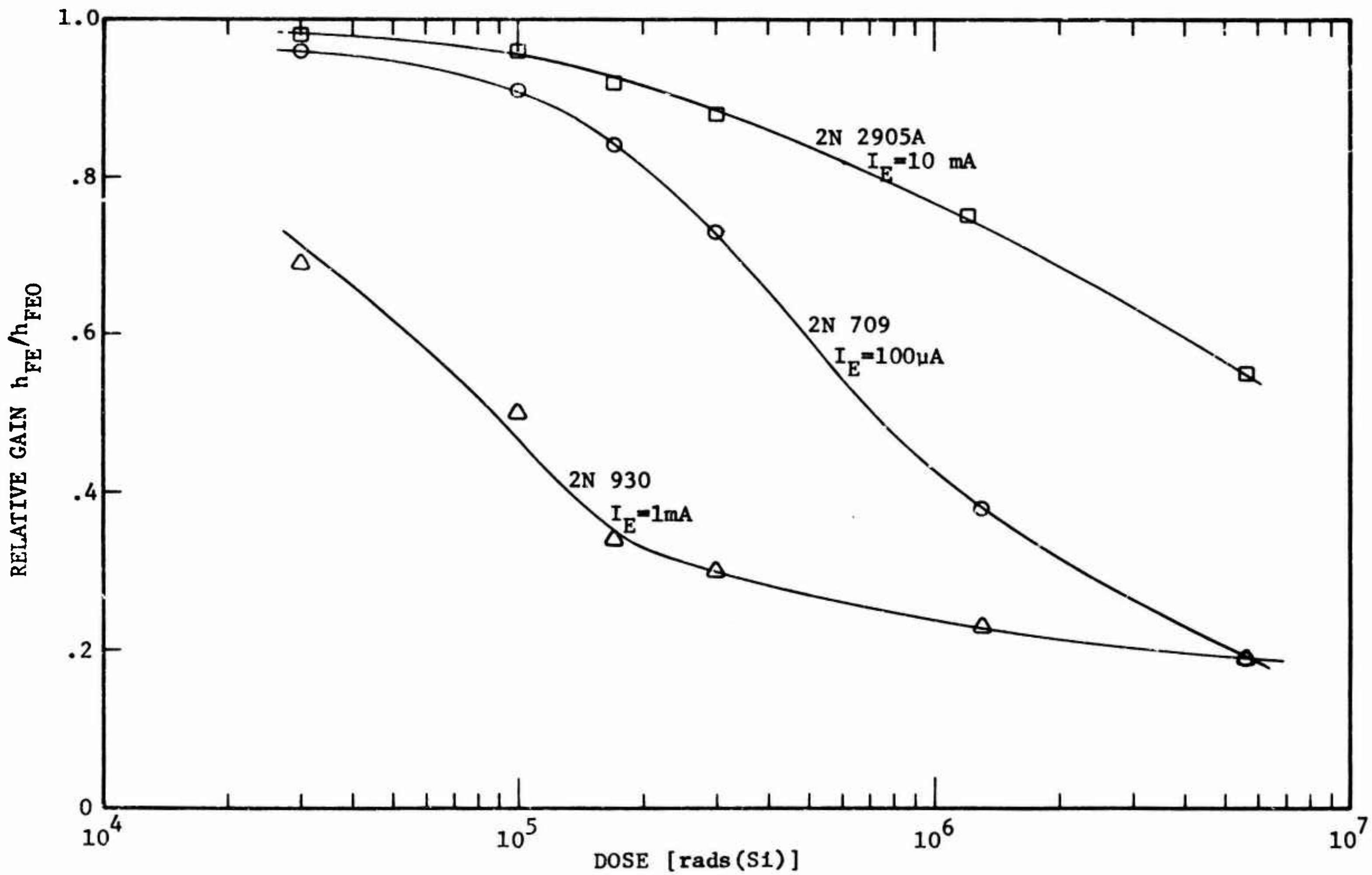

Figure 77. Illustration of the Relative Radiation Sensitivities of 2N709, 2N930 and 2N2905A

```
DEVICE 2N709   TEST 501   TEMP 22.   STRESS 1.25 E6        F4000              BRL366                          06 JUL 73

NO.   PER     TEST                                         MEDIAN         MEAN          STD. DEV.      COVAR.(%)
      CENT    IB        IE=  3UAVCB= 0 V                   5.117E-07      6.040E-07     3.747E-07      62.04

  0    0.0   -6.49E-07  .
  0    0.0   -5.79E-07  .
  0    0.0   -5.10E-07  .
  0    0.0   -4.41E-07  .
  0    0.0   -3.72E-07  .
  0    0.0   -3.02E-07  .
  0    0.0   -2.33E-07  .
  0    0.0   -1.64E-07  .
  0    0.0   -9.47E-08  .
  0    0.0   -2.54E-08  .
  0    0.0    4.39E-08  .
  2    1.6    1.13E-07  .502537
 11    8.6    1.82E-07  .488490501515516517525536538568574
  7    5.5    2.52E-07  .462469503506541547572
 13   10.2    3.21E-07  .451463464494494507508509526542570571575
 13   10.2    3.90E-07  .443465465493487495496503510535543544569
 17   13.3    4.59E-07  .439456467468472473474475492505511531534535554556557
 10    7.8    5.28E-07  .438442456458471482491549555565
 15   11.7    5.97E-07  .450451453455457470498512514518523551555560561
  7    5.5    6.67E-07  .447454460513522546576
  5    3.9    7.36E-07  .440459522550563
  3    2.3    8.05E-07  .445494564
  2    1.6    8.75E-07  .441562
  4    3.1    9.44E-07  .452479532565
  2    1.6    1.01E-06  .499521
  4    3.1    1.08E-06  .444464519522
  2    1.6    1.15E-06  .480495
  0    0.0    1.22E-06  .
  2    1.6    1.29E-06  .457458
  1    0.8    1.36E-06  .567
  2    1.6    1.43E-06  .491520
  1    0.8    1.50E-06  .545
  0    0.0    1.57E-06  .
  3    2.3    1.64E-06  .527532552
  0    0.0    1.71E-06  .
  1    0.8    1.77E-06  .590
  0    0.0    1.84E-06  .
  0    0.0    1.91E-06  .
  1    0.8    1.98E-06  .443

128                     0         5         10        15        20        25        30
```

Figure 78. Histogram of ΔI_B Illustrating the Variation in the Radiation Sensitivities Among the 2N709 Transistors of Different Wafers (Dose = 1.25 x 10^6 rads; I_E = 3 μA)

```
DEVICE 2N709    TEST 501   TEMP 22.   STRESS 1.25 E6       F4000            BRL366                     06 JUL 73

NO.   PER      TEST                                   MEDIAN       MEAN        STD. DEV.     COVAR.(%)
      CENT     I9        IE=  3UAVCB= 0 V             4.705E 00    5.398E 00   2.712E 00     50.24

 0     0.0   -4.15E 00  .
 0     0.0   -3.62E 00  .
 0     0.0   -3.09E 00  .
 0     0.0   -2.55E 00  .
 0     0.0   -2.03E 00  .
 0     0.0   -1.50E 00  .
 0     0.0   -9.59E-01  .
 0     0.0   -4.39E-01  .
 0     0.0    9.08E-02  .
 0     0.0    6.21E-01  .
 1     0.8    1.15E 00  .516
 3     2.3    1.69E 00  .537572574
 9     7.0    2.21E 00  .438500501502515536538539575
10     7.8    2.74E 00  .473489484496498490505517525541
11     8.6    3.27E 00  .443464467469487494496538510547568
15    11.7    3.80E 00  .439450454664684714744754955035245533542543570
12     9.4    4.33E 00  .449461462463472483504507509513531556
11     8.6    4.86E 00  .455470511512514534535544545571576
 8     6.3    5.39E 00  .442448453479482471523569
 7     5.5    5.92E 00  .451458492514520555564
 5     3.9    6.45E 00  .455495560561566
 4     3.1    6.98E 00  .440522546563
 6     4.7    7.51E 00  .447485525545557558
 6     4.7    8.04E 00  .457460519521528562
 6     4.7    8.57E 00  .444445544599498527
 1     0.8    9.10E 00  .557
 5     3.9    9.63E 00  .452480437551565
 1     0.8    1.02E 01  .553
 0     0.0    1.07E 01  .
 2     1.6    1.12E 01  .446549
 1     0.8    1.17E 01  .553
 0     0.0    1.23E 01  .
 1     0.8    1.28E 01  .481
 0     0.0    1.33E 01  .
 0     0.0    1.39E 01  .
 1     0.8    1.44E 01  .550
 1     0.8    1.49E 01  .548
 0     0.0    1.55E 01  .
 0     0.0    1.60E 01  .

                        0         5         10        15        20        25        30

THE FOLLOWING DEVICE(S) ARE OUTSIDE THE RANGE OF THE HISTOGRAM
00000552  2.290E 01
```

Figure 79. Histograms of I_B/I_B^o Illustrating the Variation in the Radiation Sensitivities Among the 2N709 Transistors of Different Wafers (Dose = 1.25 x 10^6 rads; I_E = 3 µA)

```
DEVICE 2N7C9    TEST 5D1   TEMP 22.   STRESS 1.25 E6        F4000              BRL366                          06 JUL 73

NO.   PER       TEST                                       MEDIAN        MEAN        STD. DEV.     COVAR.(%)
      CENT      HFE     IE=1COUAVC3= O.V                  3.670E-01     3.717E-01    1.231E-01      33.12

  0    0.0   -6.72E-02   .
  0    0.0   -4.38E-02   .
  0    0.0   -2.04E-02   .
  0    0.0    2.78E-03   .
  0    0.0    2.64E-02   .
  0    0.0    4.98E-02   .
  0    0.0    7.32E-02   .
  1    0.8    9.66E-02   .552
  1    0.8    1.20E-01   .550
  0    0.0    1.43E-01   .
  3    2.3    1.67E-01   .481548553
  3    2.3    1.90E-01   .443527567
  4    3.1    2.14E-01   .446480497549
 10    7.8    2.37E-01   .44445245851952054555195585545c5
 10    7.8    2.60E-01   .44545445346049952152853253356 2
 11    8.6    2.84E-01   .4404474484574794855225465545575 64
  5    3.9    3.07E-01   .4534565 6C563566
  6    4.7    3.31E-01   .451455455518555561
  7    7.0    3.54E-01   .44248 44149251352353555 6569
  8    6.3    3.77E-01   .45051151251453454445 71576
  8    6.3    4.01E-01   .44946145347047150 7531543
  9    7.0    4.24E-01   .43946247248349550 6509526542
  9    7.0    4.48E-01   .45546 64754854965035085105 70
  8    6.3    4.71E-01   .45746 854744844874945 05547
  7    5.5    4.94E-01   .43946446547350054156 8
  3    2.3    5.18E-01   .498525539
  3    2.3    5.41E-01   .439432517
  3    2.3    5.65E-01   .501515575
  3    2.3    5.88E-01   .502536538
  0    0.0    6.11E-01   .
  2    1.6    6.35E-01   .537572
  0    0.0    6.58E-01   .
  0    0.0    6.82E-01   .
  2    1.6    7.05E-01   .516574
  0    0.0    7.29E-01   .
  0    0.0    7.52E-01   .
  0    0.0    7.75E-01   .
  0    0.0    7.99E-01   .
  0    0.0    8.22E-01   .

128                      0          5          10          15          20          25          30
```

Figure 80. Histogram of h_{FE}/h_{FEO} Illustrating the Variation in the Radiation Sensitivities Among the 2N709 Transistors of Different Wafers (Dose = 1.25×10^6 rads; I_E = 100 μA)

```
DEVICE 2N709   TEST 501   TEMP 22.   STRESS 1.25 E6        F4000           HRL365                 06 JUL 73

NO.   PER     TEST                                     MEDIAN       MEAN        STD. DEV.     COVAR.(%)
      CENT                                             4.436E-02    5.214E-02   3.074E-02     58.96

  0    0.0   -4.75E-02  .
  0    0.0   -4.17E-02  .
  0    0.0   -3.56E-02  .
  0    0.0   -3.03E-02  .
  0    0.0   -2.46E-02  .
  0    0.0   -1.88E-02  .
  0    0.0   -1.31E-02  .
  0    0.0   -7.34E-03  .
  0    0.0   -1.66E-03  .
  0    0.0    4.07E-03  .
  0    0.0    9.7[illegible]E-03  .
  3    2.3    1.5[illegible]E-02  .502537569
 10    7.9    2.1[illegible]E-02  .483490501515516517525526538541
 14   10.9    2.70[illegible]E-02  .4614624434895005065075095425475695705715.74
 13   10.2    3.27E-02  .4494844945035045105265435445545557572575
 11    8.6    3.84E-02  .4644694834874959651153453954955[illegible]
 22   17.2    4.4[illegible]E-02  .4[illegible]
 12    9.4    4.[illegible]E-02  .4[illegible]
 10    7.8    5.[illegible]E-02  .4[illegible]
  5    3.9    6.1[illegible]E-02  .44351[illegible]
  3    2.3    6.71E-02  .4[illegible]
  3    2.3    7.29E-02  .4[illegible]
  2    1.6    7.95E-02  .[illegible]
  2    1.6    8.42E-02  .4[illegible]
  5    3.9    9.[illegible]E-02  .4[illegible]
  0    0.0    9.57E-02  .
  2    1.6    1.01E-01  .480485
  0    0.0    1.07E-01  .
  0    0.0    1.13E-01  .
  2    1.6    1.19E-01  .497492
  1    0.8    1.24E-01  .507
  0    0.0    1.30E-01  .
  1    0.8    1.36E-01  .552
  2    1.6    1.41E-01  .481520
  0    0.0    1.47E-01  .
  2    1.6    1.53E-01  .527550
  0    0.0    1.59E-01  .
  0    0.0    1.64E-01  .
  1    0.8    1.70E-01  .545

128                     0         5          10         15         20         25         30

THE FOLLOWING DEVICE(S) ARE OUTSIDE THE RANGE OF THE HISTOGRAM

0[illegible]   4.[illegible]E-01     [illegible]   1.767E-01
```

Figure 81. Histogram of $\Delta(1/h_{FE}) = \Delta I_B/I_C$ Illustrating the Variation in the Radiation Sensitivities Among the 2N709 Transistors of Different Wafers (Dose = 1.25×10^6 rads; I_E = 100 μA)

```
DEVICE 2N930   TEST 401  TEMP 22.  STRESS 3.00 E5      F4000            BRL359                        06 JUL 73
-------------------------------------------------------------------------------------------------------------------
NO.   PER      TEST                                          MEDIAN      MEAN        STD. DEV.    COVAR.(%)
      CENT     IB        IE=  1UAVCB= 0 V                    1.672E-07   1.532E-07   4.539E-08    29.63
-------------------------------------------------------------------------------------------------------------------

  0    0.0   -2.43E-08  .
  0    0.0   -1.57E-08  .
  0    0.0   -6.65E-09  .
  0    0.0    2.42E-09  .
  0    0.0    1.15E-08  .
  0    0.0    2.05E-08  .
  0    0.0    2.96E-08  .
  0    0.0    3.87E-08  .
  0    0.0    4.77E-08  .
  0    0.0    5.68E-08  .
  0    0.0    6.59E-08  .
  4    2.7    7.49E-08  .013029033040
 10    6.8    8.40E-08  .012014017018022027028030032060
 12    8.1    9.30E-08  .015016024025036038059061062065075133
 17   11.5    1.02E-07  .011019020021026031034035037039041042054055101121154
  5    3.4    1.11E-07  .049081087102119
  3    2.0    1.20E-07  .077083142
  3    2.0    1.29E-07  .128148155
  2    1.4    1.38E-07  .136143
  2    1.4    1.47E-07  .130132
  7    4.7    1.56E-07  .023035054139140149157
 18   12.2    1.65E-07  .043047049034089095096098099106107115125134141152153160
 12    8.1    1.75E-07  .057058071073090086090092108111139147
  9    6.1    1.84E-07  .044054064067069078082114118
 16   10.8    1.93E-07  .046051053056066068074085091104113123127137146150
 13    8.8    2.02E-07  .052070072075079095109120129121135144151
 10    6.8    2.11E-07  .053088100103116122124126145156
  4    2.7    2.20E-07  .093097112117
  0    0.0    2.29E-07  .
  1    0.7    2.38E-07  .110
  0    0.0    2.47E-07  .
  0    0.0    2.56E-07  .
  0    0.0    2.65E-07  .
  0    0.0    2.74E-07  .
  0    0.0    2.83E-07  .
  0    0.0    2.92E-07  .
  0    0.0    3.01E-07  .
  0    0.0    3.11E-07  .
  0    0.0    3.20E-07  .

-------------------------------------------------------------------------------------------------------------------
148                     0         5         10         15         20         25         30
```

Figure 82. Histogram of ΔI_B Illustrating the Variation in the Radiation Sensitivities Among the 2N930 Transistors of Different Wafers (Dose = 3.0×10^5 rads ; I_E = 1 μA)

```
DEVICE 2N930   TEST 401  TEMP 22.  STRESS 3.00 E5      F4000           BRL359                              06 JUL 73
---------------------------------------------------------------------------------------------------------------------
NO.   PER     TEST                                        MEDIAN       MEAN       STD. DEV.    COVAR.(%)
      CENT    IB       IE=  1UAVCB= 0 V                   2.013E 01    2.006E 01  6.296E 00    31.38
---------------------------------------------------------------------------------------------------------------------

  0    0.0   -2.91E 00  .
  0    0.0   -1.72E 00  .
  0    0.0   -5.34E-01  .
  0    0.0    6.55E-01  .
  0    0.0    1.84E 00  .
  0    0.0    3.03E 00  .
  0    0.0    4.22E 00  .
  0    0.0    5.41E 00  .
  0    0.0    6.60E 00  .
  0    0.0    7.79E 00  .
  0    0.0    8.98E 00  .
  5    3.4    1.02E 01  .013036042075C87
 10    6.8    1.14E 01  .012022028C38C40049065101119121
  8    5.4    1.25E 01  .035041055C6C062082089133
 11    7.4    1.37E 01  .011015C15027029031033054C59102143
 10    6.8    1.49E 01  .016017032003039051086125132154
  7    4.7    1.61E 01  .01403203709114C142152
 10    6.8    1.73E 01  .024025034077090126136141157160
  8    5.4    1.85E 01  .021026082C84C94099118149
  6    4.1    1.97E 01  .106134135138148155
  8    5.4    2.09E 01  .0190740910551081271301 5
 14    9.5    2.21E 01  .048064067065076073096098107114123139147150
 10    6.8    2.33E 01  .023044053057072045092116120153
 10    6.8    2.44E 01  .043046047072087010411211151 29137
  7    4.7    2.56E 01  .05507408311712213114 6
  9    6.1    2.68E 01  .045051052053056078105145156
  6    4.1    2.80E 01  .058063109113124126
  1    0.7    2.92E 01  .068
  1    0.7    3.04E 01  .144
  2    1.4    3.16E 01  .093110
  2    1.4    3.28E 01  .048111
  1    0.7    3.40E 01  .103
  0    0.0    3.51E 01  .
  0    0.0    3.63E 01  .
  0    0.0    3.75E 01  .
  0    0.0    3.87E 01  .
  1    0.7    3.99E 01  .097
  1    0.7    4.11E 01  .100
  0    0.0    4.23E 01  .

---------------------------------------------------------------------------------------------------------------------
148                     0         5         10        15        20        25        30
```

Figure 83. Histogram of I_B/I_B^0 Illustrating the Variation in the Radiation Sensitivities Among the 2N930 Transistors of Different Wafers (Dose = 3.0 x 10^5 rads; I_E = 1 μA)

DEVICE 2N930 TEST 4D1 TEMP 22. STRESS 3.00 E5 F4000 BRL359 06 JUL 73

NO.	PER CENT	TEST HFE	IE= 1MAVCB= 0.V	MEDIAN 3.004E-01	MEAN 2.967E-01	STD. DEV. 5.507E-02	COVAR.(%) 18.56
0	0.0	7.32E-02	.				
0	0.0	8.49E-02	.				
0	0.0	9.65E-02	.				
0	0.0	1.08E-01	.				
0	0.0	1.20E-01	.				
0	0.0	1.31E-01	.				
0	0.0	1.43E-01	.				
0	0.0	1.55E-01	.				
0	0.0	1.66E-01	.				
0	0.0	1.78E-01	.				
1	0.7	1.89E-01	.068				
2	1.4	2.01E-01	.045066				
11	7.4	2.13E-01	.051052053056058063067078079097100				
10	6.8	2.24E-01	.023043046048070071072089086103				
8	5.4	2.36E-01	.044047050057069073076115				
6	4.1	2.48E-01	.033059107110111114				
11	7.4	2.59E-01	.064074092096105109117124126144156				
9	6.1	2.71E-01	.094094095099105122129131145				
7	4.7	2.83E-01	.077090091109123137146				
8	5.4	2.94E-01	.019034085089113119120155				
13	8.8	3.06E-01	.014017026082085112116127135139147150151				
10	6.8	3.17E-01	.016021024025031032104130134155				
14	9.5	3.29E-01	.011027029040023037039061112128139148149160				
6	4.1	3.40E-01	.018054059135142154				
6	4.1	3.52E-01	.020055060141142157				
11	7.4	3.64E-01	.012015022029035041062121125132140				
6	4.1	3.75E-01	.033042065083102133				
4	2.7	3.87E-01	.013040075143				
4	2.7	3.99E-01	.036049101119				
0	0.0	4.10E-01	.				
1	0.7	4.22E-01	.087				
0	0.0	4.33E-01	.				
0	0.0	4.45E-01	.				
0	0.0	4.57E-01	.				
0	0.0	4.68E-01	.				
0	0.0	4.80E-01	.				
0	0.0	4.92E-01	.				
0	0.0	5.03E-01	.				
0	0.0	5.15E-01	.				
149			0 5 10 15 20 25 30				

Figure 84. Histogram of h_{FE}/h_{FEO} Illustrating the Variation in the Radiation Sensitivities Among the 2N930 Transistors of Different Wafers (Dose = 3.0×10^5 rads; I_E = 1 mA)

```
DEVICE 2N930   TEST 401   TEMP 22.   STRESS 3.00 E5        F4000            BPL359                  06 JUL 73
-------------------------------------------------------------------------------------------------------------------
NO.   PER     TEST                                      MEDIAN        MEAN        STD. DEV.     COVAR.(%)
      CENT                                             9.787E-03    9.271E-03    2.398E-03      25.87
-------------------------------------------------------------------------------------------------------------------

  0    0.0   1.59E-04  .
  0    0.0   6.36E-04  .
  0    0.0   1.11E-03  .
  0    0.0   1.59E-03  .
  0    0.0   2.07E-03  .
  0    0.0   2.54E-03  .
  0    0.0   3.02E-03  .
  0    0.0   3.50E-03  .
  0    0.0   3.97E-03  .
  0    0.0   4.45E-03  .
  0    0.0   4.93E-03  .
  7    4.7   5.40E-03  .013017022027029033040
  7    4.7   5.88E-03  .011014016018028030042
 19   12.8   6.35E-03  .012015024025026031032034035036039059060061075081087101102
 13    8.8   6.83E-03  .019020021037039041054055062065083119133
  6    4.1   7.31E-03  .049121128140154155
  4    2.7   7.79E-03  .077130136142
  2    1.4   8.27E-03  .143149
  7    4.7   8.74E-03  .126132134139140157160
  5    3.4   9.22E-03  .094111141152153
  4    2.7   9.70E-03  .023113138147
  7    4.7   1.02E-02  .034092058093107127150
 14    9.5   1.07E-02  .047050057065080089090095096106115137144146
 19   12.8   1.11E-02  .043044045048067071073082104109114120122123129131135145151
 12    8.1   1.16E-02  .038069078080084100109116118124126156
  7    4.7   1.21E-02  .051064066093103105112
 11    7.4   1.26E-02  .045052053055066070072074076091097
  3    2.0   1.31E-02  .063079117
  0    0.0   1.35E-02  .
  1    0.7   1.40E-02  .110
  0    0.0   1.45E-02  .
  0    0.0   1.49E-02  .
  0    0.0   1.54E-02  .
  0    0.0   1.59E-02  .
  0    0.0   1.64E-02  .
  0    0.0   1.69E-02  .
  0    0.0   1.73E-02  .
  0    0.0   1.78E-02  .
  0    0.0   1.83E-02  .

-------------------------------------------------------------------------------------------------------------------
144                    0         5         10         15         20         25         30
```

Figure 85. Histogram of $\Delta(1/h_{FE}) = \Delta I_B/I_C$ Illustrating the Variation in the Radiation Sensitivities Among the 2N930 Transistors of Different Wafers (Dose = 3.0×10^5 rads; I_E = 1 mA)

```
DEVICE 2N2905A TEST 6D1   TEMP 22.  STRESS 5.60 E6       F4000            BRL371                   06 JUL 73

NO.   PER     TEST                                          MEDIAN       MEAN       STD. DEV.      COVAR.(%)
      CENT    IB       IE=  3UAVCB= 0 V                   -1.810E-07  -1.783E-07   2.646E-08       14.94

  0    0.0  -2.77E-07
  0    0.0  -2.72E-07  .
  0    0.0  -2.67E-07  .
  0    0.0  -2.61E-07  .
  0    0.0  -2.56E-07  .
  1    0.7  -2.51E-07  .289
  0    0.0  -2.46E-07  .
  1    0.7  -2.41E-07  .354
  2    1.4  -2.36E-07  .281284
  1    0.7  -2.31E-07  .329
  1    0.7  -2.25E-07  .287
  2    1.4  -2.20E-07  .285313
  7    5.0  -2.15E-07  .291303307308314317334
  2    1.4  -2.10E-07  .311318
  7    5.0  -2.05E-07  .276282296310316320326
  4    2.8  -2.00E-07  .202299312347
 10    7.1  -1.94E-07  .230245278290301302315340346348
 13    9.2  -1.89E-07  .257286300309325327337342344352356359360
 12    8.5  -1.84E-07  .231248255268268292319335350351355358
 17   12.1  -1.79E-07  .217229237254261269294304321331332333358359394349357
 10    7.1  -1.74E-07  .233240262264305306322330343353
  7    5.0  -1.69E-07  .220241253260279280324
  6    4.3  -1.64E-07  .225226238247250251
 11    7.8  -1.58E-07  .227236242243259266267271273274345
  7    5.0  -1.53E-07  .224232234235258323336
  6    4.3  -1.48E-07  .218249252263270272
  5    3.5  -1.43E-07  .239246256265283
  2    1.4  -1.38E-07  .277328
  1    0.7  -1.33E-07  .275
  2    1.4  -1.27E-07  .216222
  0    0.0  -1.22E-07  .
  0    0.0  -1.17E-07  .
  2    1.4  -1.12E-07  .219244
  0    0.0  -1.07E-07  .
  0    0.0  -1.02E-07  .
  0    0.0  -9.65E-08  .
  1    0.7  -9.14E-08  .223
  0    0.0  -8.62E-08  .
  0    0.0  -8.11E-08  .

140                    0         5        10        15        20        25        30

THE FOLLOWING DEVICE(S) ARE OUTSIDE THE RANGE OF THE HISTOGRAM

C0000214 -1.20CE-09
```

Figure 86. Histogram of ΔI_B Illustrating the Variation in the Radiation Sensitivities Among the 2N2905A Transistors of Different Wafers (Dose = 5.6 x 10^6 rads; I_E = 3 μA)

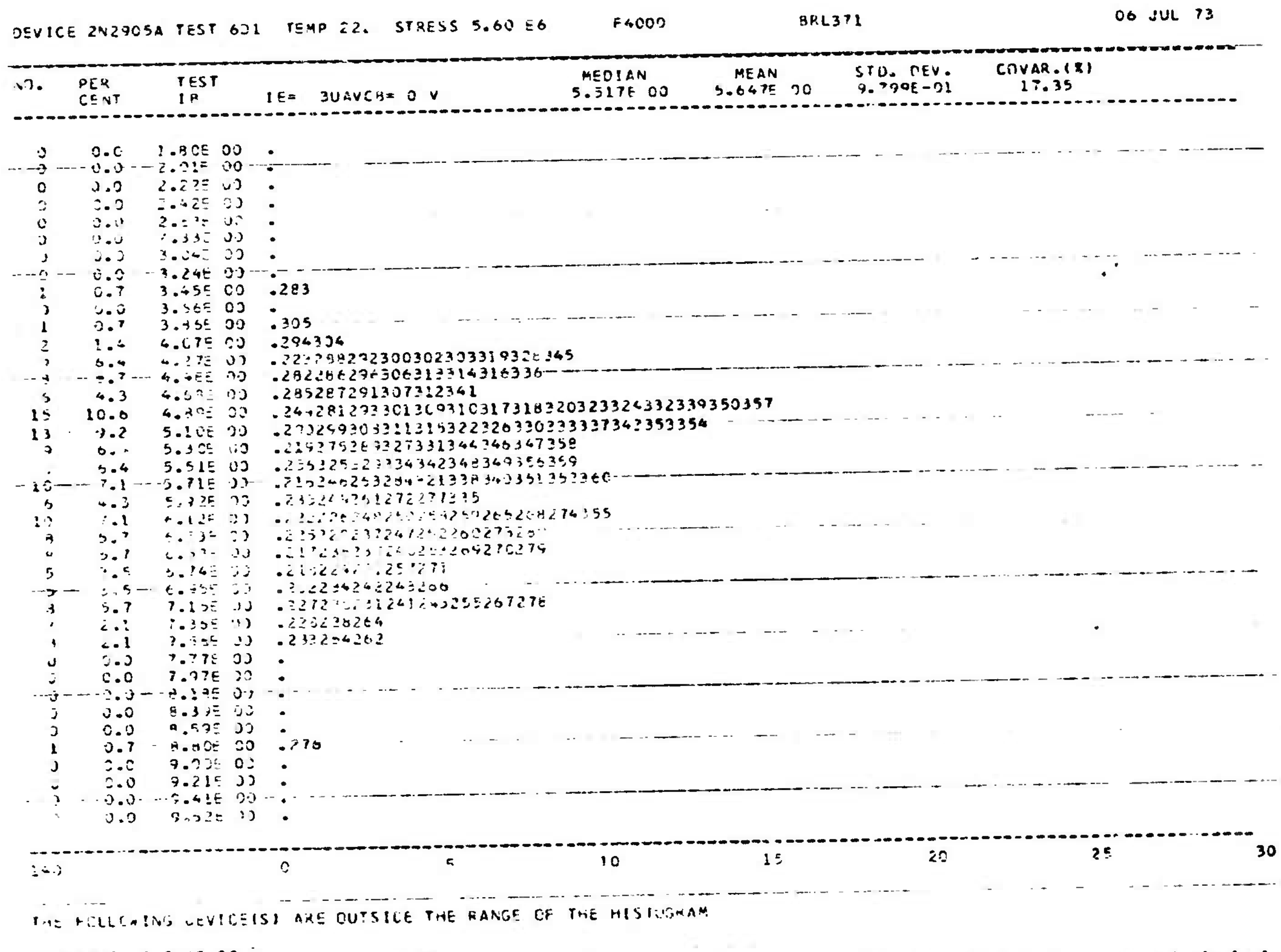

Figure 87. Histogram of I_B/I_B^o Illustrating the Variation in the Radiation Sensitivities Among the 2N2905A Transistors of Different Wafers (Dose = 5.6×10^6 rads; I_E = 3 μA)

```
DEVICE 2N2905A TEST 601   TEMP 22.   STRESS 5.40 E6        F4000             BRL371                         06 JUL 73

NO.   PER     TEST                                          MEDIAN        MEAN         STD. DEV.     COVAR.(%)
      CENT    HFE       IE=  3MAVCB= 0.V                    5.112E-01     5.082E-01    3.987E-02     7.85

  0    0.0   3.49E-01   .
  0    0.0   3.56E-01   .
  0    0.0   3.65E-01   .
  0    0.0   3.73E-01   .
  0    0.0   3.81E-01   .
  0    0.0   3.90E-01   .
  0    0.0   3.98E-01   .
  0    0.0   4.07E-01   .
  0    0.0   4.15E-01   .
  1    0.7   4.23E-01   .276
  0    0.0   4.32E-01   .
  3    2.1   4.40E-01   .233228262
 10    7.1   4.49E-01   .227228230234241242254264266267
  9    6.4   4.57E-01   .224231232239243245251255271
  6    4.3   4.65E-01   .213236252257270278
 10    7.1   4.74E-01   .225229240253258260269273279280
 13    9.2   4.82E-01   .225235237245247249250259263265272274277
  4    2.8   4.91E-01   .217245268355
  5    3.5   4.99E-01   .222261275321335
  9    6.4   5.08E-01   .219244256332340349351352360
  7    5.0   5.16E-01   .215264325331342356359
 12    8.5   5.24E-01   .322327329333334343344346347348353358
 16   11.3   5.33E-01   .223289295[illegible]311315320323[illegible]332333337339350397
  9    6.4   5.41E-01   .281293301301310317318324354
  5    3.5   5.50E-01   .245296291312341
  7    5.0   5.58E-01   .287296307314328336345
  7    5.0   5.66E-01   .282298302306313316319
  4    2.8   5.75E-01   .[illegible]294300301
  1    0.7   5.83E-01   .304
  1    0.7   5.92E-01   .305
  0    0.0   6.00E-01   .
  1    0.7   6.09E-01   .283
  0    0.0   6.17E-01   .
  0    0.0   6.25E-01   .
  0    0.0   6.34E-01   .
  0    0.0   6.42E-01   .
  0    0.0   6.51E-01   .
  0    0.0   6.59E-01   .
  0    0.0   6.67E-01   .

140                     0           5           10          15          20          25          30

THE FOLLOWING DEVICE(S) ARE OUTSIDE THE RANGE OF THE HISTOGRAM

C0090215   6.725E-01
```

Figure 88. Histogram of h_{FE}/h_{FEO} Illustrating the Variation in the Radiation Sensitivities Among the 2N2905A Transistors of Different Wafers (Dose = 5.6×10^6 rads; I_E = 3 mA)

DEVICE 2N2905A TEST 601 TEMP 22. STRESS 5.60 E6 F4000 BPL371 06 JUL 73

NO.	PER CENT	TEST		MEDIAN	MEAN	STD. DEV.	COVAR.(%)
				7.323E-03	7.423E-03	8.452E-04	11.39
0	0.0	4.61E-03	.				
0	0.0	4.76E-03	.				
0	0.0	4.91E-03	.				
1	0.7	5.07E-03	.223				
0	0.0	5.22E-03	.				
0	0.0	5.37E-03	.				
2	1.4	5.52E-03	.216244				
2	1.4	5.68E-03	.219222				
1	0.7	5.83E-03	.328				
1	0.7	5.98E-03	.323				
0	0.0	6.13E-03	.				
2	1.4	6.29E-03	.275345				
4	2.8	6.44E-03	.218246263277				
8	5.7	6.59E-03	.239242249265266322324339				
12	8.5	6.75E-03	.242252267271272330331335341343350353				
12	8.5	6.90E-03	.224227232234258262270327332333349358				
17	12.1	7.05E-03	.238254256264283321325335339342344351353356357359360				
6	4.3	7.20E-03	.229241251259274337				
6	4.3	7.36E-03	.233235273304348352				
11	7.6	7.51E-03	.225226250253260276279282293306340				
5	3.5	7.66E-03	.217226247294305				
11	7.8	7.82E-03	.240255280282290292300302309319346				
8	5.7	7.97E-03	.224246257261269301315347				
7	5.0	8.12E-03	.24[illegible]310320326				
4	2.8	8.27E-03	.231278311312				
5	3.5	8.43E-03	.230237296317318				
3	2.1	8.58E-03	.302316334				
2	1.4	8.73E-03	.313314				
3	2.1	8.89E-03	.291307329				
1	0.7	9.04E-03	.285				
4	2.8	9.19E-03	.281257308354				
0	0.0	9.34E-03	.				
2	1.4	9.50E-03	.234789				
0	0.0	9.65E-03	.				
0	0.0	9.80E-03	.				
0	0.0	9.95E-03	.				
0	0.0	1.01E-02	.				
0	0.0	1.03E-02	.				
0	0.0	1.04E-02	.				

140 0 5 10 15 20 25 30

THE FOLLOWING DEVICE(S) ARE OUTSIDE THE RANGE OF THE HISTOGRAM

00000215 1.677E-04

Figure 89. Histogram of $\Delta(1/h_{FE}) = \Delta I_B/I_C$ Illustrating the Variation in the Radiation Sensitivities Among the 2N2905A Transistors of Different Wafers (Dose = 5.6×10^6 rads; I_E = 3 mA)

```
DEVICE 2N2905A  TEST 3E1   TEMP 22.   STRESS 0.0          F4000          BRL335                    10 APR 73
--------------------------------------------------------------------------------------------------------------
NO.   PER      TEST                                   MEDIAN        MEAN       STD. DEV.    COVAR.(%)
      CENT     HFE       IE= 10MAVCB= 0.V             1.387E 02    1.385E 02   2.787E 01     0.20
--------------------------------------------------------------------------------------------------------------
  0    0.0    1.74E 01  .
  0    0.0    2.37E 01  .
  0    0.0    3.00E 01  .
  0    0.0    3.62E 01  .
  0    0.0    4.25E 01  .
  0    0.0    4.88E 01  .
  0    0.0    5.51E 01  .
  0    0.0    6.13E 01  .
  0    0.0    6.76E 01  .
  0    0.0    7.39E 01  .
  0    0.0    8.01E 01  .
  0    0.0    8.64E 01  .
 12    7.6    9.27E 01  .2[illegible]297[illegible]
  9    5.7    9.90E 01  .2[illegible]
 12    7.6    1.05E 02  .2[illegible]288298[illegible]
  9    5.7    1.11E 02  .295299[illegible]309[illegible]315[illegible]326[illegible]
  4    2.5    1.18E 02  .290293346347
  2    1.3    1.24E 02  .336341
 12    7.6    1.30E 02  .237248261268332337339340344345348357
 17   10.5    1.37E 02  .205217229256269324325327330333342350352353356358359
 16   10.2    1.43E 02  .207272240245247257278280321322328331343349351360
 16   10.2    1.49E 02  .209252302312352362502532552602732742793233335338
  3    1.9    1.55E 02  .253275355
  3    1.9    1.62E 02  .212258272
 11    7.0    1.68E 02  .204206211215249251252263265270277
 12    7.6    1.74E 02  .208210216218219223224228232233241246
 11    7.0    1.80E 02  .222227234238239243244254264271276
  4    2.5    1.87E 02  .242262266267
  0    0.0    1.93E 02  .
  0    0.0    1.99E 02  .
  0    0.0    2.06E 02  .
  0    0.0    2.12E 02  .
  0    0.0    2.18E 02  .
  0    0.0    2.24E 02  .
  0    0.0    2.31E 02  .
  0    0.0    2.37E 02  .
  0    0.0    2.43E 02  .
  0    0.0    2.49E 02  .
  0    0.0    2.56E 02  .
--------------------------------------------------------------------------------------------------------------
153                     0         5         10         15         20         25         30
```

Figure 90. Histogram of Initial Gain, h_{FE}, Marked to Illustrate the Extent of the h_{FEO} Versus h_{FE} Correlation [Marked Devices Came From the Lower Tail of the h_{FE} (Dose) Histogram]. [2N2905A, h_{FE} (10mA) $\leq$ 64 at 1.3×10^6 rad] The Pronounced Structure in the Histogram is Due to the Different Wafers

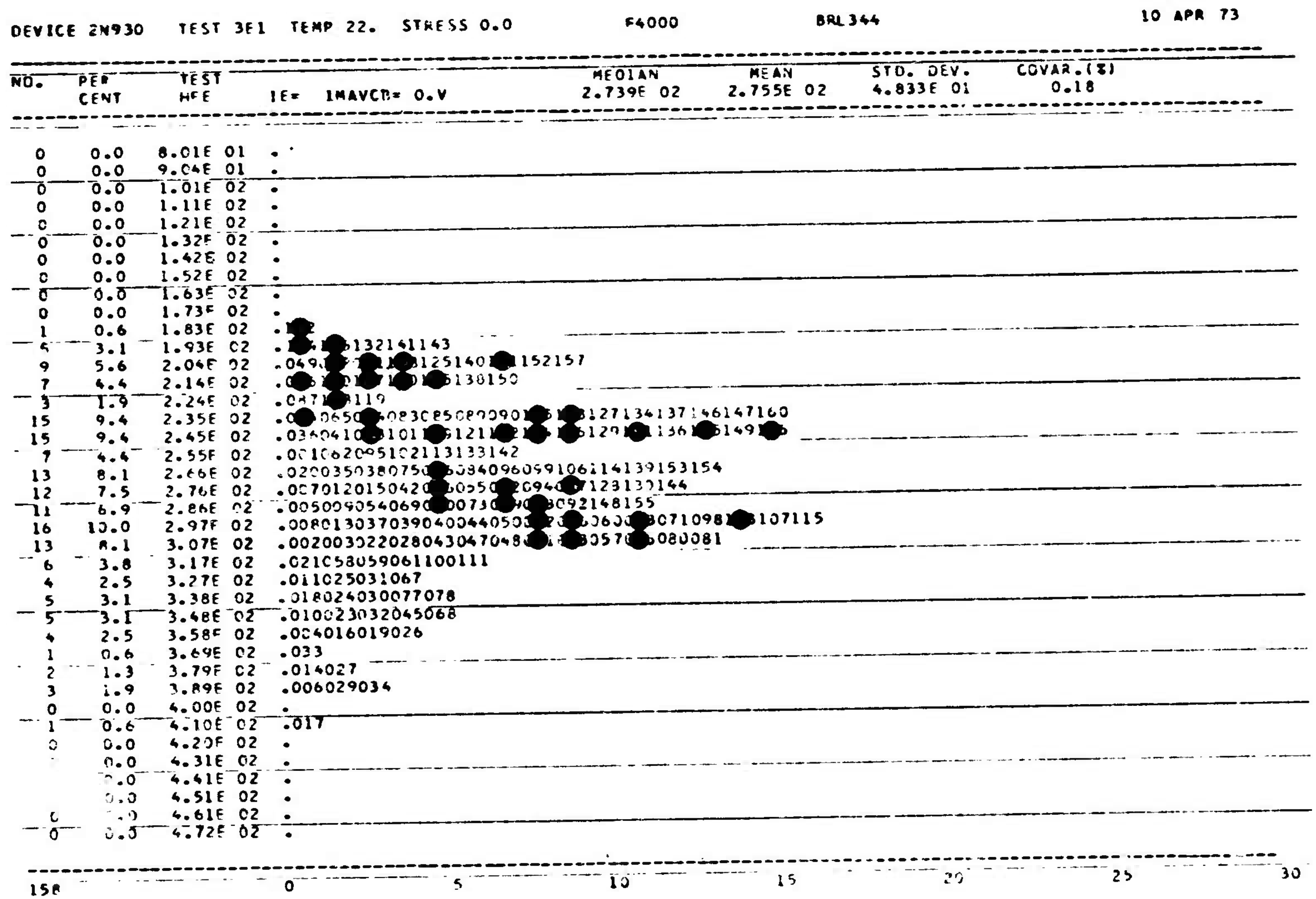

Figure 91. Histogram of Initial Gain, h_{FEO}, Marked to Illustrate the Extent of the h_{FEO} Versus h_{FE} Correlation [Marked Devices Came From the Lower Tail of the h_{FE} (Dose) Histogram]. [2N930, h_{FE} (1mA) ≤ 64 at 3.0×10^5 rad]

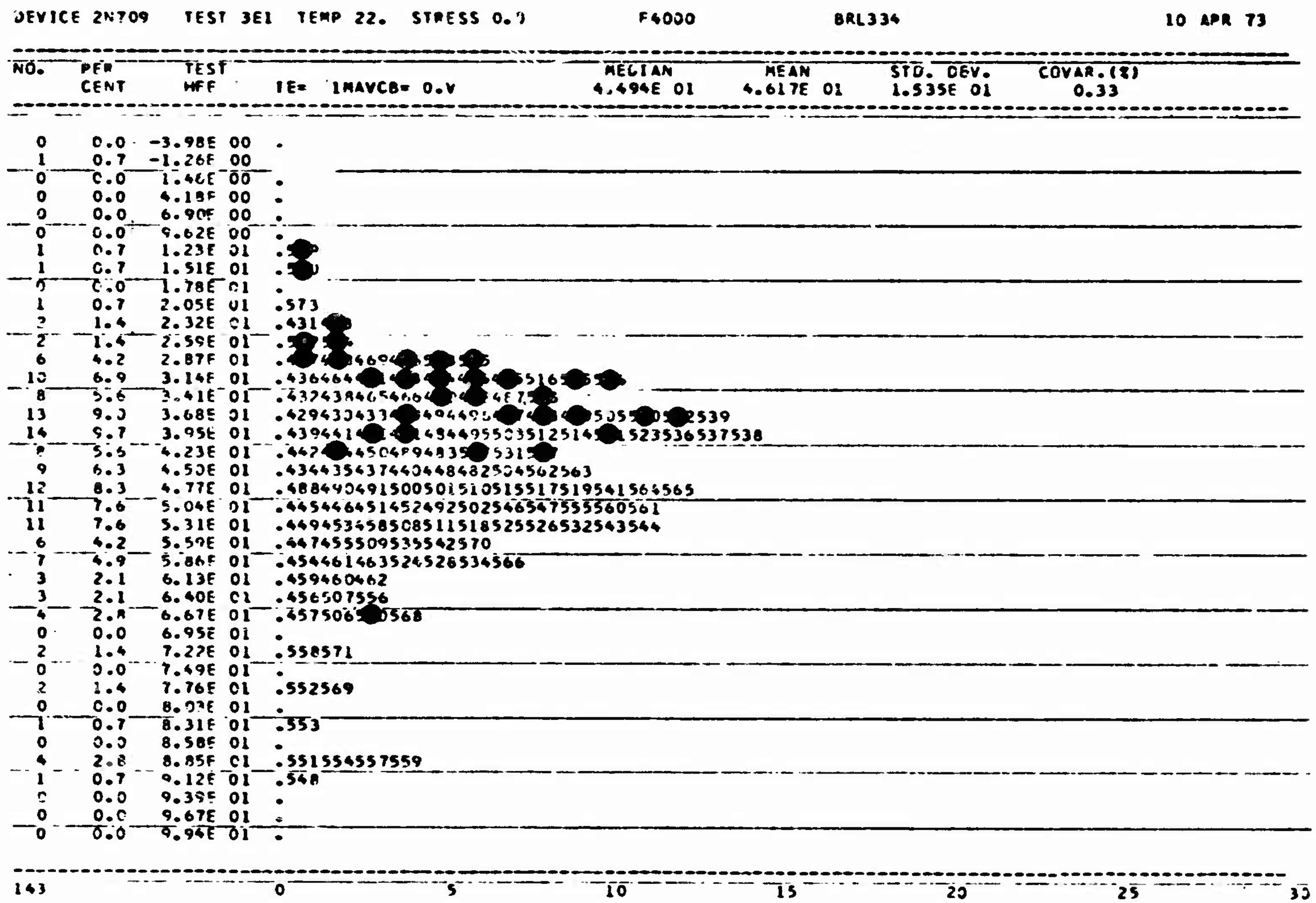

Figure 92. Histogram of Initial Gain, h_{FEO}, Marked to Illustrate the Extent of the h_{FEO} Versus h_{FE} Correlation [Marked Devices Came From the Lower Tail of the h_{FE} (Dose) Histogram]. [2N709, h_{FE} (1mA) $\leq$ 19 at 1.3×10^6 rad]

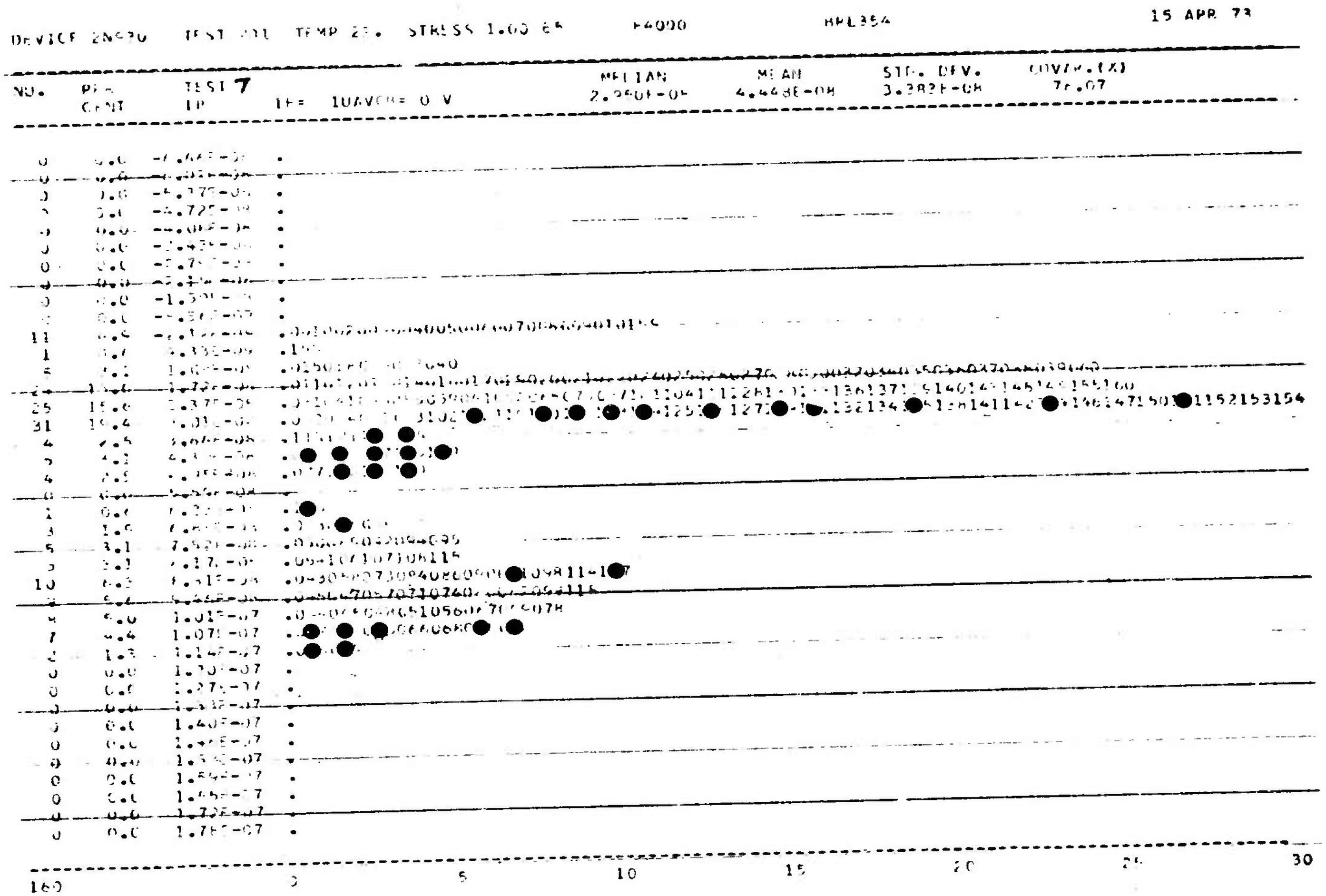

Figure 93. Histogram of Low Dose ΔI_B, Marked to Illustrate the Limitations of the Low Dose Screening. Marked Devices Came From the Upper Tail of the HIgh Dose ΔI_B Histogram (2N930, High Dose - 3 x 10^5 rads)

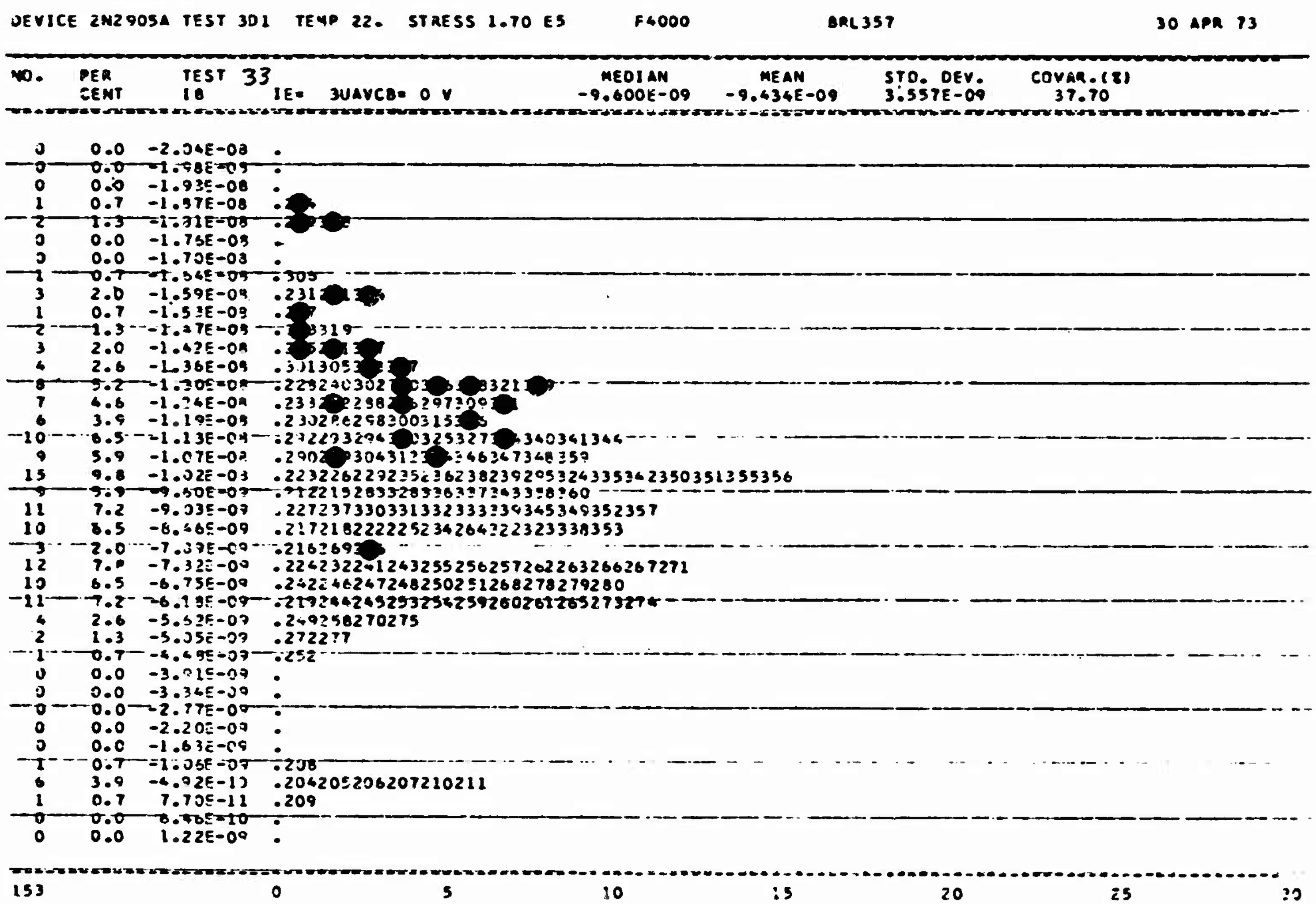

Figure 94. Histogram of Low Dose ΔI_B, Marked to Illustrate the Limitations of the Low Dose Screening. Marked Devices Came From the Upper Tail of the High Dose ΔI_B Histogram (2N2905A, High Dose - 5.6 x 10^6 rad)

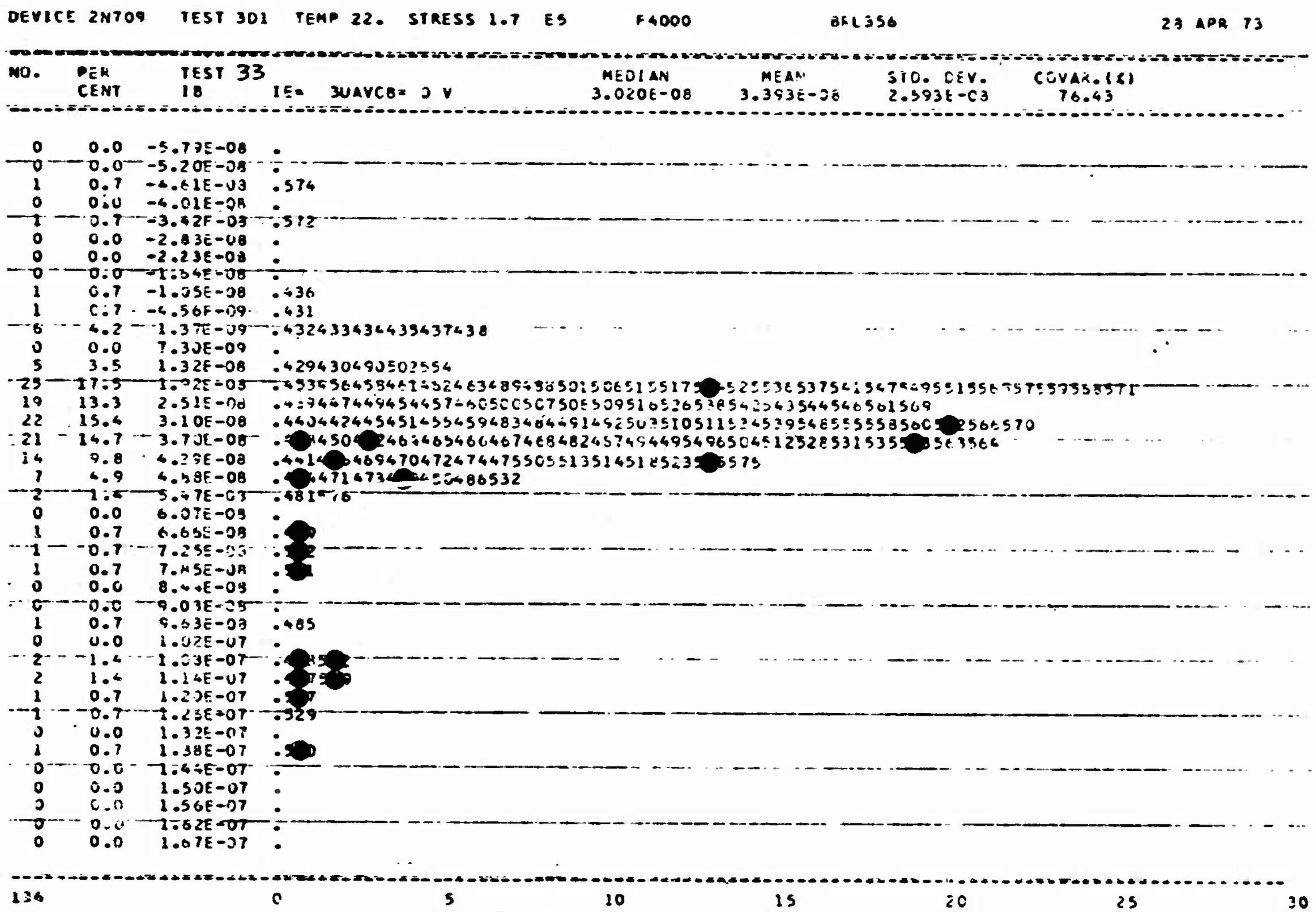

Figure 95. Histogram of Low Dose ΔI_B Marked to Illustrate the Limitations of the Low Dose Screening. Marked Devices Came From the Upper Tail of the High Dose ΔI_B Histogram (2N709, High Dose = 1.3 x 10^6 rad)

```
DEVICE UA 744   TEST 2ER   TEMP 22.   STRESS 0.0          F4000          RRL307                        2  APR 7?
-------------------------------------------------------------------------------------------------------------------
NO.   PER     TEST                                         MEDIAN       MEAN       STD. DEV.    COVAR.(%)
      CENT    18                                         -2.377E-04   -2.567E-04   7.700E-05      29.99
-------------------------------------------------------------------------------------------------------------------

  0    0.0   -5.60E-04  .
  0    0.0   -5.45E-04  .
  1    0.6   -5.30E-04  .222
  0    0.0   -5.15E-04  .
  0    0.0   -5.00E-04  .
  1    0.6   -4.85E-04  .228
  1    0.6   -4.69E-04  .197
  0    0.0   -4.54E-04  .
  5    2.8   -4.39E-04  .164185190194244
  1    0.6   -4.24E-04  .252
  3    1.7   -4.09E-04  .219223293
  4    2.2   -3.94E-04  .163206255305
  1    0.6   -3.79E-04  .157
  4    2.2   -3.64E-04  .172178136302
  2    1.1   -3.49E-04  .239265
  8    4.4   -3.34E-04  .171173174200201208249306
  3    1.7   -3.19E-04  .157253269
  7    3.9   -3.04E-04  .161184195254258277298
 10    5.6   -2.89E-04  .154202216225233234236240286378
 13    7.2   -2.74E-04  .156171119819420921421723523827928029029 1
 11    6.1   -2.59E-04  .155198204241264266279289292299301
 16    8.9   -2.44E-04  .152165169176180182196203207211218220245287304397
 18   10.0   -2.29E-04  .160162168170177210226232237242243268273274294295380386
 23   12.8   -2.14E-04  .158181187205224229231246250251260263267270271276281283284297307383394
 17    9.4   -1.98E-04  .159183189193212213215247285288300303308309379381396
 11    6.1   -1.93E-04  .151159166175192221230249261262369
  8    4.4   -1.68E-04  .227256259262278296391393
  3    1.7   -1.53E-04  .272392395
  3    1.7   -1.38E-04  .257304308
  3    1.7   -1.23E-04  .377387389
  0    0.0   -1.08E-04  .
  0    0.0   -9.31E-05  .
  0    0.0   -7.80E-05  .
  0    0.0   -6.30E-05  .
  0    0.0   -4.79E-05  .
  0    0.0   -3.29E-05  .
  0    0.0   -1.78E-05  .
  0    0.0   -2.78E-06  .
  0    0.0    1.23E-05  .

-------------------------------------------------------------------------------------------------------------------
177                     0        5        10        15        20        25        30
```

Figure 96. Histogram of the Initial Bias Currents Illustrating the Variation Among the Op Amps

DEVICE UA 744 TEST 4D1 TEMP 22. STRESS 5.60 E6 F4000 BRL331 28 APR 73

NO.	PER CENT	TEST 13 ΔIB		MEDIAN -3.522E-04	MEAN -3.370E-04	STD. DEV. 1.812E-04	COVAR.(%) 53.75
0	0.0	-1.08E-03	.				
0	0.0	-1.04E-03	.				
0	0.0	-9.96E-04	.				
0	0.0	-9.55E-04	.				
0	0.0	-9.15E-04	.				
0	0.0	-8.74E-04	.				
0	0.0	-8.33E-04	.				
0	0.0	-7.92E-04	.				
0	0.0	-7.51E-04	.				
2	1.1	-7.11E-04	.234293				
3	1.7	-6.70E-04	.236249300				
4	2.2	-6.29E-04	.208229272290				
5	2.8	-5.88E-04	.242262274280397				
6	3.3	-5.47E-04	.178195252254302309				
16	8.9	-5.06E-04	.162168172177188193206228237245267291297296388391				
12	6.7	-4.66E-04	.164186198200205210241266271279268292				
11	6.1	-4.25E-04	.182185209222243256257264268284293				
20	11.1	-3.84E-04	.175181191203212220230240250283265295377379381384385387392394				
12	6.7	-3.43E-04	.167176192204216233263294336389395396				
12	6.7	-3.02E-04	.174184201215219225231235238281288308				
19	10.6	-2.62E-04	.165169189202211217221224244247248251253261299301304378383				
18	10.0	-2.21E-04	.163170213216232239246255260267270273277278282296305306				
13	7.2	-1.80E-04	.156171173187190197226227258265275289380				
3	1.7	-1.39E-04	.194196303				
0	0.0	-9.84E-05	.				
1	0.6	-5.76E-05	.153				
3	1.7	-1.68E-05	.154156382				
4	2.2	2.40E-05	.152157158160				
3	1.7	6.48E-05	.151155159				
0	0.0	1.06E-04	.				
0	0.0	1.46E-04	.				
0	0.0	1.87E-04	.				
0	0.0	2.28E-04	.				
0	0.0	2.69E-04	.				
1	0.6	3.10E-04	.199				
0	0.0	3.50E-04	.				
1	0.6	3.91E-04	.269				
0	0.0	4.32E-04	.				
0	0.0	4.73E-04	.				

169 0 5 10 15 20 25 30

Figure 97. Histogram of ΔI_B ILlustrating the Variation in the Radiation Sensitivities Among the Op Amps (Dose = 5.6×10^6 rads)

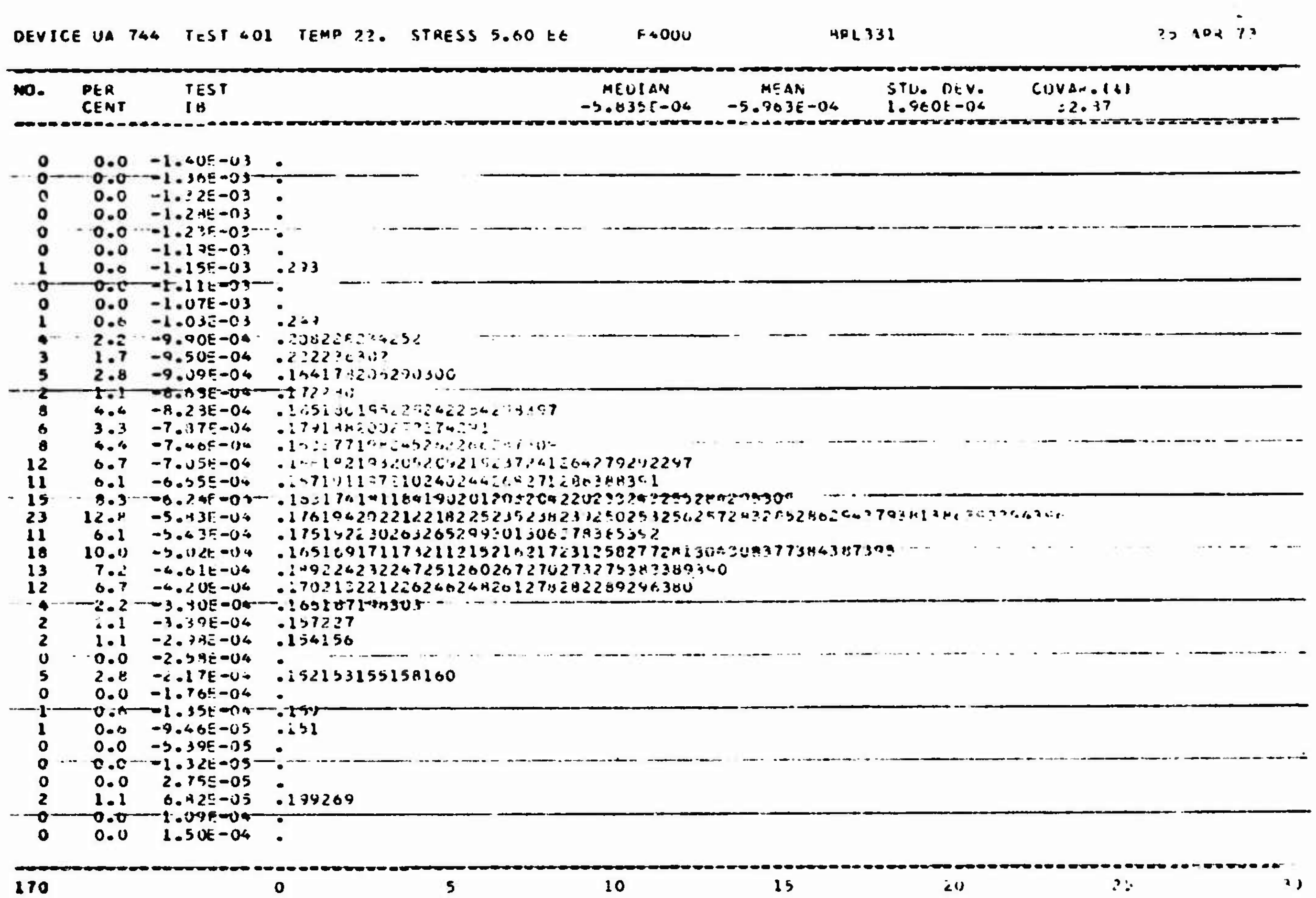

Figure 98. Histogram of I_B (5.6×10^6 rad) Illustrating the Variation Among the Op Amps

Table 77

Rank Correlation Coefficients for Total Dose Damage Prediction (Overview)

X vs. Y (a)	2N709	2N930	2N2905A
(1/f) Noise	0.3	0.2	0.3
I_B^o vs. I_B (dose)[b]	0.5-0.94	0.35-0.7	0.96-0.97
I_B^o vs. I_B/I_B^o [b]	-(0.6-0.4)	-(0.3-0.2)	0.8-0.7
I_B^o vs. $\lvert I_B(\text{dose})-I_B^o \rvert$ [b]	0.2-0.65	0.2-0.4	0.6-0.7
$1/I_B^o$ vs. $(1/I_B^o - 1/I_B)$ [b]	0.91-0.94	0.97-0.8	0.98-0.96
ΔI_B (low injection) vs. ΔI_B (high injection)	$\xrightarrow{\hspace{2em}}$ 0.96-0.55-0.2 [e]	0.98-0.90	$\xrightarrow{\hspace{2em}}$ 0.90-0.80-0.55 [e]
h_{FEO} vs. h_{FE} (dose)	$\xrightarrow{\hspace{2em}}$ 0.56-0.80-0.95 [e]	$\xrightarrow{\hspace{2em}}$ 0.36-0.49-0.68 [e]	0.97-0.97
h_{FEO} vs. $h_{FEO}-h_{FE}$ (dose)	0.91-0.94	0.97-0.83	0.96-0.95
h_{FEO} vs. h_{FE}/h_{FEO}	-(0.6-0.4)	-(0.3-0.2)	-(0.8-0.7)
h_{FEO} vs. $\Delta h_{FE}/h_{FEO}$	0.5-0.6	0.3-0.2	0.8-0.7
$1/h_{FEO}$ vs. $\Delta(1/h_{FE})$	0.2-0.7	-(0.4-0.2)	-(0.75-0.6)
I_B^o [c]	-0.5	-(0.6-0.55)	0.7-0.85
I_B^o (T)[d,c]	-0.4	-0.4	0.7-0.8
ΔI_B (due to ΔT)[c]	-0.4	-0.4-0	0.75-0.8
ΔI_B (due to burn-in)[c]	0	-0.3 to 0.3	-(0.3-0.2)
I_{EBO}^o (or BV_{EBO}^o)	-0.4	-0.3	0.6-0.75
I_{EBO}^o (T) (or BV_{EBO}^o)	-0.4	-0.3	0.6-0.75
ΔI_{EBO} (due to ΔT) (or ΔBV_{EBO})	-0.4	0.2	0.6-0.7
ΔI_{EBO} (due to burn-in)	0	---	---
2N930 Pre-burn-in: (1/f) Noise	---	0.3	---
2N930 Pre-burn-in: I_B^o	---	-0.4	---
2N930 Pre-burn-in: I_B^o (T)	---	-0.4	---

(a) Unless otherwise noted, the Y parameter is Radiation Sensitivity ≡ the change or the relative change in the low injection I_B.
(b) All I_B values were taken at relatively high injection level.
(c) All I_B values were taken at low injection level.
(d) "T" indicates other than room temperature.
(e) These multiple entries represent variation with emitter current. Arrows correspond to the direction of increasing current.

Table 78

Summary of Data to Illustrate the Radiation Sensitivity of 2N709

		1.0×10^5 rads	3.0×10^5 rads	COV %	1.3×10^6 rads	COV %	5.6×10^6 rads	COV %
ΔI_B (Amps.)	I_B at V_{BE} = 0.45V	---	3.4×10^{-9}	166	6.5×10^{-8}	79	2.5×10^{-7}	73
	I_B at I_E = 3 μA	---	8.1×10^{-8}	80	5.5×10^{-7}	67	1.1×10^{-6}	37
	I_B at I_E = 1 mA	---	5.0×10^{-6}	43	1.7×10^{-5}	48	3.5×10^{-5}	36
$\frac{I_B}{I_B^0}$	I_B at V_{BE} = 0.45V	---	1.45	39	8.7	79	27.1	76
	I_B at I_E = 3 μA	---	1.6	25	5.0	56	9.8	52
	I_B at I_E = 1 mA	---	1.24	7.5	1.8	20	2.66	27
$\frac{h_{FE}}{h_{FEO}}$	h_{FE} at I_E = 100 μA	---	0.74	16	0.41	48	0.20	43
	h_{FE} at I_E = 1 mA	---	0.81	8.6	0.55	19	0.36	21
	h_{FE} at I_E = 10 mA	---	0.35	2.7	0.70	5.9	0.55	8.7
$\Delta(1/h_{FE})$	h_{FE} at I_E = 100 μA	---	9.3×10^{-3}	56	4.7×10^{-2}	64	1.1×10^{-1}	41
	h_{FE} at I_E = 1 mA	---	5.3×10^{-3}	44	1.8×10^{-2}	48	3.7×10^{-2}	37
	h_{FE} at I_E = 10 mA	---	3.8×10^{-3}	36	1.0×10^{-2}	21	1.8×10^{-2}	19

Table 79

Summary of Data to Illustrate the Radiation Sensitivity of 2N930

			1.0×10^5 rads		3.0×10^5 rads		1.3×10^6 rads		5.6×10^6 rads	
				COV %		COV %		COV %		COV %
ΔI_B (Amps)	I_B at	V_{BE} = 0.45V	7.9×10^{-8}	77	2.3×10^{-7}	40	3.3×10^{-7}	19	4.3×10^{-7}	13
		I_E = 1 µA	4.4×10^{-8}	76	1.4×10^{-7}	41	2.0×10^{-7}	20	2.5×10^{-7}	15
		I_E = 100 µA	8.7×10^{-7}	63	2.1×10^{-6}	37	3.0×10^{-6}	19	3.7×10^{-6}	15
		I_E = 10 mA	2.5×10^{-5}	53	4.5×10^{-5}	41	6.8×10^{-5}	36	9.2×10^{-5}	20
$\frac{I_B}{I_B^0}$	I_B at	V_{BE} = 0.45V	5.7	65	15.0	44	20.0	37	25.7	35
		I_E = 1 µA	6.5	65	18.3	41	23.9	35	32.2	21
		I_E = 100 µA	3.0	45	5.8	31	7.7	18	9.4	15
		I_E = 10 mA	1.6	22	2.1	21	2.7	12	3.2	10
$\frac{h_{FE}}{h_{FEO}}$	h_{FE} at	I_E = 100 µA	0.36	34	0.17	24	0.13	18	0.105	16
		I_E = 1 mA	0.50	29	0.30	19	0.23	15	0.19	13
		I_E = 10 mA	0.65	22	0.47	16	0.37	12	0.31	10
		I_E = 50 mA	0.80	12	0.65	12	0.53	11	0.45	8.4
$\Delta(1/h_{FE})$	h_{FE} at	I_E = 100 µA	8.9×10^{-3}	63	2.2×10^{-2}	36	3.1×10^{-2}	20	3.9×10^{-2}	16
		I_E = 1 mA	4.3×10^{-3}	56	8.7×10^{-3}	36	1.3×10^{-2}	20	1.6×10^{-2}	16
		I_E = 10mA	2.6×10^{-3}	53	4.6×10^{-3}	40	6.9×10^{-3}	36	9.4×10^{-3}	20

Table 80

Summary of Data to Illustrate the Radiation Sensitivity of 2N2905A

			1.0×10^5 rads	COV %	3.0×10^5 rads	COV %	1.3×10^6 rads	COV %	5.6×10^6 rads	COV %
ΔI_B (Amps.)	I_B at	V_{BE} = 0.45V	1.8×10^{-9}	250	-5.1×10^{-9}	120	-6.3×10^{-8}	21	-2.3×10^{-7}	13
		I_E = 3 μA	-5.7×10^{-9}	40	-1.5×10^{-8}	36	-5.3×10^{-8}	19	-1.8×10^{-7}	15
		I_E = 30 mA	-5.6×10^{-5}	18	-9.1×10^{-5}	19	-1.2×10^{-4}	13	-2.0×10^{-4}	10
$\frac{I_B}{I_B^O}$	I_B at	V_{BE} = 0.45V	0.98	7.7	1.1	11	1.9	17	4.3	27
		I_E = 3 μA	1.15	3.9	1.4	5.4	2.4	13	5.6	17
		I_E = 30 mA	1.25	2.3	1.4	4.4	1.6	4.9	1.9	5.7
$\frac{h_{FE}}{h_{FEO}}$	h_{FE} at	I_E = 3 mA	---	---	0.87	2.4	0.71	5.5	0.51	7.9
		I_E = 30 mA	---	---	0.71	4.5	0.64	5.1	0.53	5.7
		I_E = 300 mA	---	---	0.91	1.5	0.80	1.9	0.67	2.3
$\Delta(1/h_{FE})$	h_{FE} at	I_E = 3 mA	3.8×10^{-4}	41	1.2×10^{-3}	31	3.2×10^{-3}	15	7.4×10^{-3}	11
		I_E = 30 mA	1.9×10^{-3}	18	3.1×10^{-3}	19	4.2×10^{-3}	13	6.7×10^{-3}	11
		I_E = 300 mA	5.7×10^{-4}	43	2.0×10^{-3}	36	5.5×10^{-3}	13	1.0×10^{-2}	8.4

Table 81

Results of Rank Correlations Between Radiation Sensitivity (Low Dose) and Radiation Sensitivity (High Dose)

Device Type	Bias Condition for I_B	Radiation Sensitivity: I_B(irradiated) - I_B^o Low Dose rad(Si)	High Dose rad(Si)	Correlation Coefficient
2N709	V_{BE} = 0.45V	1.7×10^5	1.3×10^6	0.678
	I_E = 3 µA	1.7×10^5	1.3×10^6	0.663
	V_{VE} = 0.45V	3.0×10^5	1.3×10^6	0.893
	I_E = 3 µA	3.0×10^5	1.3×10^6	0.821
2N930	V_{BE} = 0.45V	3.0×10^4	3.0×10^5	0.699
	I_E = 1 µA	3.0×10^4	3.0×10^5	0.639
	V_{BE} = 0.45V	1.0×10^5	3.0×10^5	0.752
	I_E = 1 µA	1.0×10^5	3.0×10^5	0.726
2N2905A	V_{BE} = 0.45V	1.7×10^5	5.6×10^6	0.329
	I_E = 3 µA	1.7×10^5	5.6×10^6	0.675
	V_{BE} = 0.45V	3.0×10^5	5.6×10^6	0.296
	I_E = 3 µA	3.0×10^5	5.6×10^6	0.681

Table 82

Summary of Data Illustrating the Procedure and the Results of the Low Dose Screening (2N930)

Bias Conditions	3×10^5 rads		1×10^5 rads		N (% of Total Sample)	M (% of Total Sample)
	Rows R	Devices N	Rows P	Devices M		
$I_B(V_{BE} = 0.45V)$	1	2	13	60	1.3	40.3
	2	6	13	60	4.0	40.3
	3	11	14	63	7.4	42.3
	4	19	15	73	12.8	49.0
	5	35	15	73	23.5	4[illegible].0
$I_B(I_E = 1\ \mu A)$	1	1	10	54	0.7	36.2
	2	5	13	94	3.4	63.1
	3	17	13	94	11.4	63.1
	4	32	13	94	21.5	63.1
$I_B(I_E = 100\ \mu A)$	1	1	9	51	1	34.2
	2	5	10	53	5	35.6
	3	17	13	81	17	54.4
$I_B(I_E = 10\ mA)$	1	1	5	39	1	26.2
	2	3	6	48	3	32.2
	3	6	7	57	6	38.3
	4	17	7	57	17	38.3
	5	22	7	57	22	38.3
	6	29	10	64	29	43.0

Table 83

Summary of Data Illustrating the Procedure and the Results of the Low Dose Screening (2N2905A)

Bias Conditions	5×10^6 rads		1.7×10^5 rads		N(% of Total Sample)	M (% of Total Sample)
	Rows R	Devices N	Rows P	Devices M		
$I_B(I_E = 300\ mA)$	2	4	6	36	2.8	25.5
	3	15	10	99	10.6	70.2
	4	26	10	99	18.4	70.2
$I_B(I_E = 1\ mA)$	4	8	9	32	5.7	22.7
	6	16	12	63	11.3	44.7
	7	23	18	124	16.3	87.9
$I_B(I_E = 3\ \mu A)$	3	5	9	25	3.5	17.7
	5	7	9	25	5.0	17.7
	6	16	13	57	11.3	40.4
	7	19	13	57	13.5	40.4
	8	25	18	105	17.7	74.5
$I_B(V_{BE} = 0.45V)$	3	5	12	93	3.5	66.0
	4	16	16	126	11.3	89.4
	5	22	18	138	15.6	97.9

Table 34

Summary of Data Illustrating the Procedure and the Results of the Low Dose Screening (2N709)

Bias Condition	Rows *R	Devices N	N(% of Total Sample)	Rows *P	Devices M	M(% of Total Sample)
I_B at I_E = 10 mA	1	2	1.5	3	3	2.3
	2	4	3.0	6	9	6.8
	5	7	5.3	7	11	8.3
	6	11	8.3	10	33	24.8
	7	15	11.3	10	33	24.8
	8	23	17.3	12	47	35.3
I_B at I_E = 100 μA	1	1	0.75	1	7	5.3
	3	4	3.0	1	7	5.3
	4	7	5.3	3	9	6.8
	7	11	8.3	9	22	16.5
	9	14	10.5	9	22	16.5
	11	20	15.0	12	55	41.3
I_B at I_E = 3 μA	1	1	0.75	1	7	5.3
	2	2	1.5	2	8	6.0
	3	5	3.8	9	17	12.8
	7	10	7.5	9	17	12.8
	9	17	12.8	13	41	30.8
	11	23	17.3	15	84	63.2

*In these histograms, all devices with good data, but such large ΔI_B as to fall outside the histogram plot, were called row 1.

Table 85

Rank Correlation Coefficients for Damage Prediction at 5.6×10^6 rads - μA744

Change in Bias Current, ΔI_B vs.:	Rank Correlation
I_B^o	-0.061
low frequency noise current	0.091
I_B^o (22°C) - I_B^o (-50°C)	0.112
I_B^o (75°C) - I_B^o (22°C)	0.157
I_B^o (75°C) - I_B^o (-50°C)	0.190
I_B^o (-50°C)	-0.099
I_B^o (75°C)	0.082
Relative Change in Bias Current, $\Delta I_B/I_B^o$ vs.:	
I_B^o	0.546
low frequency noise current	-0.316
I_B^o (22°C) - I_B^o (-50°C)	-0.403
I_B^o (75°C) - I_B^o (22°C)	-0.486
I_B^o (75°C) - I_B^o (-50°C)	-0.492
I_B^o (-50°C)	0.463
I_B^o (75°C)	0.237

Table 86

Summary of Data Illustrating the Procedure and the Results of the Low Dose Screening for the μA744 Op Amp

Rows R	Devices N	N(% of Total Sample)	Rows P	Devices M	M(% of Total Sample)
1	2	1.4	13	56	39.7
2	5	3.5	14	74	52.5
3	9	6.4	14	74	52.5
4	14	9.9	15	106	75.2
5	20	14.2	15	106	75.2

REFERENCES

1. Sawyer, D.E., "Prevalent Error Sources in Tra[illegible] Delay-Time Measurements", IEEE Trans. On Nucl. Sci. NS-19, No. 6, 121 (1972)

2. Frank, M., and Larin, F., "Effect of Operating Conditions and Transistor Parameters on Gain Degradation", IEEE Trans. on Nucl. Sci., NS-12, 126 (1965)

3. Ramsey, C.E., Vail, P.J., "Current Dependence of the Neutron Damage Factor", IEEE Trans on Nucl. Sci. NS-17, No. 6, 310 (1970)

4. Gwyn, C.W., and Gregory, B.L., "Designing Ultrahard Bipolar Transistors", IEEE Trans. on Nucl. Sci. NS-18, No. 6, 340 (1971)

5. Rosenberg, C., Arimura, I., and Unwin, A.M., "Statistical Analysis of Neutron-Induced Gain Degradation of Power Transistors", IEEE Trans. on Nucl. Sci. NS-17, No. 6, 160 (1970).

6. Niehous, D., Frank, M., Stoll., E., and Swick, E., "Neutron Hardness Assurance for Power Transistors", IEEE Trans. On Nucl. Scie. NS-17, No. 6, 154 (1970). See also, "Neutron Screening Techniques for Hardened Bipolar Power Transistors', Bendix Corp. Technical Report, SAMSO Contract NR F04701-69-C-0170, August, 1971.

7. Smith, D.M. and Hahn, L.A. "Neutron Hardness Assurance of Bipolar Transistors by Collector Resistance Technique", IEEE Trans. on Nucl. Sci. NS-19, No. 6, 125 (1972)

8. Larin, F., Radiation Effects in Semiconductor Devices, John Wiley & Sons (1968) p. 173

9. Shedd, W., Buchanan, B., and Dolan, R., "Radiation Effects on Junction Field Effect Transistors", IEEE Trans. on Nuc. Sci., NS-16, pp 87-95, Dec. 1969.

10. Buchanan, B., Dolan, R., and Roosild, S., "Comparison of Neutron Radiation Tolerance of Bipolar and Junction Field Effect Transistors", Proc. IEEE, Dec. 1967

11. Gregory, B.L. and Smits, F.M., "A Comparison of Radiation Tolerance of Field Effect and Bipolar Transistors", IEEE Trans. on Elec. Dev., May 1965

12. Buchanan, B.L., Dolan, R.P. and Shedd, W.M. "Radiation Tolerance of Bipolar and Field Effect Transistors as a Function of Lifetime and Doping", Trans. of Met. Soc. of AIME, 245, Mar. 1969.

13. George, W., "Radiation Hardened Junction Field Effect Transistors", AFCRL-70-0339, Scientific Report No. 2, Motorola, Inc., Prepared for AFCRL under contract No. F19628-68-C-0141, January 1970

14. Stein, H.J. and Gereth, R., "Introduction Rates of Electrically Active Defects in n- and p-Type Silicon By Electron and Neutron Irradiation", Jour. Appl. Phys, 39 No. 6, 2890, May 1968.

15. Dacey, G.C., and Ross, I.M., "Unipolar 'Field-Effect' Transistor", Proc. IRE, Aug. 1953.

16. Graeme, Tobey and Huelsman (Editors), Operational Amplifiers, McGraw Hill, 1971.

17. Carr, E.A., "Simplified Techniques for Predicting TREE Responses", IEEE Trans. on Nucl. Sci., NS-12, Oct. 1965.

18. Sivo, L.L., Hughes, H.L., King, E.E., "Investigation of Radiation Induced Interface States Utilizing Gated-Bipolar and MOS Structures", IEEE Trans. Nucl. Sci., NS-19, 313 (1972).

19. Thornton, C.G., and Simmons, C.D., "A New High Current Mode of Transistor Operation", IRE Trans. On Electron Devices, Vol. ED-5, pp. 6-10, January 1968.

20. English, A.C., "Mesoplasmas and 'Second Breakdown' In Silicon Junctions" Solid State Electronics, Vol. 6, pp. 511-521, September-October 1963

21. Portnoy, W.M. and Gamble, F.R., "Fine Structure and Electromagnetic Radiation in Second Breakdown", IEEE Transactions on Electron Devices ED-11, pp. 470-478, October 1964.

22. Scarlett, R.M., Shockley, W., and Haitz, R.H., "Thermal Instabilities and Hot Spots in Junction Transistors", Physics of Failure in Electronics (Edited by F.M. Goldberg and J. Vaccaro), pp. 194-203, Spartan Books Inc., Baltimore and Cleaver-Hume Press, London 1963.

23. Schafft, H.A., and French, J.C., "Breakdown Characteristics of Semiconductor Materials," Electro-Technology, Vol. 75, pp.77-82, June 1965

24. Ford, G.M., "Collector to Emitter Breakdown Related to Thermal Runaway in Inhomogeneous Base Germanium Power Transistors", Solid State Design, Vol. 4, pp 29-36, June 1963

25. Budenstein, P.P., Pontius, D.H., and Smith, W.B., Second Breakdown and Damage in Semiconductor Devices, U.S. Army Missile Command, Report No. RG-TR-72-15, April 1972.

26. Melchior, H., and Strutt, M. J. O., "Secondary Breakdown in Transistors," Proc. IEEE (Correspondence), Vol. 52, pp. 439-440, April 1964

27 Egelkrout, D.W., "Second Breakdown and Radiation Effects in Semiconductor Junction Devices," The Boeing Company, D2-121704-1, December 1967.

28. English, A.C., and Power, H.M., "Mesoplasma Breakdown in Silicon Junctions", Proc. IEEE (Correspondence), Vol.51, p. 501, March 1963

29. Weitzsch, F., "Zur Theorie Des Zweiten Durchbruchs Bei Transistoren", Archiv Der Elektrischen Ubertragung, Vol. 19, pp. 27-42, January 1965

30. Hakim, E.B., and Reich, B., "Effects of Neutron Radiation on Second Breakdown," IEEE Proceedings, (Correspondence) Vol. 52, p. 735, June 1964

31. [redacted]

32. Reich, B., Hakim, E.B., Hunter, E.T., "The Effects of Neutron Radiation on Second Breakdown and Thermal Behavior of Silicon Transistors", IEEE Transactions on Nuclear Science, NS-15, No. 6, Dec. 1968

33. Caldwell, R.S., Bowman, W.C., and Folsom, J.A., NEREM, Record 28, 20 (1966)

34. Carr, E.A., and Binder, D., IEEE Trans. Nucl. Sci., NS-16, No. 6, 120 (1969)

35. Tasca, D.M. and Peden, J.C., Feasibility Study of Developing A Non-Destructive Screening Procedure for Thermal Second Breakdown, General Electric Company Space Division Philadelphia, Pennsylvania, July 1971

36. Warner, R.M., Jr., Integrated Circuit Design Principles and Fabrication, Motorola, Inc, Semiconductor Products Division, McGraw Hill, 1965

37. Clark, L.E., and George, W.L., Current Crowding In Hardened Power Transistors, Motorola Semiconductor Products Division, Phoenix Arizona, (Paper presented at 1972 IEEE Meeting on Nuclear and Space Radiation Effects.

38. Reich, B., Hakim, E.B., "Bulk Reliability Effects in Semiconductor Devices, Current Crowding in Transistors", USAERDL Technical Report 2333, February 1963

39. Seminar on "Second Breakdown in Power Transistors", Marshall Space Flight Center, Huntsville Alabama, January 15, 1968, J. K. Morris, Chairman

40. Chang, Z.F., and Turner, C.R., "Characterization of Second Breakdown in Power Transistors", RCA Appl. Note SMA-21.

41. Buhanan, D., "Investigation of Current-Gain Temperature Dependence in Silicon Transistors", IEEE Transactions on Electron Devices, ED-16, No. 1 (January 1969)

42. Dixon, W.J., and Massy, F.J. Jr., Introduction to Statistical Analysis, McGraw Hill Third Ed. 1969

43. Private communication with Tom Auspach of Honeywell

44. Circuit Analysis of the X Switch, Honeywell Report No. WCCA-2-10, October, 1971